

**Project Acronym:**  
SOUNDPET(INTEGRATED/0918/0008)

MRI-guided Focused ultraSOUND system for cancer in PETs  
(dogs and cats)

**Deliverable: 6.7**

**Title:** Evaluation of the FUS positioning system for microbubbles-mediated blood-brain barrier disruption in mice

**Prepared by:**

Marios Stavrou (CUT)  
Anastasia Antoniou (CUT)  
Elena Georgiou (CING)  
Ioanna Kousiappa (CING)  
**Christakis Damianou (CUT)**

**Date: 05/04/2023**



**Ευρωπαϊκή Ένωση**  
Ευρωπαϊκά Διαρθρωτικά  
και Επενδυτικά Ταμεία



Κυπριακή Δημοκρατία



**Διαρθρωτικά Ταμεία**  
της Ευρωπαϊκής Ένωσης στην Κύπρο

## Table of Contents

SUMMARY .....	3
INTRODUCTION .....	4
MATERIALS AND METHODS .....	7
Positioning Focused Ultrasound Device .....	7
Experimental protocol No.1 .....	8
<i>Anaesthesia</i> .....	8
<i>Retro-orbital Injection</i> .....	8
<i>Treatment protocol</i> .....	9
<i>Transcardiac perfusion</i> .....	10
<i>Brain dissection</i> .....	11
<i>Tissue embedding</i> .....	11
<i>Immunohistochemistry</i> .....	11
Experimental protocol No.2 .....	11
<i>Anaesthesia</i> .....	11
<i>Intravenous injection</i> .....	12
<i>Treatment protocol</i> .....	12
<i>Brain dissection &amp; Immunohistochemistry</i> .....	13
RESULTS.....	13
Protocol calibration for efficient BBB disruption .....	13
<i>Experimental protocol No.1</i> .....	13
<i>Experimental protocol No.2</i> .....	18
Feasibility of delivering A $\beta$ (1-40) antibody in the brain tissue – the effect of antibody amount .	37
A $\beta$ (1-40) antibody alone versus antibody plus FUS – constant antibody amount .....	40
Testing whether FUS mediated BBB disruption facilitates AAV9 penetration into the CNS .....	51
DISCUSSION .....	54
REFERENCES.....	55

## SUMMARY

In this deliverable, we evaluated the feasibility of focussed ultrasound (FUS) and microbubbles (MBs) mediated blood-brain barrier (BBB) disruption in mice using a single element spherically focused transducer of 1 MHz as integrated with the manual positioning device and also identified the US protocol required for opening the BBB. Next, we investigated whether FUS-mediated BBB disruption (BBBD) enhances the delivery of specific therapeutic agents in the mouse brain. All mice experiments were carried out in collaboration with the Cyprus Institute of Neurology and Genetics (CING) at the premises of the Institute. All involved mice were obtained from the animal house facility of CING.

Single sonications were performed using pulsed FUS with a duty factor (DF) of 1% for a total duration of 100 s. The electric power (20-70 W) and amount of MBs (5-20  $\mu$ L) were varied to optimize BBBD. The success and extent of BBBD was assessed using the Evans Blue (EB) dye method as well as Fibrinogen and Fibronectin immunostaining. The safety of the protocol was assessed by Hematoxylin and Eosin (H&E) staining. FUS at electric power of 50-60 W, in synergy with 5  $\mu$ L MBs, was considered optimum for efficient BBBD and used to examine the feasibility of delivering therapeutic agents in the mouse brain parenchyma. No procedure-related brain damage was observed at none of the tested power levels and there was no evidence of hemorrhage. Despite optimizing treatment parameters, the success of BBBD is highly dependent on whether efficient ultrasound coupling is achieved.

Using the optimized protocol parameters, we examined the capability of A $\beta$  (1-40) antibody to enter the brain parenchyma following FUS-mediated BBBD in the 5XFAD mouse model of the Alzheimer's disease. Sonicated mice showed clear evidence of antibody delivery, whereas non-sonicated mice (antibody alone) did not show any signs of the antibody in their brains. The antibody volume is an important factor to be considered as the higher the volume, more antibody binds to amyloid plaques.

Furthermore, FUS-induced BBBD was performed prior to intravenously injecting different doses of the AAV9 vector to optimally transduce the brain of P30 WT mice. The biodistribution of the vector in the Central Nervous System (CNS) was examined by measuring vector genome copy numbers (VGCNs) in extracted DNA from different CNS areas, as well as oligodendrocyte enhanced green fluorescent protein (EGFP) expression rates in different CNS areas. The sonicated mice that were injected with 50  $\mu$ l of the AAV9 vector had a tendency for higher levels of EGFP in many brain areas compared to the non-sonicated mice and appear to have the highest transduction rates. However, further experiments with a larger mice population are needed to confirm this and obtain sufficient evidence.

The study was approved by the Veterinary services of Cyprus (License number: CY/EXP/PR.L05/2021). Appropriate animal handling and procedures were followed according to the Animal health and welfare committee for the SOUNDPET (INTEGRATED/0918/0008) project in order to ensure maximum animal wellbeing. Animals were euthanized while under the effect of deep anesthesia.

## INTRODUCTION

The Blood brain barrier (BBB) consists of tightly linked capillary endothelial cells and serves as the brain's defense against biological toxins controlling the transfer of substances from the blood vessels to the brain parenchyma and vice versa [1]. Paracellular permeability is limited to substances with a molecular weight up to 400-500 Da, thus prohibiting the delivery of most therapeutic agents into the brain [2]. The highly selective nature of BBB is the main obstacle against the application of potential disease-modifying therapies for diseases of the Central Nervous System (CNS), including brain tumors and neurodegenerative diseases such as the Alzheimer's disease (AD) and Parkinson's disease (PD) [3-4]. Accordingly, drug delivery into the brain tissue has been a major challenge for researchers in the field and efforts have spanned decades.

Among the drug-based methods employed in the clinical setting for BBB disruption (BBBD), the most commonly used one involves endovascular administration of an osmotic agent called mannitol to the tumor using a catheter, which causes the endothelial cells to shrink, thus opening the BBB tight junctions [5-6]. The most clinically studied non-drug method is the Magnetic Resonance Imaging (MRI)- guided Focused Ultrasound (MRgFUS), followed by MRI- guided laser ablation and cranial implantable US [5].

It is by now generally accepted that pulsed FUS in synergy with microbubbles (MBs) can cause temporal BBBD by loosening the endothelial cell junctions through a mechanism known as cavitation [7-8]. At sufficiently high acoustic pressure, MBs begin to oscillate stably causing transient increase of permeability in the targeted area while above a threshold of pressure inertial cavitation occurs where MBs collapse violently [9-10]. In the former case, the endothelial ligaments recover completely within a few hours post-sonication [11]. Inertial cavitation is responsible for the majority of adverse effects observed with this strategy, such as micro-hemorrhages [10].

Accordingly, BBBD by pulsed FUS in the presence of gaseous MBs has emerged as a feasible method of delivering large molecules normally hampered by the BBB to the brain. An indicative example is a study by Choi et al. [12] who showed that substances with high molecular weight of up to 70 kDa can reach the brain tissue through diffusion mechanisms following FUS plus MBs-mediated BBBD in the hippocampus of wild type (WT) mice. This finding was particularly important in that the size of diffused substances was similar to that of drugs for key CNS diseases [12]. This strategy has been later confirmed by numerous preclinical studies to enhance the penetration of therapeutic agents, such as therapeutic peptides, genes, and antibodies into the CNS of non-transgenic and transgenic mouse models of neurological diseases, with an increasing number of clinical trials exploring clinical utility [13–16]. Typically, initial evidence of the success and extend of BBBD is obtained by contrast-enhanced MRI and the well-known Evans Blue (EB) dye method [13-14], [16].

Neurodegenerative disorders such as AD, PD, and Huntington's disease are characterized by progressive neuronal dysfunction and there is currently no established method of treatment that can stop or reduce their progression. AD is the prevalent neurodegenerative disorder and cause of dementia and is characterized by the presence of intracellular neurofibrillary tangles and extracellular amyloid plaques owing to Amyloid  $\beta$  peptides ( $A\beta$ ) aggregation [17-18]. AD typically starts in the hippocampus and then spreads to other areas of the brain as advances [18]. Available treatments are not curative but may slow disease progression and alleviate symptoms.

Given the acute demand for disease-modifying therapies, the development of FUS therapeutics for AD has received and is still receiving remarkable research interest. Transgenic mouse models of AD constitute the main research tool in such studies since they are inexpensive, reproducible, and exhibit abundant plaque load. The ability of MBs-enhanced FUS without exogenous agents to reduce the  $A\beta$  pathology has been well demonstrated [19–21]. A single trans-skull MRgFUS treatment was shown to increase the levels of endogenous immunoglobulins (IgM and IgG) in the cortex of the TgCRND8

mouse model, which were detected bound to plaques 4 days posttreatment [19]. FUS-mediated endogenous antibody delivery and glia cells activation were considered as the mechanisms responsible for the observed plaque burden reduction [19]. Later, Shen et al. [20] reported that FUS in synergy with MBs applied twice a week for 6 weeks in triple transgenic AD mice triggered behavioral changes and improved the spatial memory, which were associated with reduced A $\beta$  pathology and tau phosphorylation, as well as improved neuronal health of the sonicated hippocampus compared to the sham group. The findings of Poon et al. [21] support that the therapeutic effects of a single FUS treatment last for at least two weeks, and also that multiple MRI-guided treatments repeated at a two-week interval is a practical method to reduce the A $\beta$  plaque load in advanced AD patients.

The positive effects of FUS in the mitigation of AD pathological features can be enhanced by administrating exogenous therapeutic agents. According to a study by Hsu et al. [22], the effects of FUS on plaque reduction were enhanced using a specific inhibitor of the glycogen synthase kinase-3 (GSK-3); a key molecule in the onset of AD. Administration of an GSK-3 inhibitor in APP<sup>swe</sup>/PSEN1-dE9 transgenic mice prior to MBs-enhanced FUS reduced the A $\beta$  plaque synthesis by suppressing the GSK-3 protein activity, thus resulting in higher plaque reduction compared to when the inhibitor or FUS were applied alone [22]. Another study targeted an A $\beta$  peptide species deposited in AD brain termed Pyroglutamate-3 A $\beta$  (pGlu-3 A $\beta$ ) [23]. The FUS-mediated administration of an anti-pGlu-3 A $\beta$  vaccine was found to promote plaque clearance and partial protection from cognitive decline in APP<sup>swe</sup>/PS1 $\Delta$ E9 mice [23]. Others attempted to support neuronal health as a measure for disease mitigation [24]. Repeated delivery of a pharmacological agent termed D3 (TrkA agonist) that promotes neuronal function by MRgFUS-induced BBBD was found to impart positive cognitive effects in TgCRND8 AD mice [24]. Expect from decreasing A $\beta$  pathology, the combination of FUS and D3 induced numerous additional effects including functional recovery, reduction of dystrophic neurites around the plaques, and enhanced hippocampal neurogenesis [24].

A number of studies aimed to investigate the efficiency of FUS-mediated BBBD to facilitate the supply of large disease-specific antibodies in the brain and the resultant therapeutic effects. The feasibility of delivering an anti-Ab antibody called BAM-10 into the brain of the TgCRND8 mouse model using transcranial MRgFUS has been investigated by Jordao et al [25]. Immunofluorescent staining revealed binding of the antibody to the plaques in the targeted brain areas that was accompanied by reduction of plaque pathology a few days later, also confirming that a single treatment is sufficient to trigger therapeutic effects [25].

FUS-induced BBBD was also shown to facilitate the supply of an anti-pyroglutamate-3 A $\beta$  monoclonal antibody (mAb) called 07/2a in the brain of aged APP/PS1dE9 transgenic mice [26]. A more than 5-fold increase in the mAb levels was observed in the brain of mice treated with FUS plus antibody at 4 and 72 h post-treatment compared to those treated with antibody alone. Immunohistochemistry revealed that the combined therapy further triggered immune responses since the glial activity of resident Iba1<sup>+</sup> and phagocytic CD68<sup>+</sup> microglial cells in the sonicated brain was enhanced compared to the non-sonicated part. Furthermore, a short-term increase in Ly6G immune cells occurred in the sonicated regions indicating that the combined therapy promoted neutrophil infiltration in the brain [26]. The long term effects of the 07/2a mAb administered alone have been examined in a study by Crehan et al. [27], where a 4-month immunotherapy with the specific antibody caused remarkable reduction of pGlu-3 A $\beta$  and A $\beta$  plaques in APP/PS1dE9 mice with positive effects on cognition. The same group further demonstrated that three successive treatments with the 07/2a mAb combined with FUS mediated BBBD performed on a weekly basis resulted in a faster improvement of spatial learning and memory of a higher percentage of aged APP/PS1dE9 mice compared to the mice group treated only with the mAb [28].

Recently, Bajracharya et al. [29], developed a tau-specific mAb termed RNF5 and evaluated its ability to reduce tau aggregates in K369I tau transgenic K3 mice when repetitively administered alone or in combination with low-intensity scanning ultrasound (SUS) plus MBs once a week for 3 months. Immunohistochemical results revealed that the antibody alone caused a reduction in tau levels similar to that observed in the case of MBs-enhanced SUS. Their combination did not result in further decrease of tau levels despite the increased antibody levels observed in the brain. A possible explanation given by the authors is that accumulation of the RNF5 mAb in a specific p-tau-negative hippocampal layer reduced the RNF5 concentration available to attach to tau aggregates. Thereby, this study underlined the need to examine the localization of antibodies following FUS-induced BBB opening in a cellular level since this seems to affect the therapeutic efficacy [29].

Another anti-A $\beta$  antibody tested for its efficacy to improve cognition in AD mice is the Aducanumab. While this antibody administered alone was proved to reduce the A $\beta$  pathology, it seems that higher doses of the antibody should reach the brain to produce clear positive cognitive effects [30]. Leinenga et al. [30] compared the effects of this antibody when administered alone or in synergy with MBs-enhanced SUS in APP23 AD mice. While the superiority of the combined approach in terms of plaque reduction over the antibody and SUS groups was controversial and dependent on the examined brain area, only the mice that received the combined treatment showed significant improvement in spatial memory. Furthermore, the combined approach offered a 5-fold increase in the antibody amount compared to the non-sonicated mice (only antibody) a few days post-treatment. Notably, Aducanumab is the first therapeutic agent to be tested in combination with FUS in AD patients in a phase I ongoing clinical trial [31].

The A $\beta$  (1-40) antibody is an antibody against the amyloid peptides A $\beta$ (1-40) representing the most abundant A $\beta$  isoform in the brain [32]. The FUS-mediated delivery of the specific antibody was previously tested in a very small mice population (n=3), where a 3-fold increase in fluorescence intensity of the antibody staining was observed in the brain regions treated with MBs-enhanced MRgFUS in comparison with the non-sonicated regions, with H&E staining providing evidence of hemorrhages in the sonicated brain tissue [33]. While this study provides promising results on FUS-mediated enhanced A $\beta$  (1-40) antibody delivery, further experiments in a larger mouse population are needed to confirm these early findings and optimize the therapeutic protocol for safe and efficient A $\beta$  (1-40) antibody delivery.

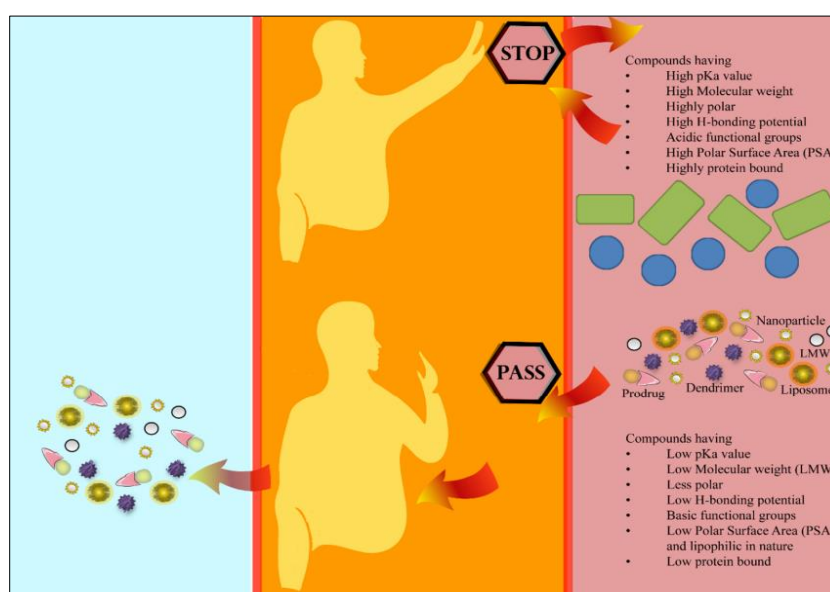


**Figure 1:** Physicochemical properties of compounds to cross the blood brain barrier.<sup>4</sup>

## MATERIALS AND METHODS

### Positioning Focused Ultrasound Device

A robotic system with a platform for stable position for the animal **and** a single element FUS transducer that reaches the mouse head with a top to bottom approach was built and tested (Figure 2). The device was manufactured on a polyjet 3D printing machine (Object30 pro, Stratasys, Minnesota, USA) with 1 degree of freedom (DOF).<sup>5</sup> It has the following components: single element spherically focused transducer (Piezo Hannas, Wuhan, Hubei, China) with  $f = 1$  MHz, radius of curvature = 80 mm, diameter = 50 mm, and efficiency = 32.5% and an amplifier with a build-in signal generator (AG series, T&G Power conversion Inc., Rochester, NY).<sup>5</sup> A laser pointer accessory was implemented into the system. This is a simple and ergonomic way to optimize the head position before the sonication process so that each mouse is sonicated at the exact same brain location. The mouse was placed on the positioning device and coupling gel was applied on the mouse head for improving ultrasonic coupling (Figure 2).

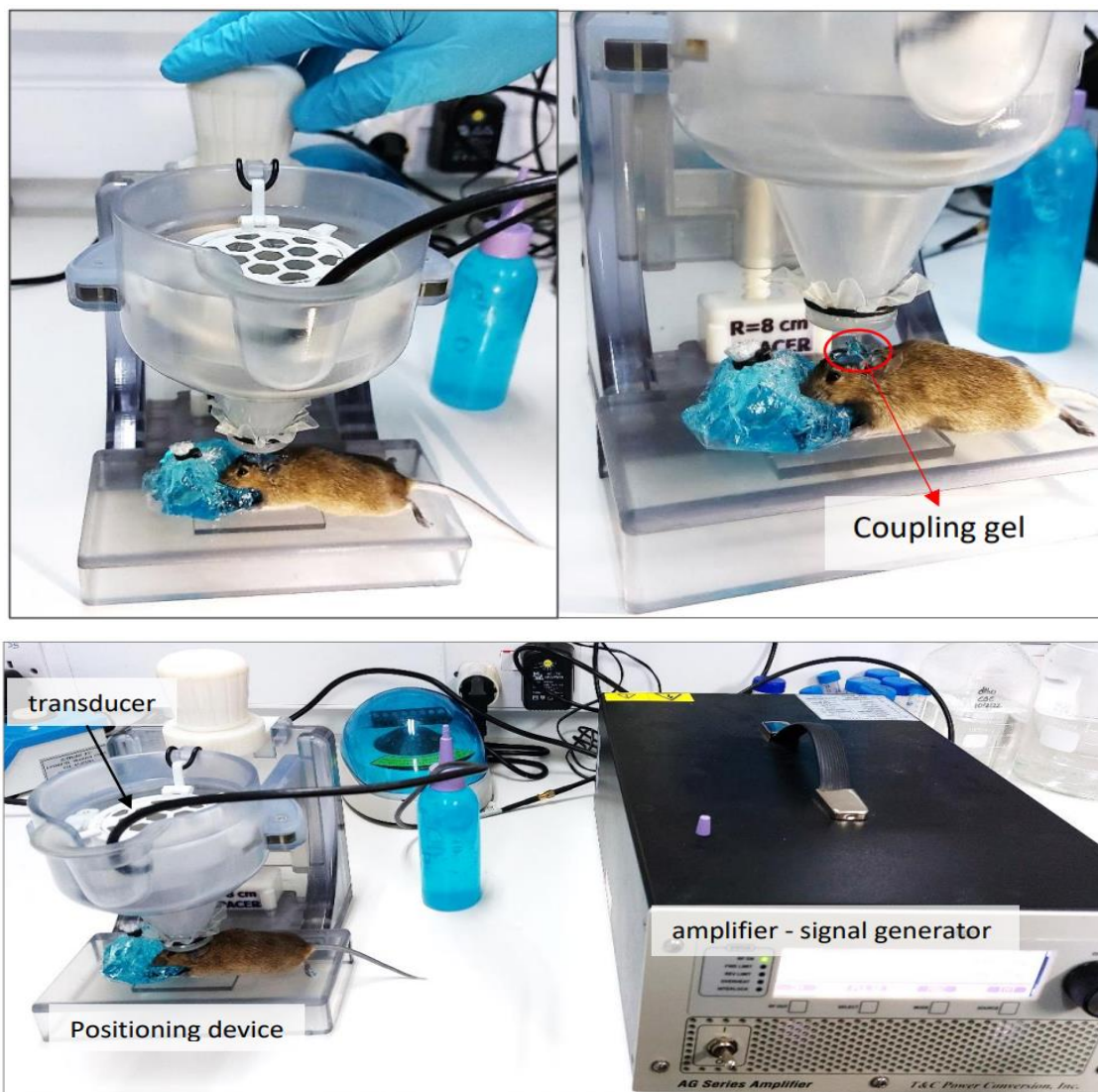


**Figure 2:** Experimental set-up for transcranial application of FUS for microbubble mediated BBB opening in mice.

## Experimental protocol No.1

### *Anaesthesia*

Mice were weighed and intraperitoneal injection of Avertin was used to cause rapid and deep anaesthesia to ensure no animal suffering. The dose of Avertin was weight-dependent for each animal (Figure 3a). Hair was removed from mouse head using hair removal cream (Veet Hair Removal Cream Body & Legs for Sensitive Skin™) (Figure 3b).

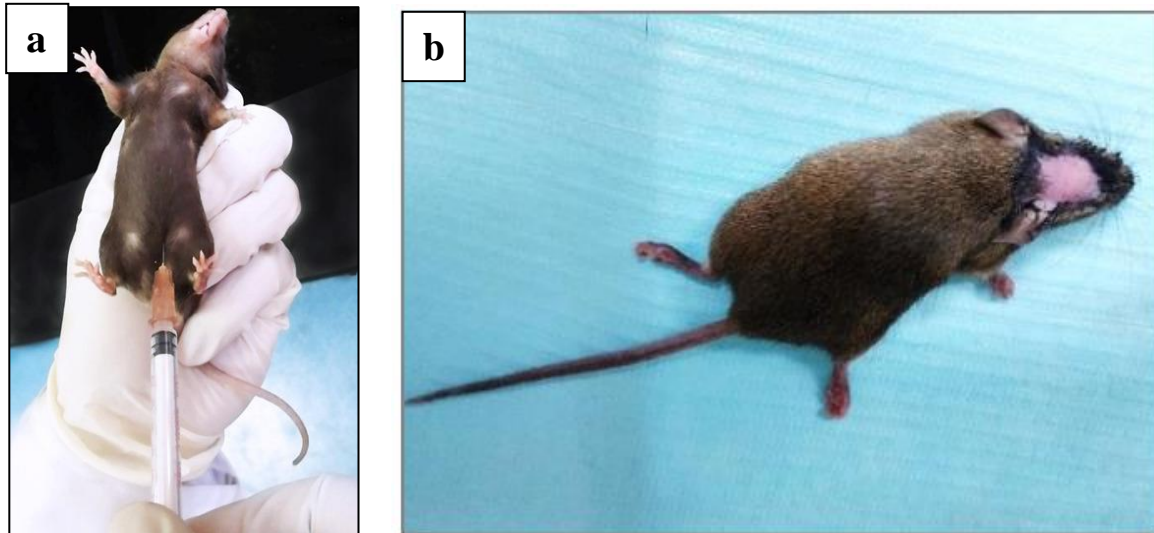


**Figure 3:** Intraperitoneal injection of Avertin (a) and hair removal for improving ultrasonic coupling (b).

### *Retro-orbital Injection*

Retro-orbital injection was used to deliver the EB or A $\beta$  (1-40) antibody and 5  $\mu$ L of MBs (Figure 4).

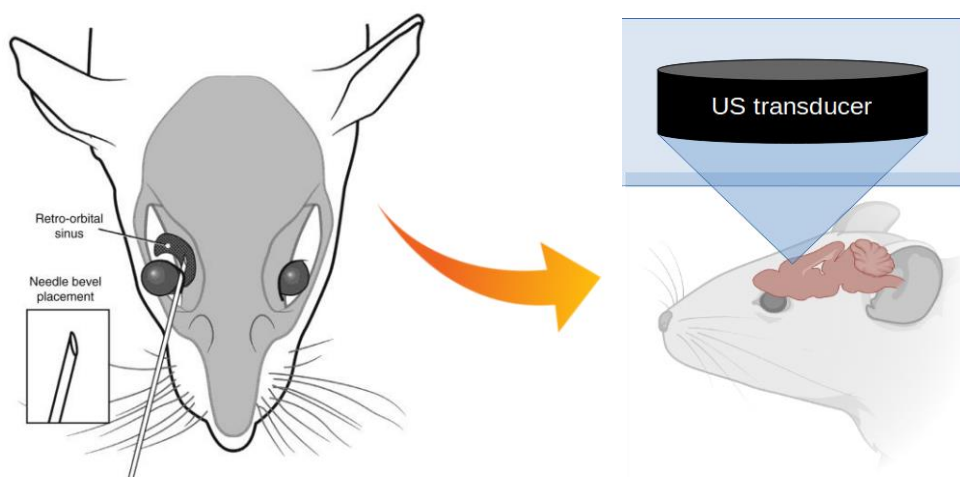


**Figure 4:** Retro-orbital injection of EB or A $\beta$  (1-40) antibody and MBs followed by transcranial application of FUS. Modified from Yardeni *et al.*, 2011.<sup>34</sup>

## Treatment protocol

A total of 34 mice were included in this experimental part (11 for protocol calibration and 23 for antibody study). The following sonication parameters were used: Pulsed FUS with  $F = 1.04$  MHz,  $P = 30, 40, 50$  or  $60$  W (based on the experiment),  $DF = 1\%$ , Pulse repetition period (PRP) = 1000 ms, Pulse duration (PD) = 10 ms, and sonication duration = 100 s. The mouse was left for 40 minutes (protocol calibration experiment with the wild type mice) or 4 hours (experiments with the  $A\beta$  1-40 antibody and 5XFAD mice), which is the time window that the BBB remains open after FUS sonication, before performing transcardiac perfusion. FUS sonication was performed within a 3-4 minutes time window following the injection of MBs (Bracco Imaging, Turin, Italy) and EB (Sigma, St. Louis, MO, USA).

In the following figures (Figures 5 & 6) the experimental parameters of each experiment that we performed are noted (e.g., sonication parameters, MBs volume, antibody volume). Wild type (WT) (B6/SJL) mice were used for protocol calibration for efficient BBBD using various electrical power values (30/40/50/60W) (Figure 5). 5XFAD mice were used to explore the feasibility of delivering  $A\beta$  (1-40) antibody to the brain using different amount of antibody (25, 50, 100  $\mu$ L) and also the difference between antibody alone versus antibody plus FUS (constant antibody amount) (Figure 6).

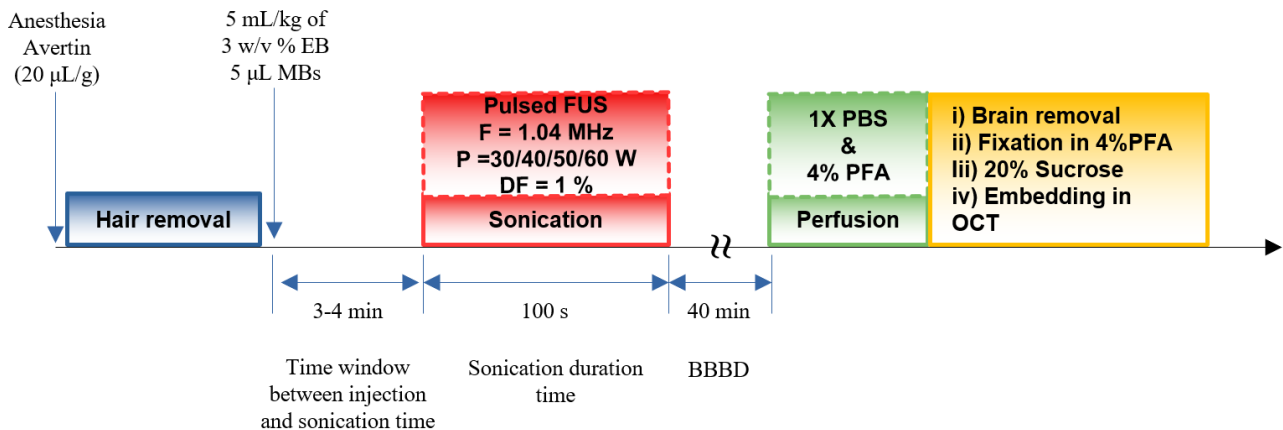


**Figure 5:** Timeline and experimental parameters of protocol calibration for efficient BBB disruption (BBBD) in WT mice (B6/SJL) exploring the effect of power (30/40/50/60W).

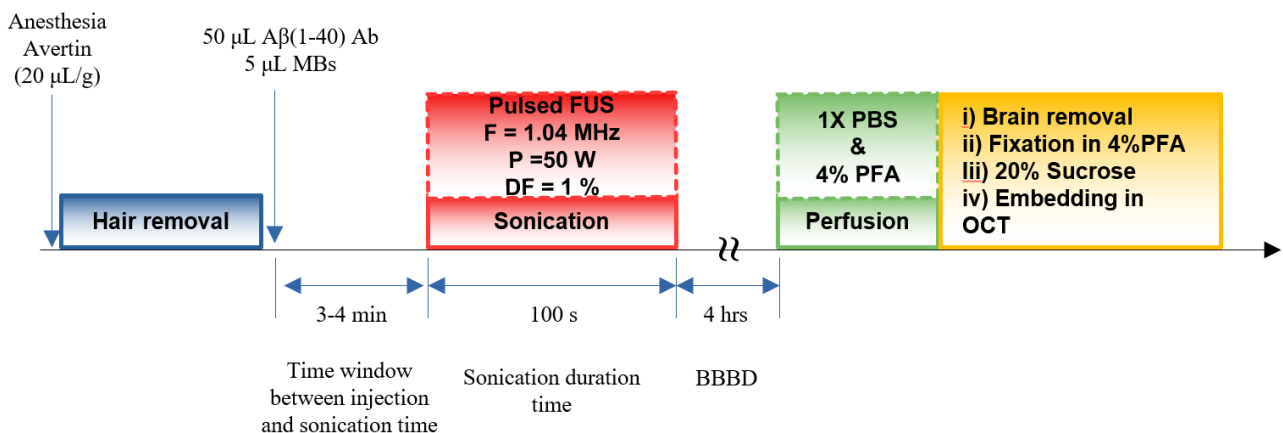


**Figure 6:** Timeline and experimental parameters used to explore the feasibility of delivering  $A\beta$  (1-40) antibody – the effect of antibody amount (a) and Antibody alone versus antibody plus FUS (constant antibody amount) in 5XFAD mice (b).

### ***Transcardiac perfusion***

Transcardiac perfusion was used to clear blood and preserve the brain for immunostaining analysis. Firstly, the skin on the chest was gripped using forceps and an incision was made using scissors in order to expose the xiphoid (arrowhead-shaped white bone) and then lateral incisions were made beneath the ribcage using scissors to expose the diaphragm and liver. Incisions in the diaphragm along the entire length of the rib cage and two cuts through the two sides of the rib cage up to the collarbone and then the sternum is reflected up towards the head of the mouse in order to fully expose the heart and the liver (Figure 7).

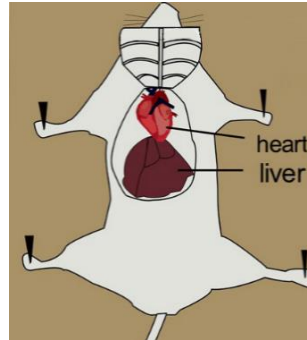


**Figure 7:** Thoracotomy was essential for the transcardiac perfusion. Adapted from Wu *et al.*, 2021.<sup>35</sup>

The heart was secured at a steady position and the needle was inserted into the left ventricle at an angle parallel to the midline of the heart (Figure 8A-C). A small incision was made on the right atrium using scissors and saline perfusion was performed by manually pushing the syringe (Figure 8D). As the procedure progresses, the liver turns white from red (Figure 8E-F). This is an indication that the perfusion was successful. Saline was switched with 4% of Paraformaldehyde (PFA) and ~15-20 ml 4% PFA was infused into circulation of adult mice. Body twitching, tail flicking and head moving will be observed and then the whole mouse body becomes stiff. 4% Paraformaldehyde (PFA) was used to cross-link protein and DNA and preserve the tissue and cell structures.

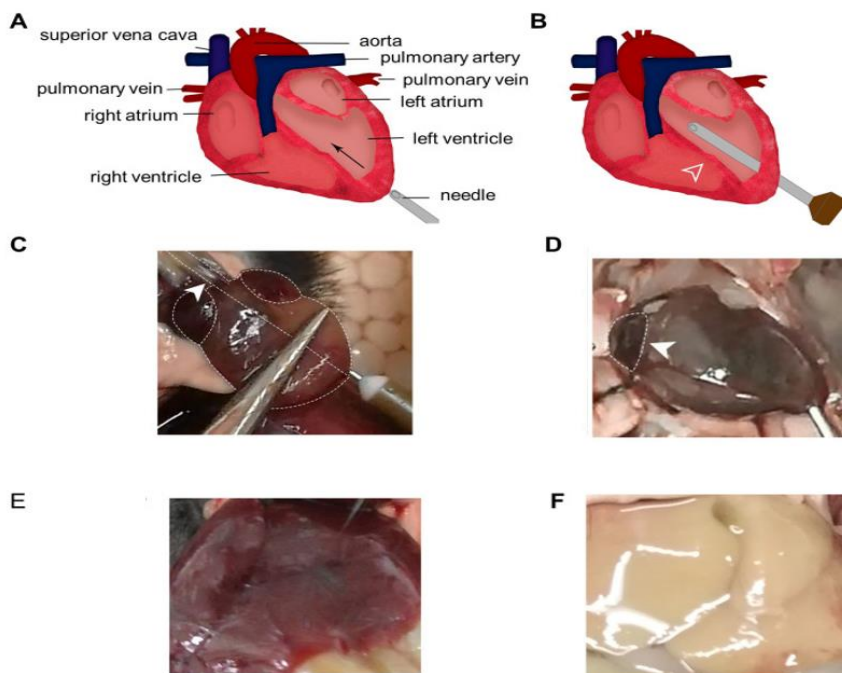


**Figure 8:** Transcardiac perfusion. Heart diagram and needle position (A). Needle was inserted into the left ventricle of the heart (B). The needle goes into the aorta (C). A small incision was made on the right atrium (D). The liver contains blood and appears red before the perfusion (E). Decolorization of the liver tissue after successful perfusion (F). Adapted from Wu *et al.*, 2021.<sup>35</sup>

### ***Brain dissection***

The mouse head was removed from the body using scissors and the skin was removed by performing an incision along the midline from the neck to the nose. The two flaps of skin were removed and exposed the skull. The bones were trimmed off using dissecting scissors and any traces of residual muscles on the skull were removed. The skull is carefully removed using scissors and forceps, exposing the brain. The brain is then removed, washed in PBS, placed for 2 hours in 4% PFA. It is then removed from PFA, washed with PBS, placed into 20% sucrose solution (diluted in Phosphate Buffer 0.1M) overnight at 4 °C and wait until it sinks to the bottom of the container. Sucrose solution is important for the cryoprotection of fixed tissue prior to embedding and freezing.

### ***Tissue embedding***

Acetone-Dry ice bath was prepared, and OCT was used to fill the cryomould that contained the brain tissues. A pair of forceps was used to place the cryomould into the acetone-dry ice bath. The OCT was frozen in 5 minutes. The frozen OCT containing the brain tissue was removed from the acetone-dry ice bath, then removed from the cryomould and stored in the -80°C freezer.

### ***Immunohistochemistry***

The tissue was permeabilized by immersing the frozen sections in acetone for 10 minutes at -20°C. It was washed three times with 1X PBS (Phosphate Buffer Saline) and blocking solution (5% Bovine Serum Albumin + 0.5% Triton X-100) was applied for 1 hour on the sections at room temperature in a humidified chamber. The blocking solution was then removed and the primary antibody, anti- $\beta$ -amyloid primary monoclonal 6E10, (diluted in blocking solution) was applied to the tissue sections and incubated overnight at 4°C. The following day, the primary antibody was removed, and the tissue sections were washed three times with 1X PBS and then secondary antibodies, Fluorescein (FITC) goat anti-mouse, 1:100 and Alexa Fluor<sup>®</sup> 594 goat anti-rabbit, 1:500 (diluted in blocking solution) were applied for 1 hour at room temperature, followed by three washes with 1X PBS and incubation for 30 seconds with 4',6-diamidino-2-phenylindole (DAPI, Sigma-Aldrich), a nuclear staining. The tissues were washed two times for 5 minutes with 1X PBS, dried and mounted with mounting media in order to prepare them for microscopy.

## **Experimental protocol No.2**

### ***Anaesthesia***

Before the experiments, the hair was removed from the mice head using hair removal cream (Veet Hair Removal Cream Body & Legs for Sensitive Skin<sup>™</sup>). Mice were initially anesthetized using isoflurane and placed on the device platform for sonication. The experiments were carried out under continuous administration of anaesthesia (Figure 9).

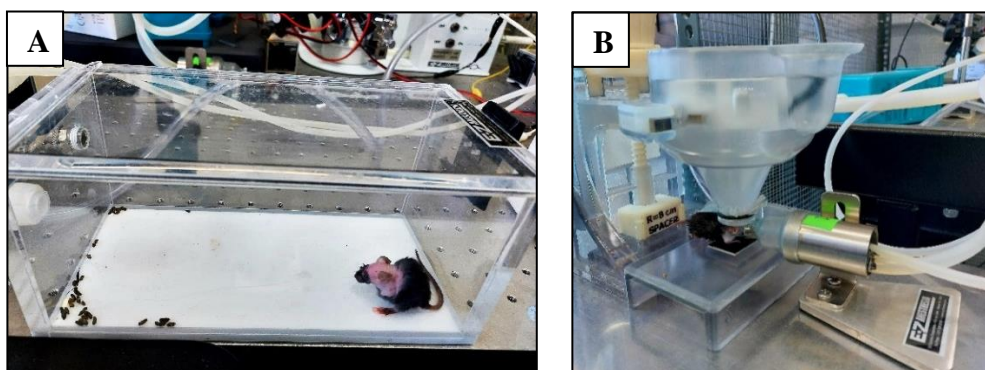


**Figure 9:** Mice anesthetized using isoflurane (A) and experiments performed under continuous isoflurane administration (B).

### ***Intravenous injection***

Tail vein injection was used to deliver the EB, MBs, and AAV9 vector to the mice (Figure 10).



**Figure 10:** Intravenous administration of EB/MBs/vector.

### ***Treatment protocol***

A total of 29 mice were included in this part (21 for protocol testing and calibration and 8 for the AAV9 vector study). Note that in the first experiment of this part the mice were anesthetized with Avertin while following treatment were again anaesthetized intraperitoneally with Avertin and transcardially perfused with saline followed by fresh 4% paraformaldehyde (PFA) using a similar procedure as described above. However, this approach was abandoned in the following experiments, where isoflurane anesthesia was used, and perfusion was not performed. The relevant timeline and parameters used for protocol calibration can be seen in Figure 11, whereas the sonication protocol used for AAV9 vector delivery is shown in Figure 12. Protocol calibration was done in WT mice while experiments with the AAV9 vector were carried out in P30 WT mice.

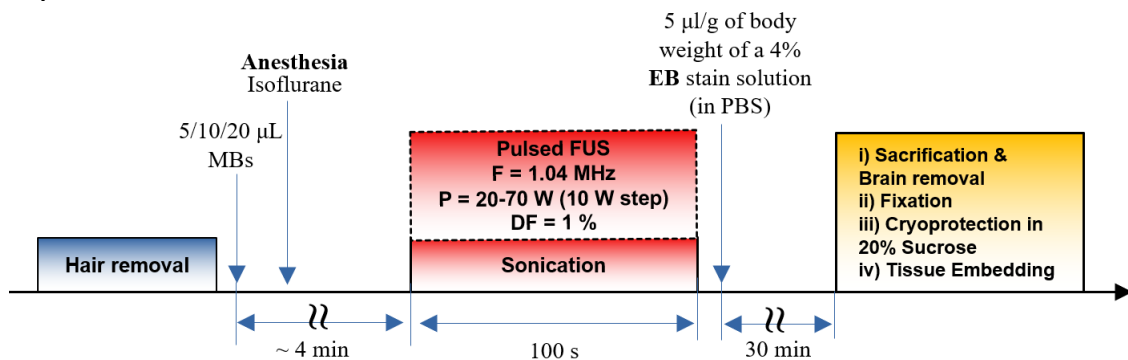


**Figure 11:** Timeline and experimental parameters of protocol calibration for efficient BBB in WT mice.

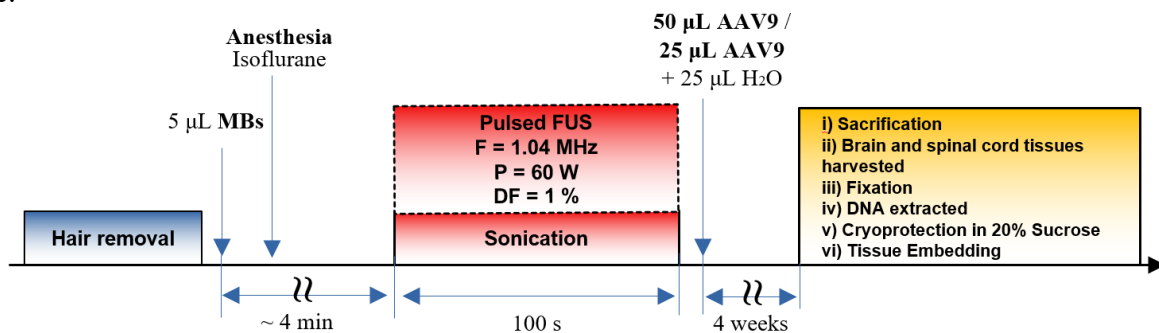


**Figure 12:** Timeline and experimental parameters used for AAV9 vector delivery through the FUS mediated opened BBB in P30 WT mice.

### ***Brain dissection & Immunohistochemistry***

Thirty (30) minutes following EB injection the mice were anaesthetized intraperitoneally with Avertin and sacrificed (Figure 11). Brain and spinal cord tissues were harvested and fixed overnight at 4 C°, then cryoprotected in 20% sucrose in 0.1 M phosphate buffer. Longitudinal brain sections were obtained (15mm). Slides containing brain sections were directly visualized using a fluorescence microscope to assess the EB leakage. Brain sections were also processed for immunostaining with Fibrinogen and Fibronectin antibodies. These antibodies determine the tissue integrity. Specifically, cryosections from brain were immunostained for fibronectin (DAKO, Glostrup, Denmark, 1:100) and FITC-labeled polyclonal fibrinogen antibody (DAKO, 1:500) to assess serum protein leakage into the brain parenchyma. Different brain areas were examined.

In the experiments involving the AAV9 vector, mice were sacrificed 4 weeks following FUS and vector administration (Figure 12). Cryosections from brain were immunostained for EGFP (Invitrogen, 1:1000) and DNA was extracted from brain, cerebellum, brainstem, and spinal cord for VGCNs determination.

## **RESULTS**

### **Protocol calibration for efficient BBB disruption**

#### ***Experimental protocol No.1***

Experiments were performed in order to evaluate the feasibility of FUS plus MBs-mediated BBB disruption in mice (WT B6/SJL) using a single element spherically focused transducer as integrated with the manual positioning device and examine how the ultrasound protocol influences BBB opening.

Mice (WT B6/SJL) were injected with EB (5 mL/kg) and 5  $\mu$ L MBs followed by FUS using the following sonication parameters: Pulsed FUS --> F = 1.04 MHz, P = 30/40/50/60 W, DF = 1%, PRP = 1000 ms, PD = 10 ms (Figure 13-18). Mouse 1 was injected with EB and 5  $\mu$ L of MBs and treated with an electrical power value of 30 Watt (Figure 14).

Mice (WT B6/SJL) were injected with EB, which was used to assess the permeability of the BBB to macromolecules. It binds albumin when entering the bloodstream, but albumin cannot pass the BBB, therefore the neural tissue remains unstained. In case the BBB has been compromised, albumin-bound EB enters the brain. Fluorescence of EB and protein complexes is observed at a wavelength of 680 nm for the excitation wavelength of 620 nm.

There was leakage of EB in the brain. It was visible in the naked eye but did not cover a large brain area. In mouse 2 (40 Watt), EB was diffused in the whole left cerebrum (Figure 15), whereas in mouse 3 (50 Watt) the diffusion was not very large and does not go very deep in the cerebrum (Figure 16). In mouse 4 (60 Watt), the diffusion is very large, and it goes deep through the entire half brain (Figure 17). Similar observations were seen in mouse 5 which it was sonicated with the same electrical power value (60 Watt) as the mouse 4, the diffusion is very large, and it goes deep through the entire half brain (Figure 18). In addition, a mouse injected with EB but without any MBs or FUS was used as a control. It did not show any EB leakage in the brain parenchyma (Figure 19). On the other hand, mouse injected with EB and followed by FUS in the absence of MBs was characterized by EB leakage in the brain parenchyma (Figure 20).

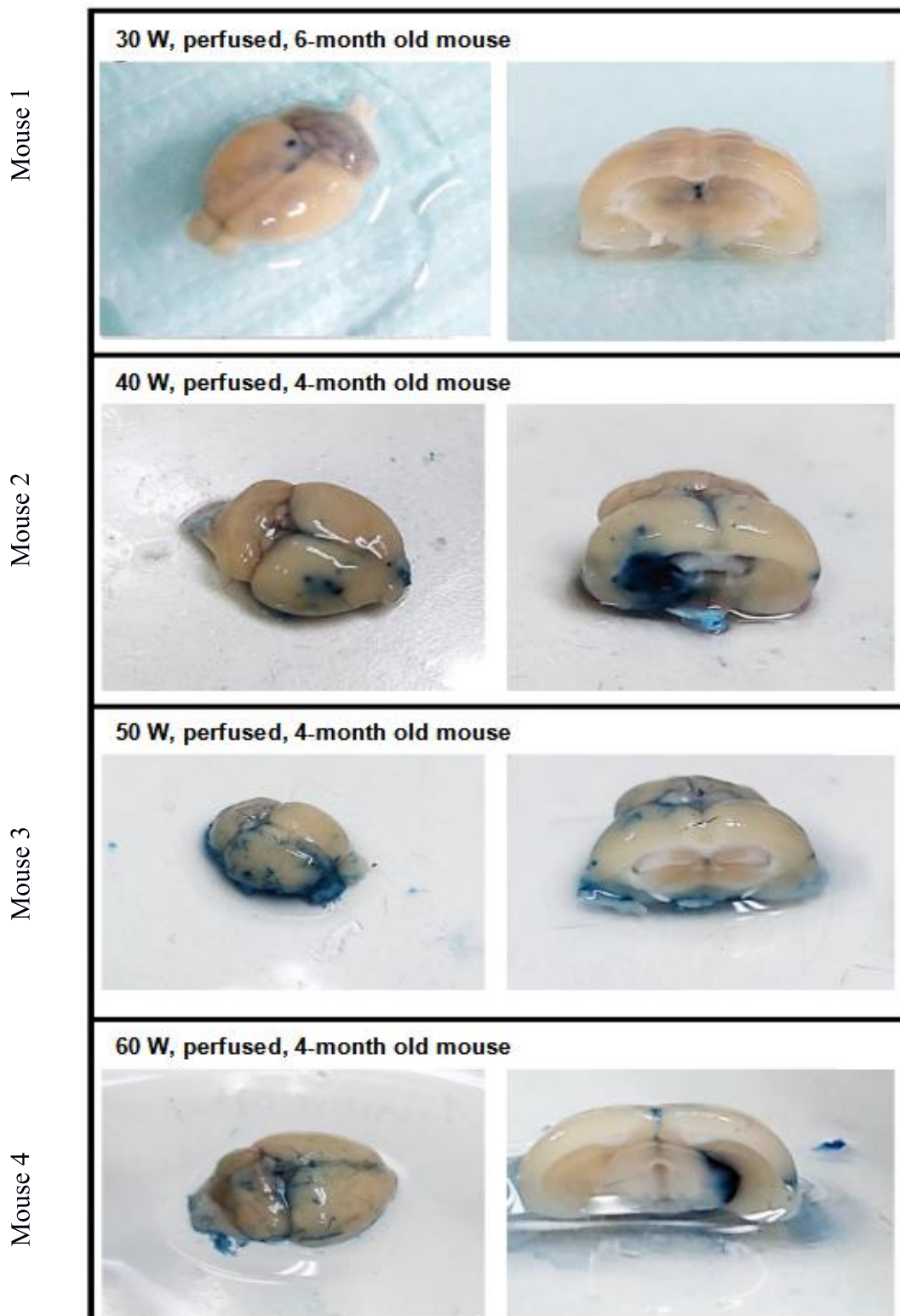


**Figure 13:** Freshly perfused mouse brains after the injection with EB, 5  $\mu$ L of MBs and different electric power values (30-60W) but the same sonication parameters for each mouse.

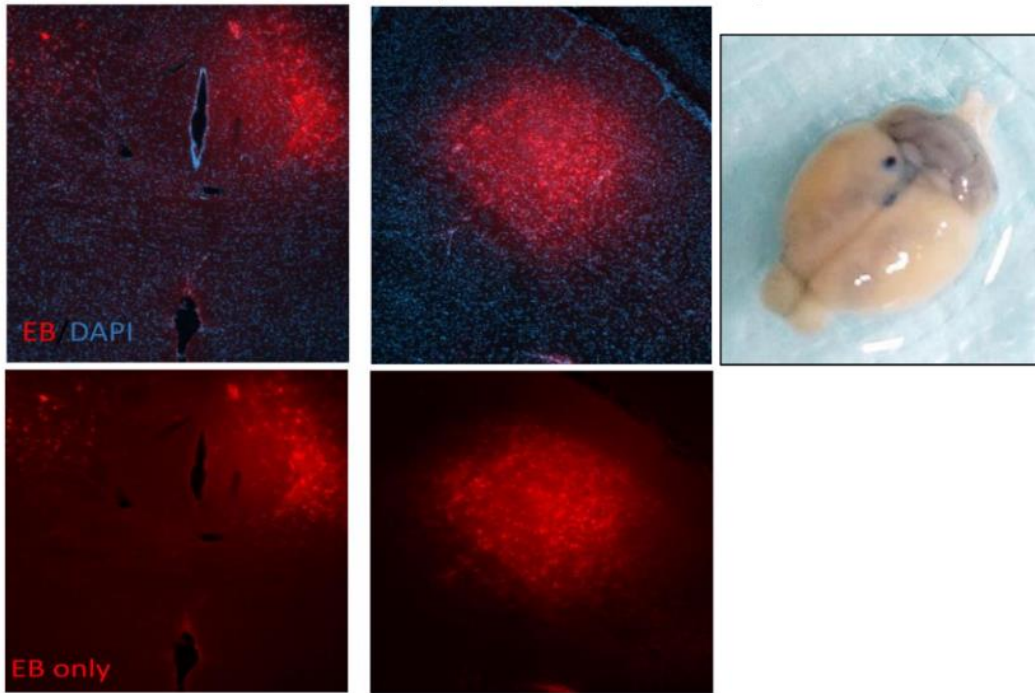


**Figure 14:** Fluorescence images of unstained brain sections taken from a perfused mouse (Mouse 1) that was injected with EB, 5  $\mu$ L of MBs followed by FUS with electrical power value 30W.

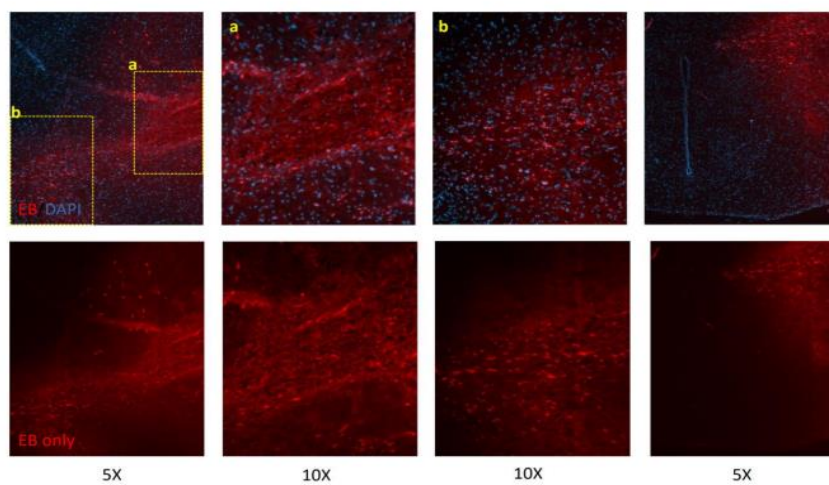
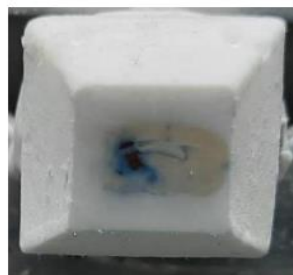


**Figure 15:** Fluorescence images of unstained brain sections taken from a perfused mouse (Mouse 2) that was injected with EB, 5  $\mu$ L of MBs followed by FUS with electrical power value 40W.

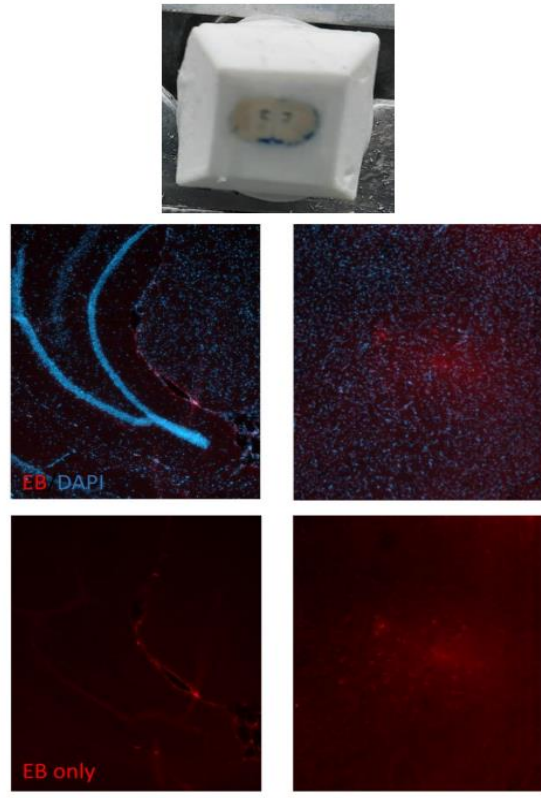


**Figure 16:** Fluorescence images of unstained brain sections taken from a perfused mouse (Mouse 3) that was injected with EB, 5  $\mu$ L of MBs followed by FUS with electrical power value 50W.

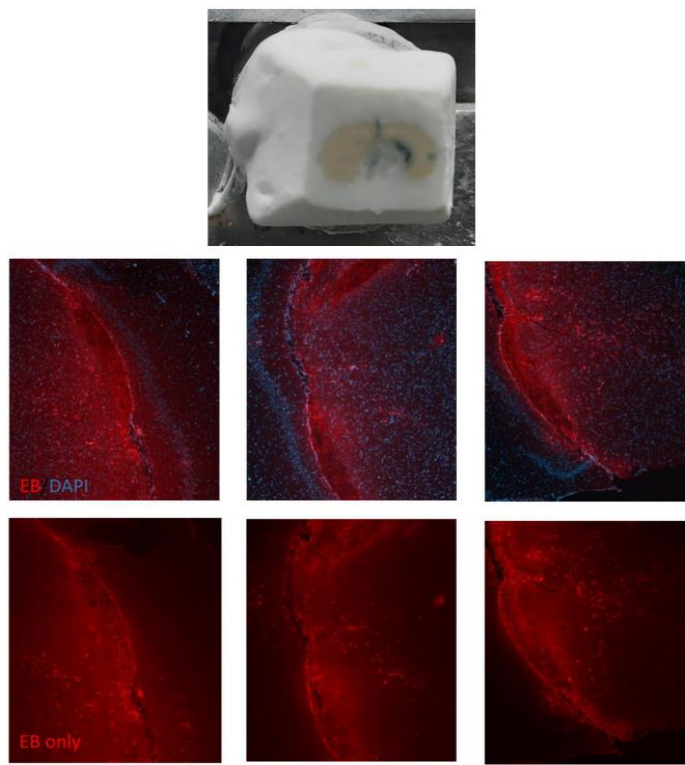


**Figure 17:** Fluorescence images of unstained brain sections taken from a perfused mouse (Mouse 4) that was injected with EB, 5  $\mu$ L of MBs followed by FUS with electrical power value 60W.

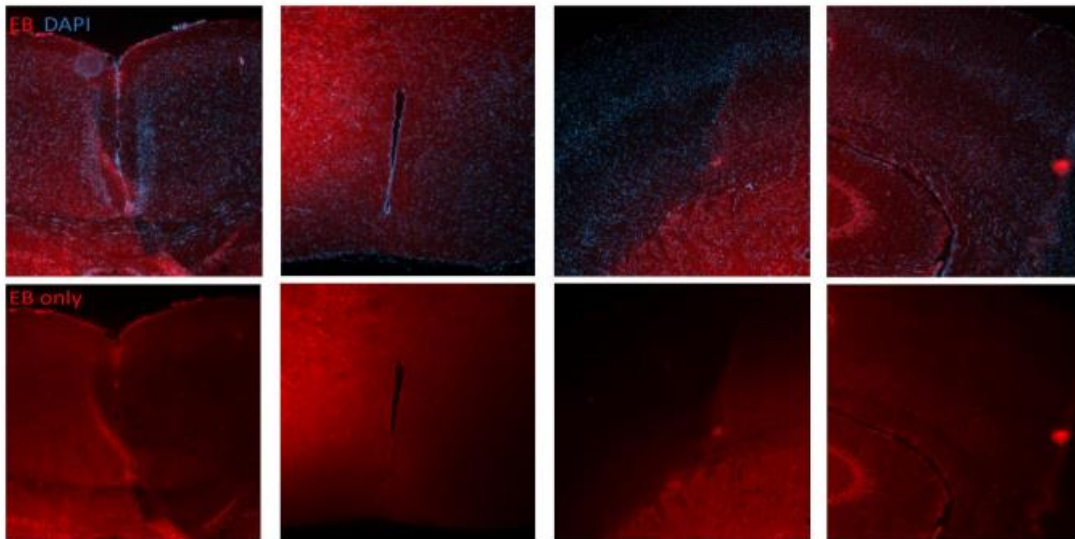
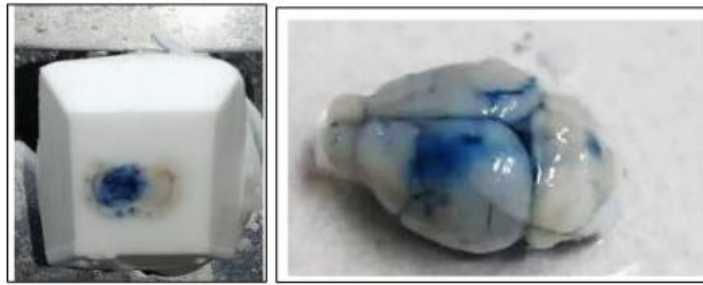


**Figure 18:** Fluorescence images of unstained brain sections taken from a perfused mouse (Mouse 5) that was injected with EB, 5  $\mu$ L of MBs followed by FUS with electrical power value 60W.

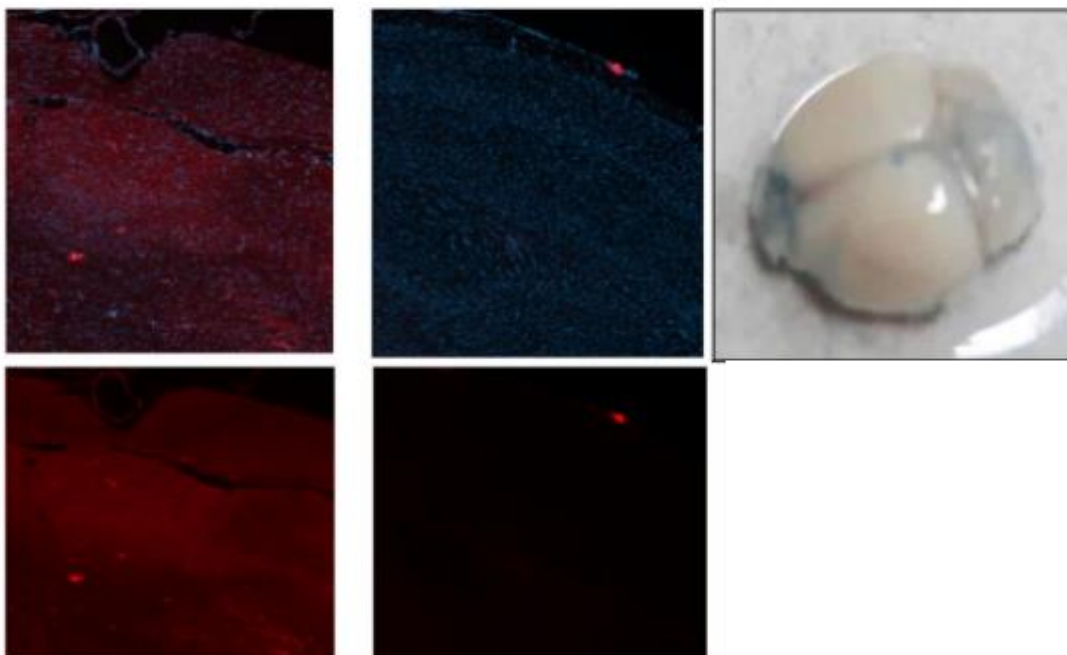


**Figure 19:** Fluorescence images of unstained brain sections taken from a mouse that was only injected with EB.

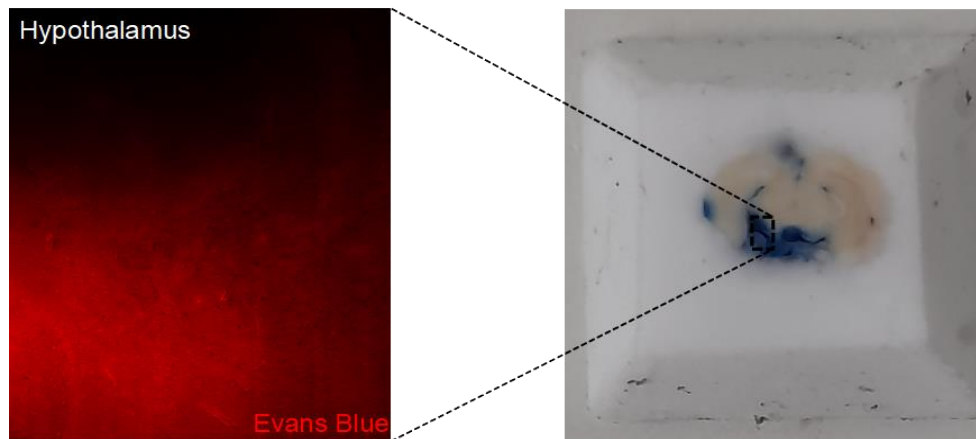


**Figure 20:** Brain of a WT mouse injected with EB followed by transcranial application of FUS with an electrical power value 50W in the absence of MBs. Fluorescence image of brain section showed EB leakage in the brain parenchyma.

### *Experimental protocol No.2*

Three 1 month-old WT mice were tested for the first test (+ 2 control mice). An electric power of 10 W was used. The first mouse was injected with 85  $\mu$ L EB and after 5 minutes with 10  $\mu$ L MBs diluted with saline. Afterwards, at 15 s, the mouse was anesthetized with Avertin intraperitoneally for rapid and deep anesthesia to ensure no animal suffering. The dose of Avertin was weight-dependent for each animal. The mouse was sonicated at the brain for 60 seconds. The 2<sup>nd</sup> mouse was injected with 20  $\mu$ L MBs and after 5 minutes we did anesthesia with Avertin and sonication at the brain for 60 second. The intravenous injection with EB was done after 2,5 hours post-sonication. The test in the 3<sup>rd</sup> mouse was the same as with the 2<sup>nd</sup> with the only difference that the mouse was injected with 10  $\mu$ L MBs.

Thirty (30) minutes after the EB injection the mice were anaesthetized intraperitoneally with Avertin and then transcardially perfused with saline followed by fresh 4% paraformaldehyde (PFA). Brain and spinal cord tissues were harvested and further fixed overnight at 4 C<sup>o</sup>, and then cryoprotected. Longitudinal brain sections were obtained (15 mm) and processed for immunostaining with Fibrinogen and Fibronectin antibodies. We have examined 4 areas from brain tissues: Corpus Callosum, Internal Capsule, Cerebellum and Pons. Two (2) WT mice were used for control. One (1) mouse was injected with EB only and 1 mouse was non-injected.

Representative photos of Fibrinogen and Fibronectin immunofluorescence staining in the corpus callosum, internal capsule, cerebellum and pons show that in controls (M1 and M5) low levels of fibrinogen and fibronectin are evident. The 2<sup>nd</sup> mouse (M2) shows low levels too, because the MBs injection was not done correctly due to the fact that the vein turned blue from EB, which had been injected first. In mouse 3 and mouse 4 (M3 and M4) higher level of fibrinogen and fibronectin were detected in all the brain areas we examined (Figures 21-28). Nevertheless, we are not sure that the FUS worked based on the pictures provided. We believe that the experiment should definitely be repeated with optimal setting including anesthesia (isoflurane) and FUS parameters/equipment.

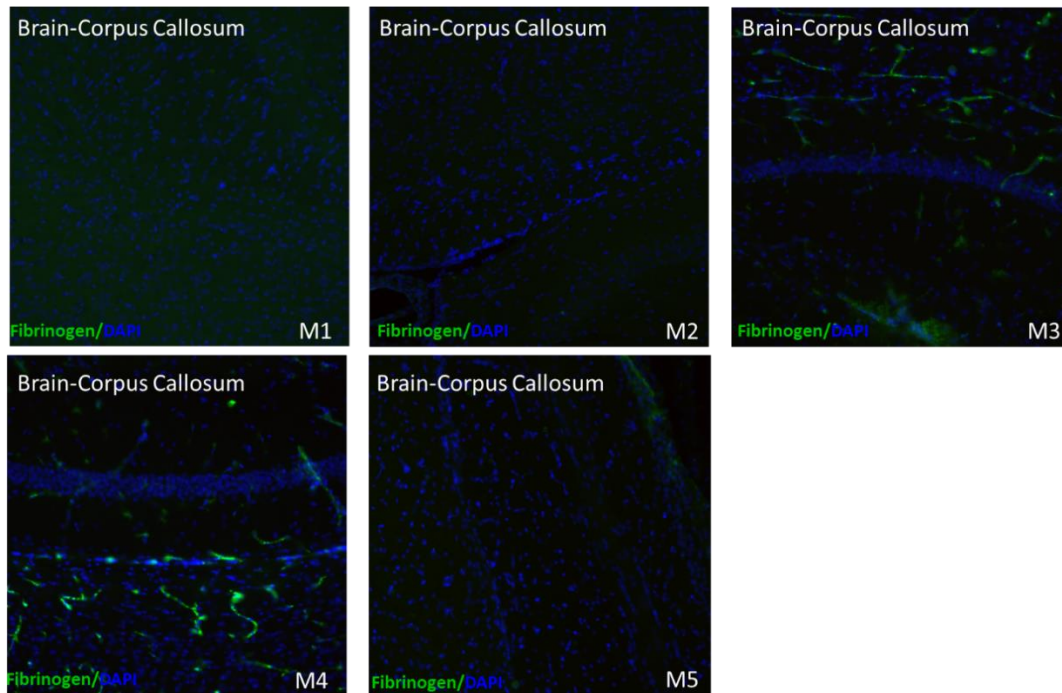


**Figure 21:** Representative photos (10x) from all the tested mice of Fibrinogen immunofluorescence staining in Corpus Callosum. M1: WT mouse injected with EB only, M2: WT mouse injected first with EB and MBs diluted with saline after 5 min. M3: WT mouse injected first with MBs and EB after 2,5 hours. M4: WT mouse injected first with MBs and EB after 2,5 hours. M5: WT mouse non-injected.

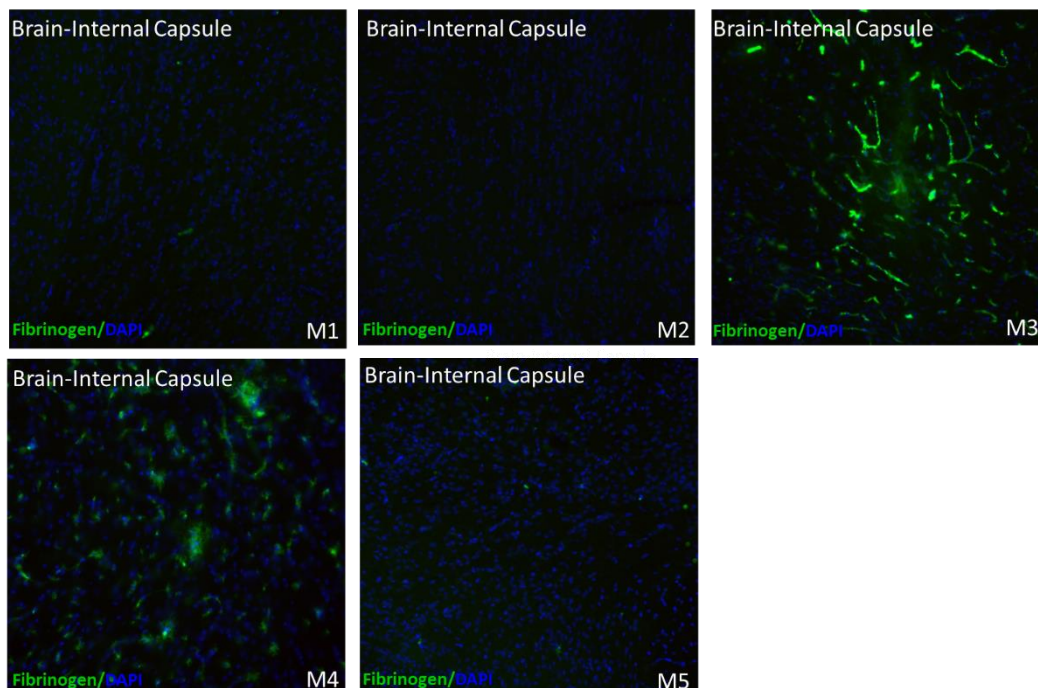


**Figure 22:** Representative photos (10x) from all the tested mice of Fibrinogen immunofluorescence staining in internal capsule. M1: WT mouse injected with EB only, M2: WT mouse injected first with EB and MBs diluted with saline after 5 min. M3: WT mouse injected first with MBs and EB after 2,5 hours. M4: WT mouse injected first with MBs and EB after 2,5 hours. M5: WT mouse non-injected.

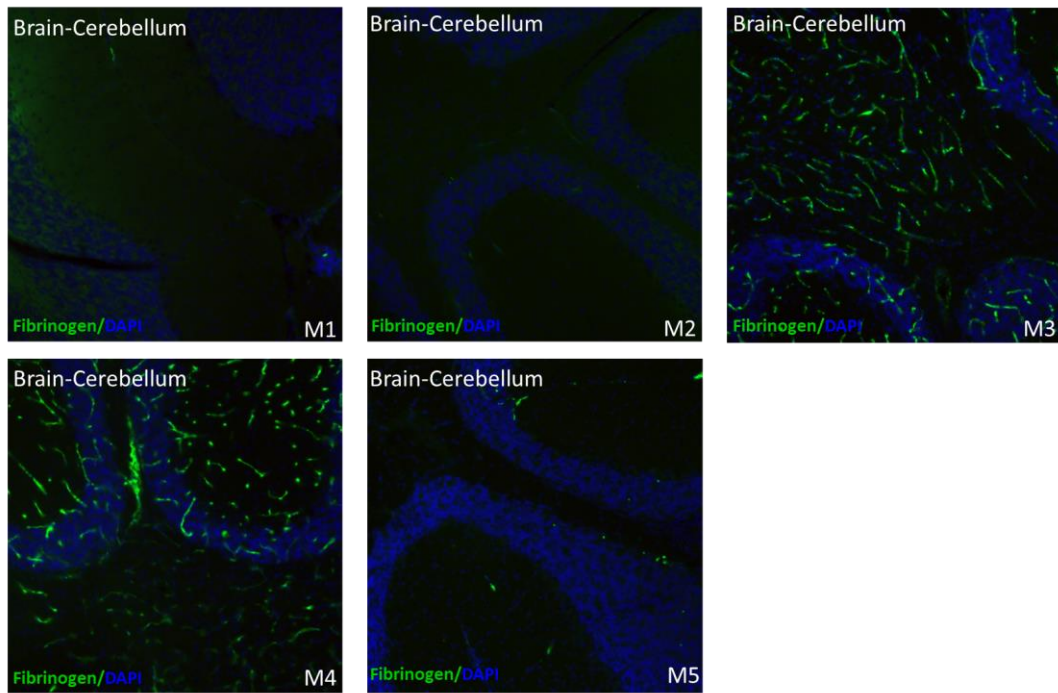


**Figure 23:** Representative photos (10x) from all the tested mice of Fibrinogen immunofluorescence staining in cerebellum. M1: WT mouse injected with EB only, M2: WT mouse injected first with EB and MBs diluted with saline after 5 min. M3: WT mouse injected first with MBs and EB after 2,5 hours. M4: WT mouse injected first with MBs and EB after 2,5 hours. M5: WT mouse non-injected.

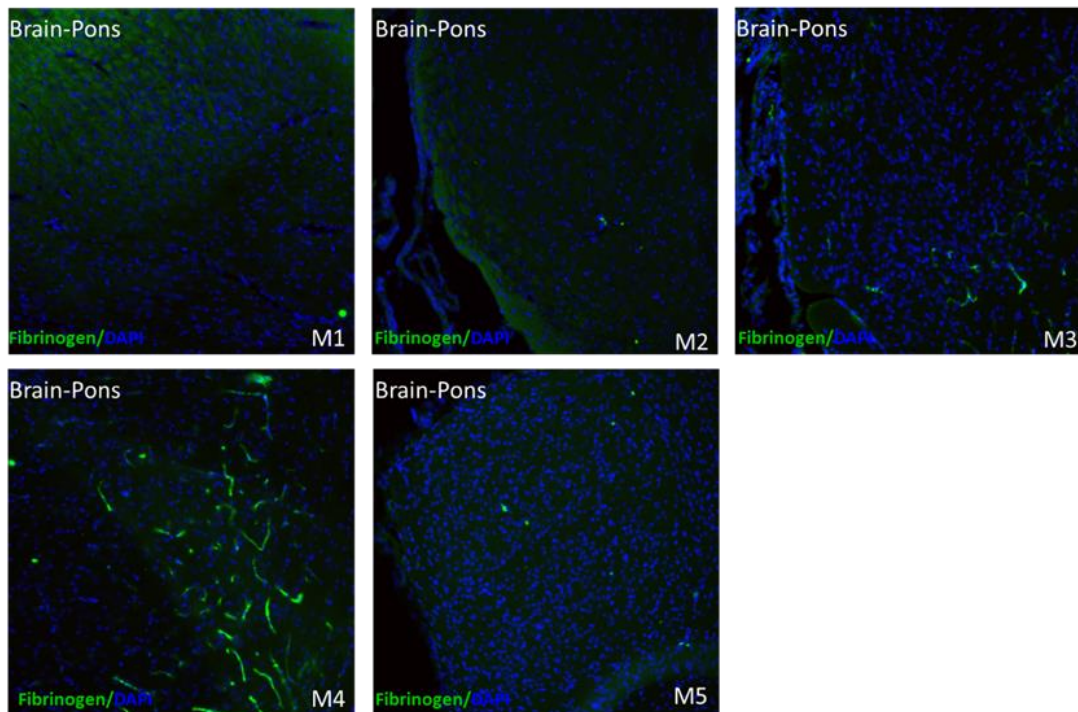


**Figure 24:** Representative photos (10x) from all the tested mice of Fibrinogen immunofluorescence staining in pons. M1: WT mouse injected with EB only, M2: WT mouse injected first with EB and MBs diluted with saline after 5 min. M3: WT mouse injected first with MBs and EB after 2,5 hours. M4: WT mouse injected first with MBs and EB after 2,5 hours. M5: WT mouse non-injected.

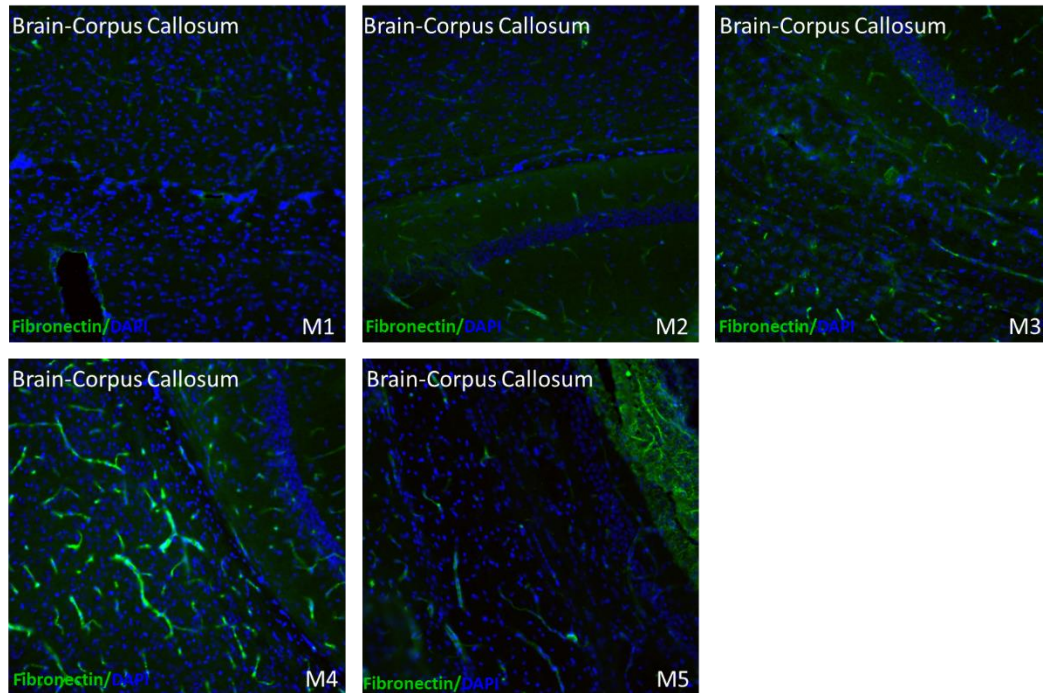


**Figure 25:** Representative photos (10x) from all the tested mice of Fibronectin immunofluorescence staining in corpus callosum. M1: WT mouse injected with EB only, M2: WT mouse injected first with EB and MBs diluted with saline after 5 min. M3: WT mouse injected first with MBs and EB after 2,5 hours. M4: WT mouse injected first with MBs and EB after 2,5 hours. M5: WT mouse non-injected.

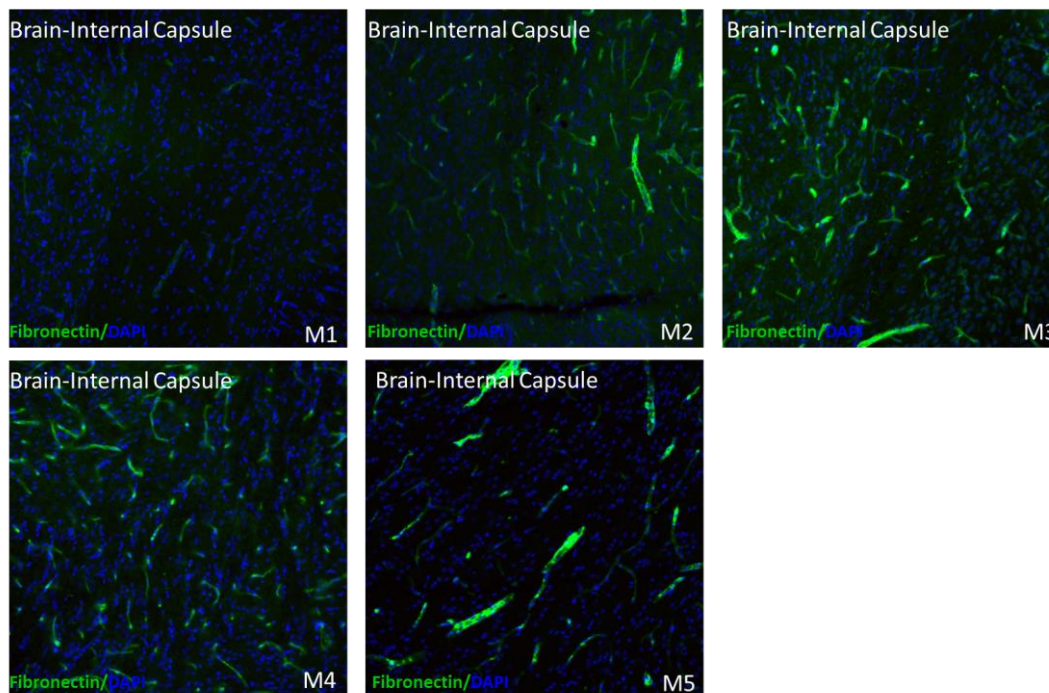


**Figure 26:** Representative photos (10x) from all the tested mice of Fibronectin immunofluorescence staining in internal capsule. M1: WT mouse injected with EB only, M2: WT mouse injected first with EB and MBs diluted with saline after 5 min. M3: WT mouse injected first with MBs and EB after 2,5 hours. M4: WT mouse injected first with MBs and EB after 2,5 hours. M5: WT mouse non-injected.

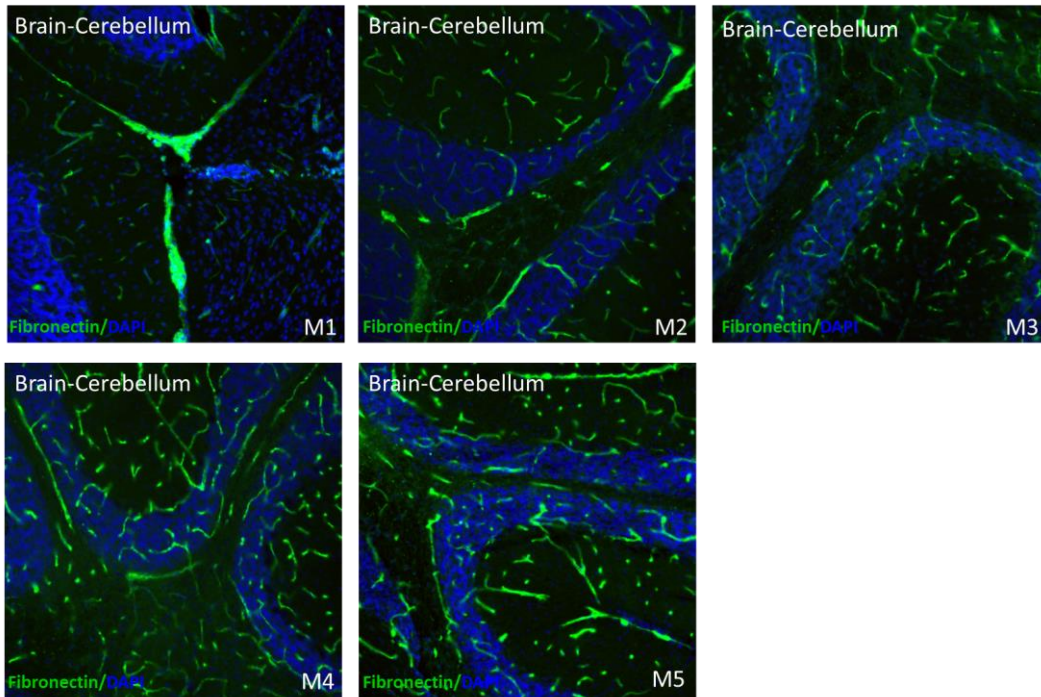


**Figure 27:** Representative photos (10x) from all the tested mice of Fibronectin immunofluorescence staining in cerebellum. M1: WT mouse injected with EB only, M2: WT mouse injected first with EB and MBs diluted with saline after 5 min. M3: WT mouse injected first with MBs and EB after 2,5 hours. M4: WT mouse injected first with MBs and EB after 2,5 hours. M5: WT mouse non-injected.

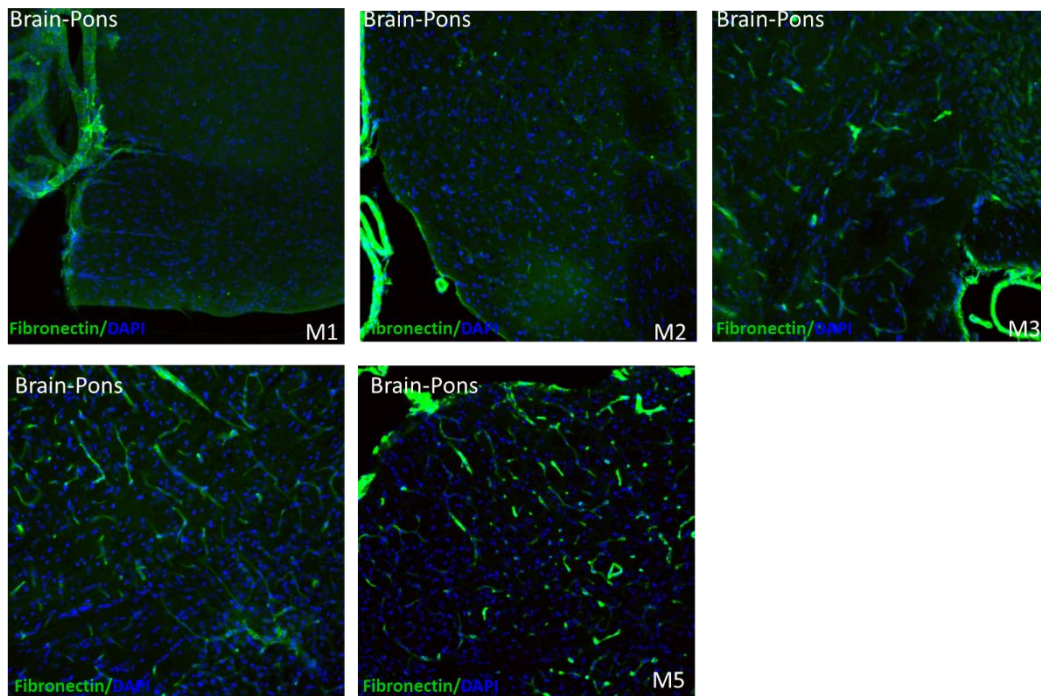


**Figure 28:** Representative photos (10x) from all the tested mice of Fibronectin immunofluorescence staining in pons. M1: WT mouse injected with EB only, M2: WT mouse injected first with EB and MBs diluted with saline after 5 min. M3: WT mouse injected first with MBs and EB after 2,5 hours. M4: WT mouse injected first with MBs and EB after 2,5 hours. M5: WT mouse non-injected.

In the next experiment, we tested 5 WT mice of 1 month-old (+ 2 mice for control). Initially, the first mouse was injected with 20  $\mu$ L MBs. The mouse was then anesthetized with isoflurane for 2 min for rapid anesthesia to ensure no animal suffering. Then, the mouse was sonicated for 60 s (Electric power: 20 W, MGC: 7.8%). After the sonication, the mouse was injected intravenously with EB. The 2<sup>nd</sup> mouse was injected with 20  $\mu$ L MBs. Similarly, the mouse was anesthetized and sonicated for 60 s (Electric power: 30 W, MGC: 9%). The difference in the 3<sup>rd</sup> mouse was the amount of MBs of 10  $\mu$ L and the power of 20 W, MGC: 7.8%. In the 4<sup>th</sup> mouse, the injected amount of MBs was 10  $\mu$ L and the electric power was 30 W, MGC: 7.8%. The 5<sup>th</sup> mouse was injected with 20  $\mu$ L MBs and the electric power was 30W, MGC: 9%.

Thirty (30) minutes after the EB injection the mice were anaesthetized intraperitoneally with Avertin and sacrificed. Slides containing brain sections were directly visualized using a fluorescence microscope. Cryosections from brain were immunostained for fibronectin and FITC-labeled polyclonal fibrinogen antibody to assess serum protein leakage into the parenchyma. Two (2) WT mice were used for control. One (1) mouse was injected with EB only and 1 mouse was non-injected.

Representative photos of EB in many brain areas (Figures 29-33) show EB leakage into the brain parenchyma indicating BBB disruption. We observe that the M3 mouse shows high levels of EB in many brain areas than the other mice. Fibrinogen and Fibronectin immunofluorescence staining in corpus callosum, internal capsule and cerebellum (Figures 34-39) show low levels of fibrinogen and fibronectin in controls (M6 and M7). All the tested mice show higher level of Fibrinogen and Fibronectin in all brain areas we examined than the control mice. According to the EB staining, the protocol used in M3 mouse (10  $\mu$ L MBs and electric power of 20 W (MGC: 7.8 %)) is maybe the best. Nevertheless, we have repeated these conditions to be sure for actual experiment.

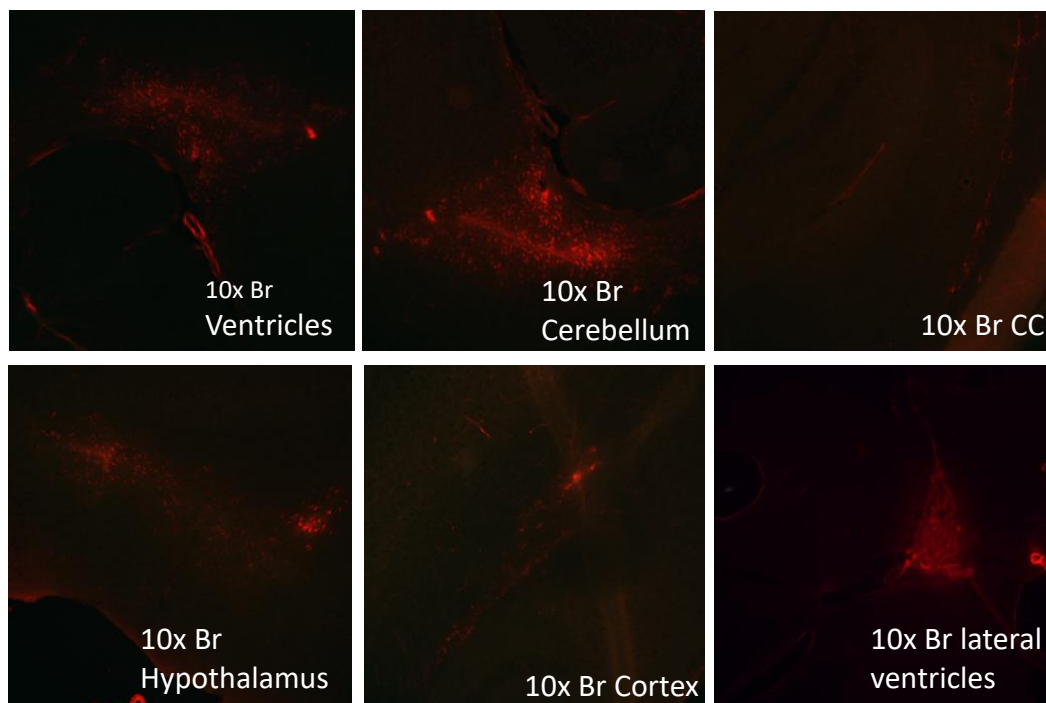


**Figure 29:** Representative photos (10x) of EB from the 1<sup>st</sup> and 2<sup>nd</sup> mouse in many brain areas.

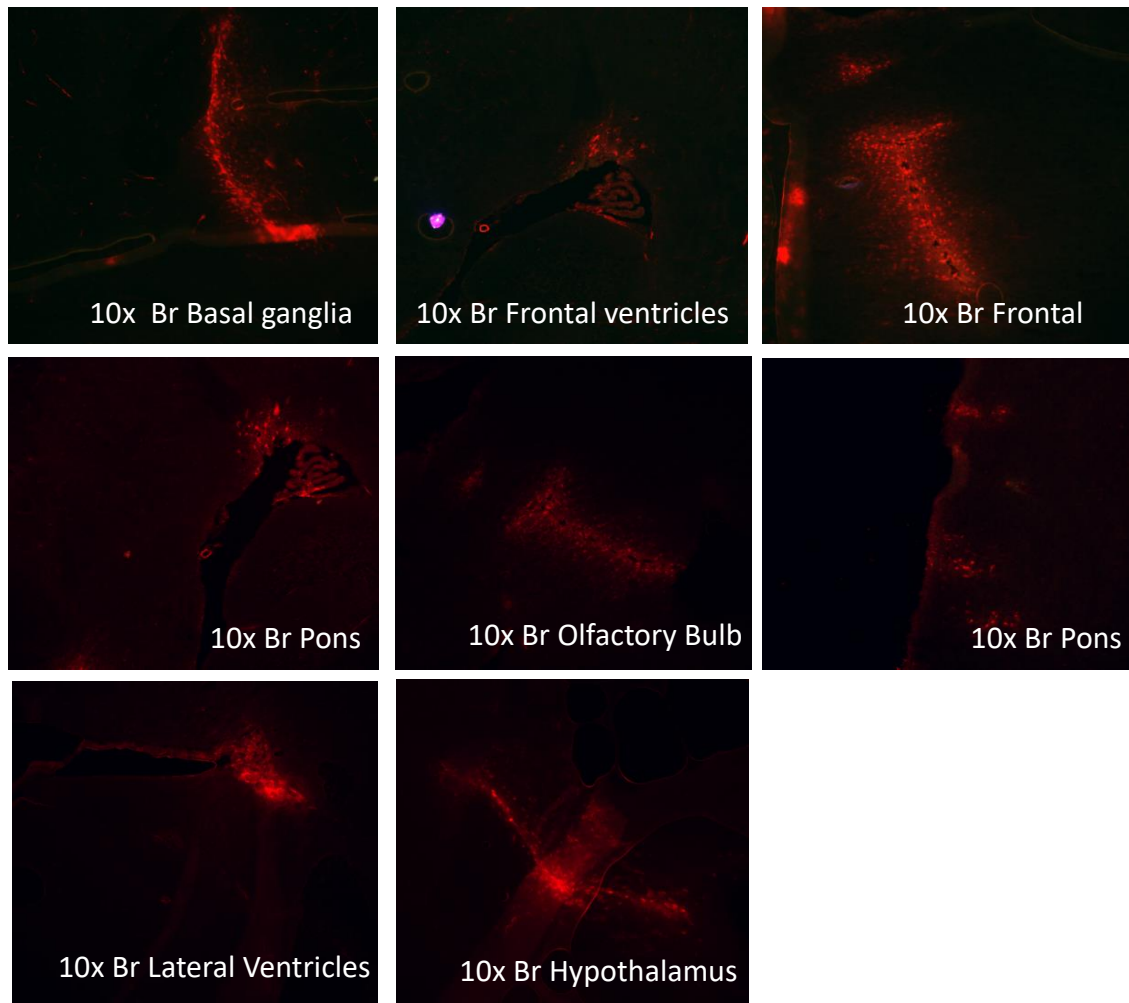


**Figure 30:** Representative photos (10x) of EB from the 3<sup>rd</sup> mouse in many brain areas.

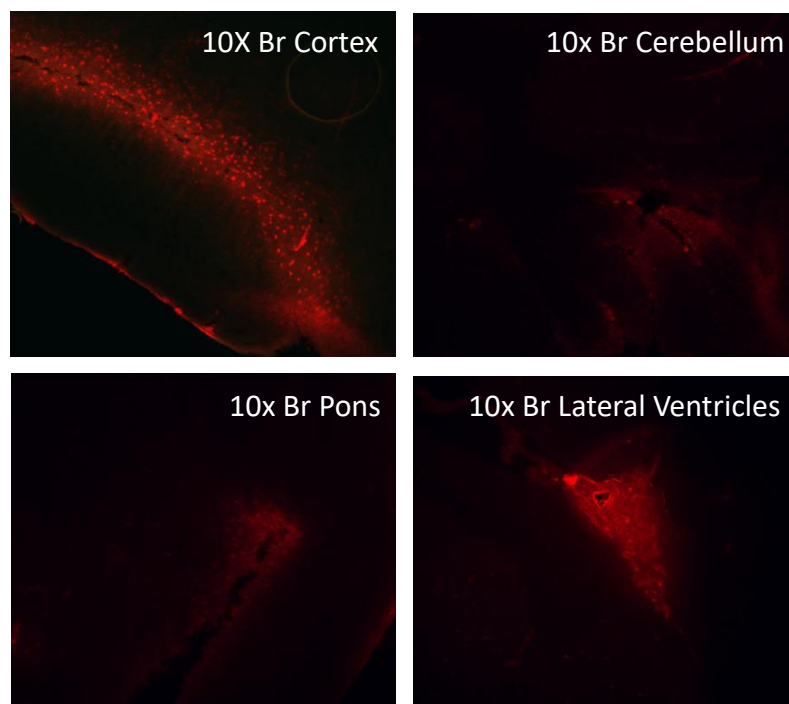


**Figure 31:** Representative photos (10x) of EB from the 4<sup>th</sup> mouse in many brain areas.

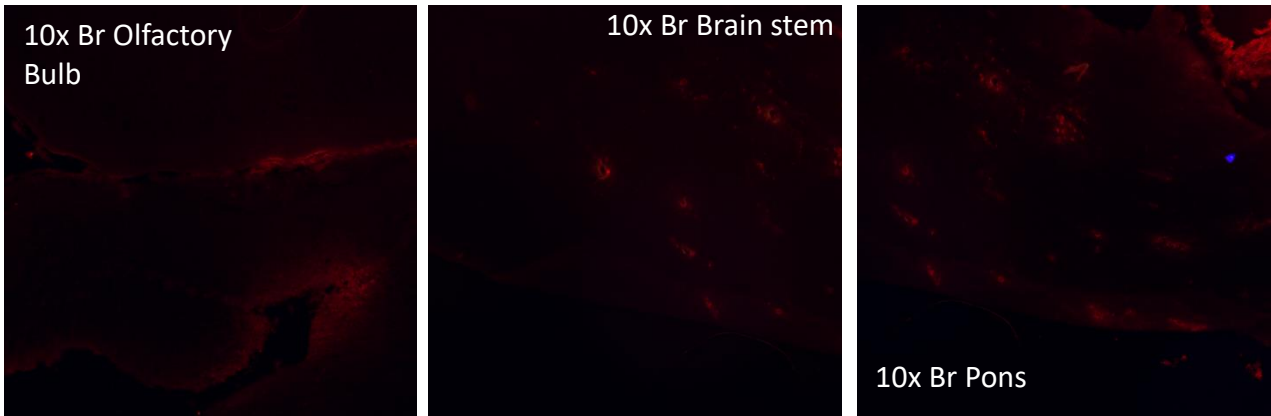


**Figure 32:** Representative photos (10x) of EB from the 5<sup>th</sup> mouse in many brain areas.

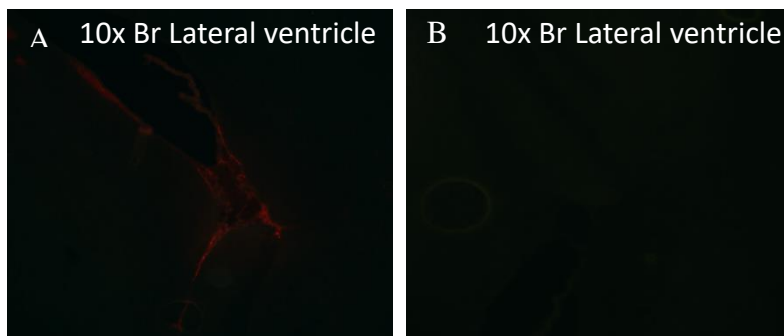


**Figure 33:** Representative photos (10x) of EB from the control mice in brain area (Lateral ventricle). A: Mouse with EB only, B: Non-injected mouse

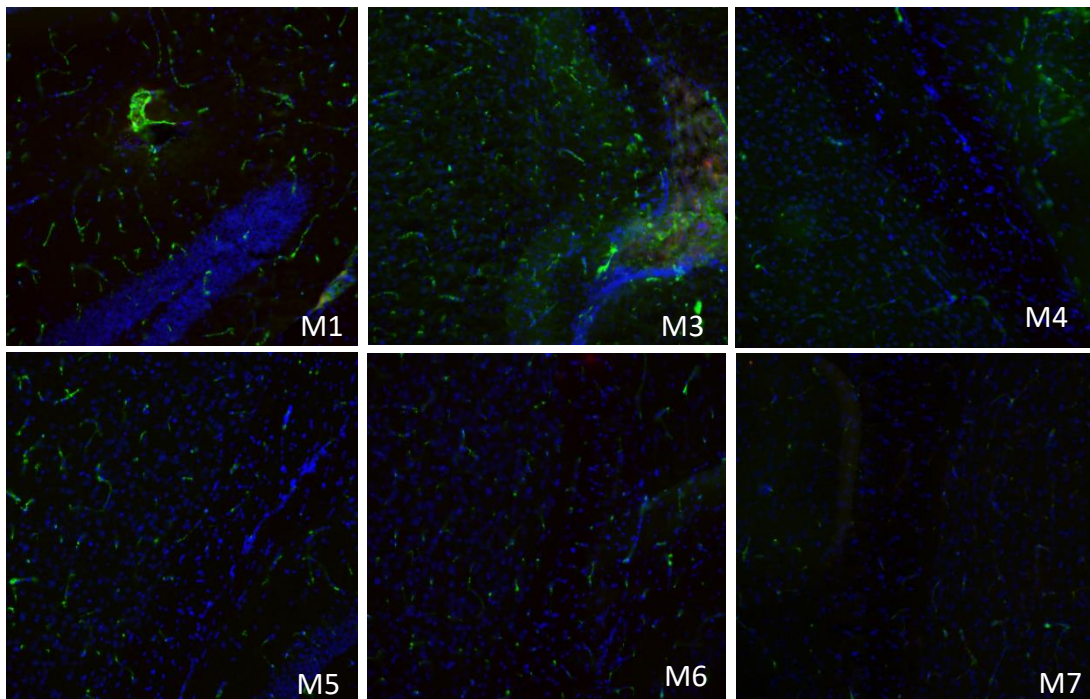


**Figure 34:** Representative photos (10x) from all the tested mice of Fibrinogen immunofluorescence staining in Corpus Callosum. M1: Injected with 20 $\mu$ L MBs-Electric power = 20W (MGC : 7.8 %), M3: Injected with 10 $\mu$ L MBs-Electric power = 20W (MGC : 7.8 %), M4: Injected with 10 $\mu$ L MBs-Electric power = 30W (MGC : 7.8 %). M5: Injected with 20 $\mu$ L MBs-Electric power = 30W (MGC : 7.8 %), M6: Injected only with EB, M7: Non injected mouse.

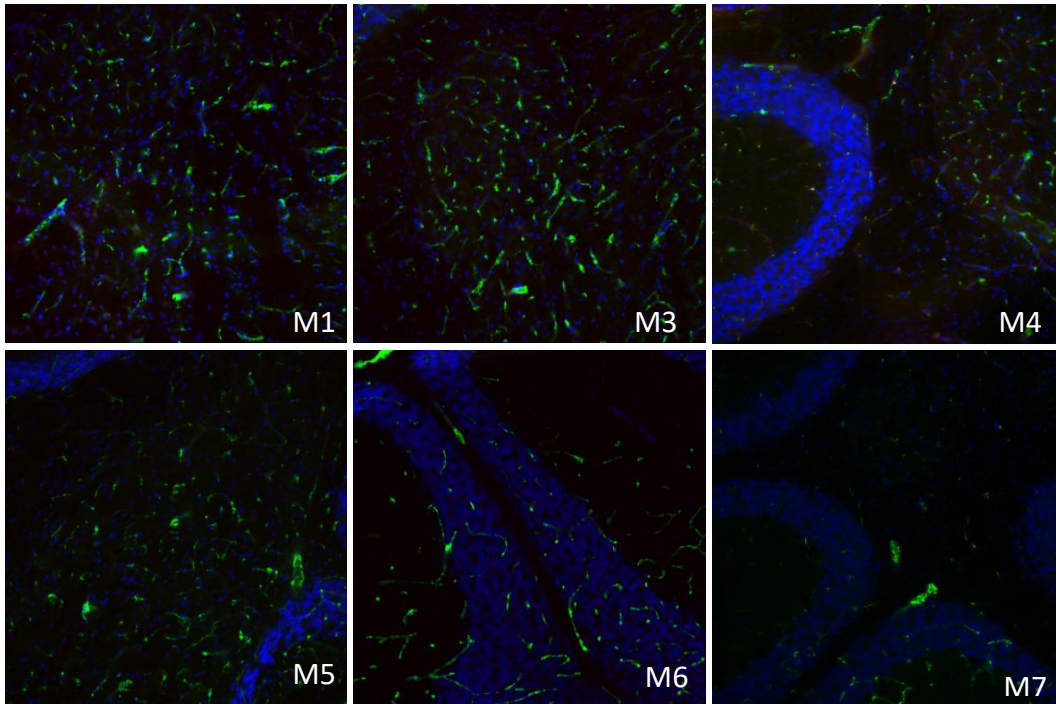


**Figure 35:** Representative photos (10x) from all the tested mice of Fibrinogen immunofluorescence staining in Cerebellum. M1: Injected with 20 $\mu$ L MBs-Electric power = 20W (MGC : 7.8 %), M3: Injected with 10 $\mu$ L MBs-Electric power = 20W (MGC : 7.8 %), M4: Injected with 10 $\mu$ L MBs-Electric power = 30W (MGC : 7.8 %). M5: Injected with 20 $\mu$ L MBs-Electric power = 30W (MGC : 7.8 %), M6: Injected only with EB, M7: Non injected mouse.

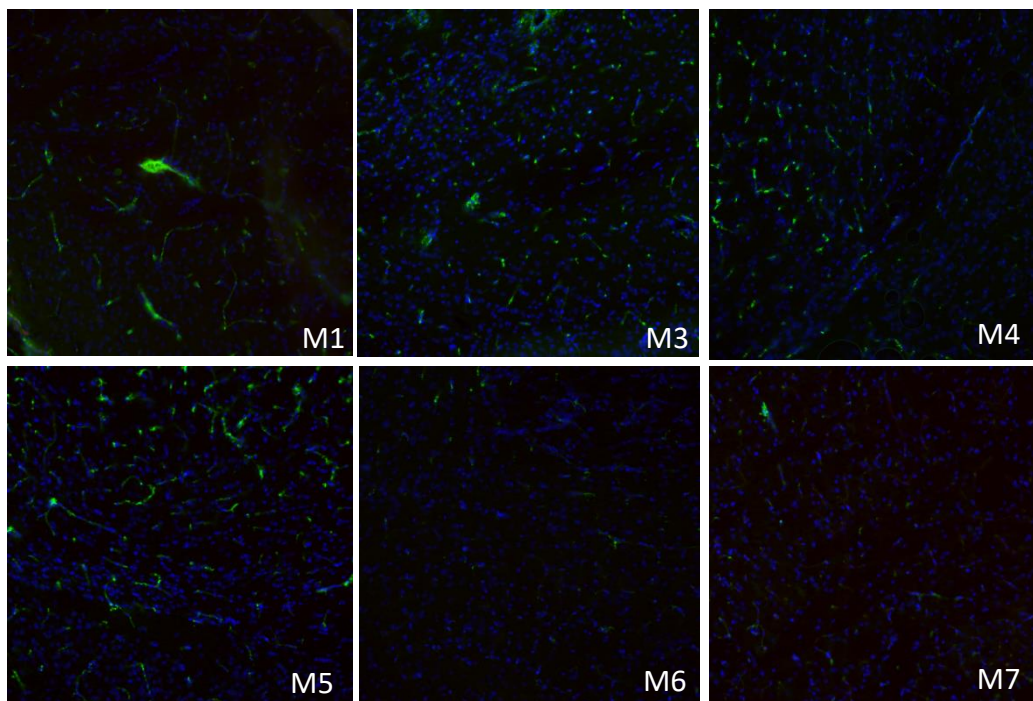


**Figure 36:** Representative photos (10x) from all the tested mice of Fibrinogen immunofluorescence staining in internal capsule . M1: Injected with 20 $\mu$ L MBs-Electric power = 20W (MGC : 7.8 %), M3: Injected with 10 $\mu$ L MBs-Electric power = 20W (MGC : 7.8 %), M4: Injected with 10 $\mu$ L MBs-Electric power = 30W (MGC : 7.8 %). M5: Injected with 20 $\mu$ L MBs-Electric power = 30W (MGC : 7.8 %), M6: Injected only with EB, M7: Non injected mouse.

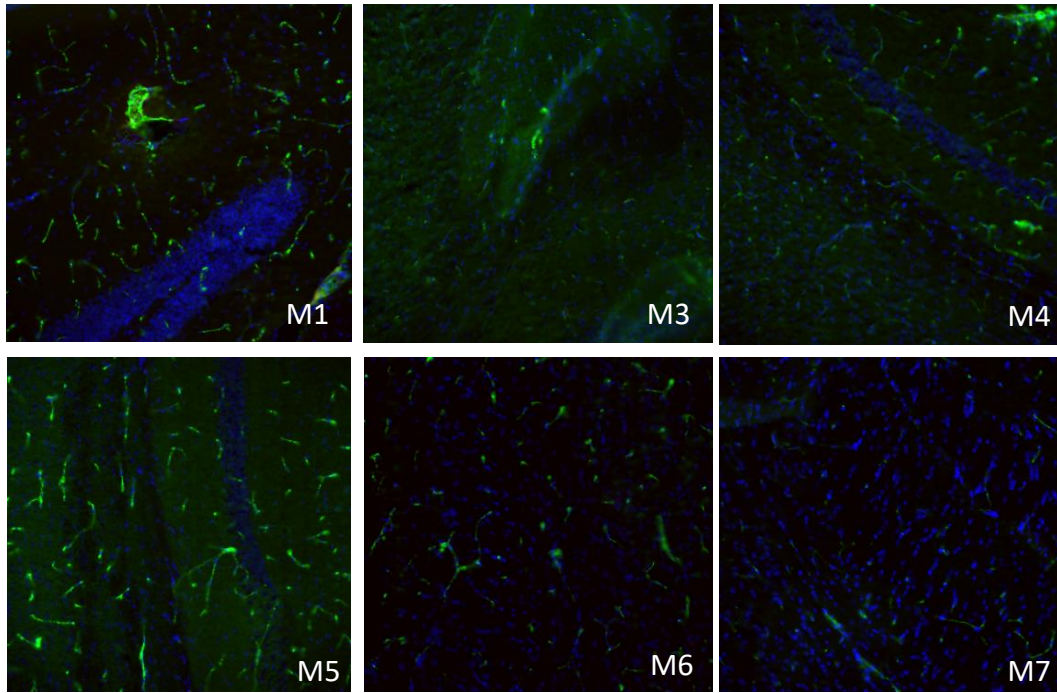


**Figure 37:** Representative photos (10x) from all the tested mice of Fibronectin immunofluorescence staining in Corpus Callosum. M1: Injected with 20 $\mu$ L MBs-Electric power = 20W (MGC : 7.8 %), M3: Injected with 10 $\mu$ L MBs-Electric power = 20W (MGC : 7.8 %), M4: Injected with 10 $\mu$ L MBs-Electric power = 30W (MGC : 7.8 %). M5: Injected with 20 $\mu$ L MBs-Electric power = 30W (MGC : 7.8 %), M6: Injected only with EB, M7: Non injected mouse.

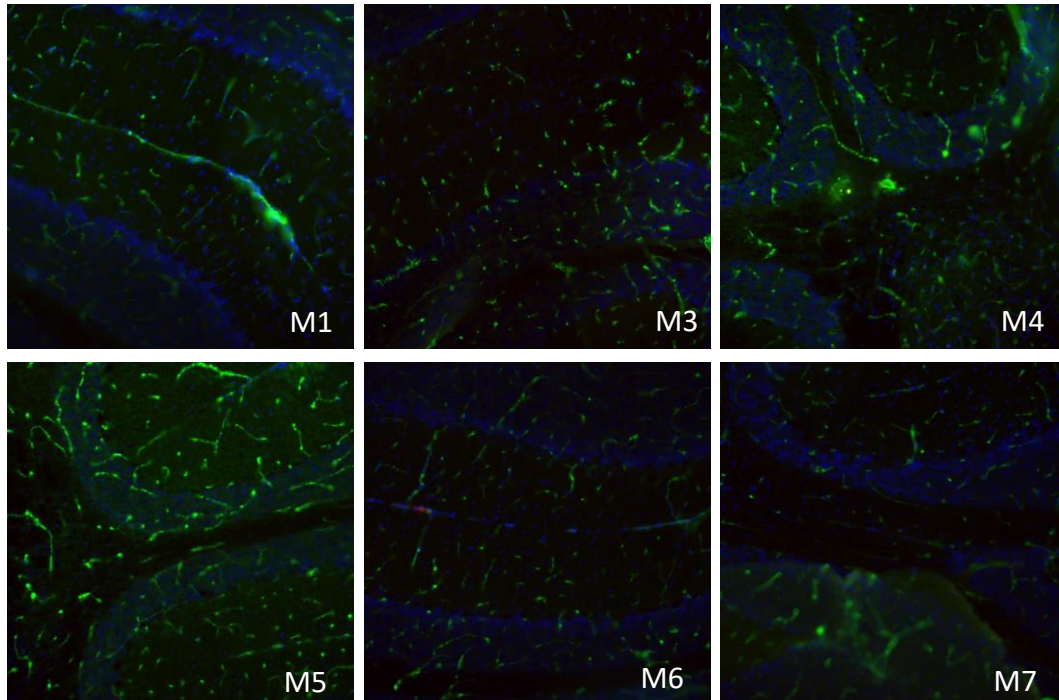


**Figure 38:** Representative photos (10x) from all the tested mice of Fibronectin immunofluorescence staining in Cerebellum. M1: Injected with 20 $\mu$ L MBs-Electric power = 20W (MGC : 7.8 %), M3: Injected with 10 $\mu$ L MBs-Electric power = 20W (MGC : 7.8 %), M4: Injected with 10 $\mu$ L MBs-Electric power = 30W (MGC : 7.8 %). M5: Injected with 20 $\mu$ L MBs- Electric power = 30W (MGC : 7.8 %), M6: Injected only with EB, M7: Non injected mouse.

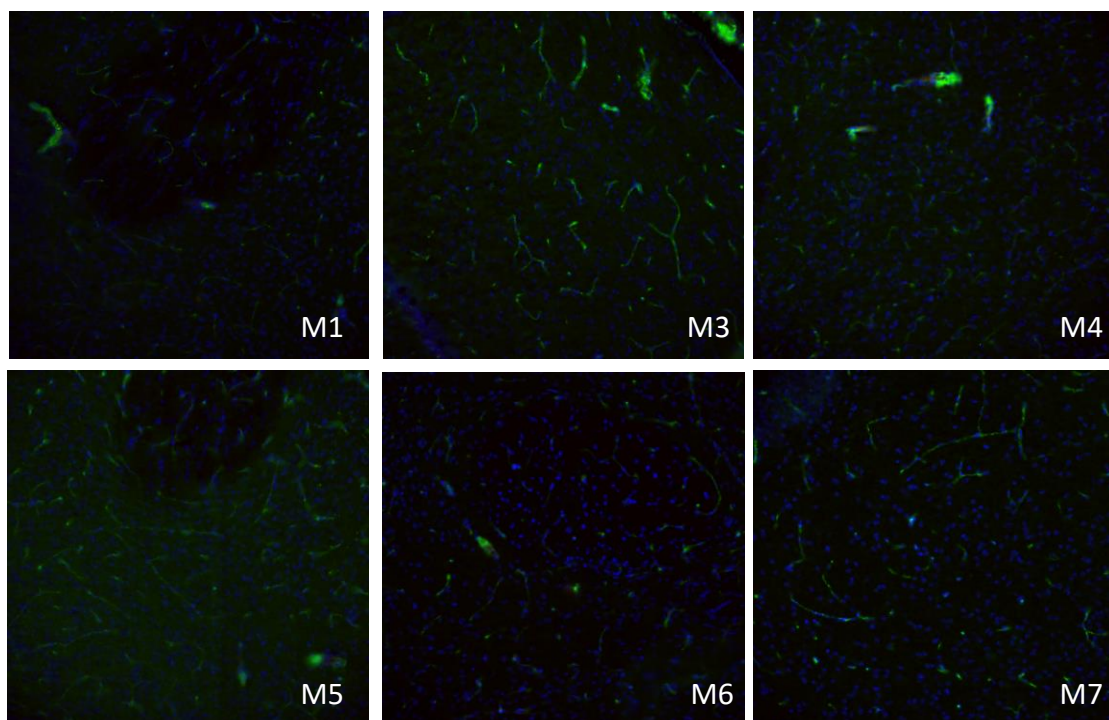


**Figure 39:** Representative photos (10x) from all the tested mice of Fibronectin immunofluorescence staining in internal capsule. M1: Injected with 20 $\mu$ L MBs-Electric power = 20W (MGC : 7.8 %), M3: Injected with 10 $\mu$ L MBs-Electric power = 20W (MGC : 7.8 %), M4: Injected with 10 $\mu$ L MBs-Electric power = 30W (MGC : 7.8 %). M5: Injected with 20 $\mu$ L MBs-Electric power = 30W (MGC : 7.8 %), M6: Injected only with EB, M7: Non injected mouse.

According to the results from previous trial, in this test, we have tested the effect of electric power while keeping the amount of MBs constant (5 $\mu$ L). We tested 7 WT mice of 1 month-old (Table 1). The rest parameters remained the same (1 % DF, 100 s sonication duration).

**Table 1:** Electric power tested for protocol calibration for constant amount of MBs.

Group	# of mice	Electric power (W)	MBs ( $\mu$ L)
A	2	40	5
B	2	50	5
C	2	60	5
D	1	70	5

Thirty (30) minutes after the EB injection, the mice were anaesthetized intraperitoneally with Avertin and sacrificed. Slides containing brain sections were directly visualized using a fluorescence microscope. Cryosections from brain were immunostained for fibronectin and FITC-labeled polyclonal fibrinogen antibody to assess serum protein leakage into the parenchyma. Two (2) WT mice were used for control; 1 mouse was injected with EB only and 1 mouse was not non-injected.

Representative photos of EB in many brain areas (Figures 40-44) and Fibrinogen and Fibronectin immunofluorescence staining in corpus callosum, internal capsule and cerebellum (Figures 45-50) show that in controls (M8 and M9), low levels of fibrinogen and fibronectin are evident and the EB leakage into the brain parenchyma indicates BBB disruption. Compared to the previous experiments, we observed higher amount of EB at all electric powers. It seems that the M5 mouse (74Watt) and M6-M7 mice (60 Watt) show similarly higher levels of EB in many brain areas than

the other mice. Concerning the immunostaining with Fibrinogen and Fibronectin antibodies, all the tested mice show higher level in all brain areas we examined than the control mice. According to the EB staining, we believe that the range of 60-74 W electric power with 5  $\mu$ L MBs is the most effective protocol.

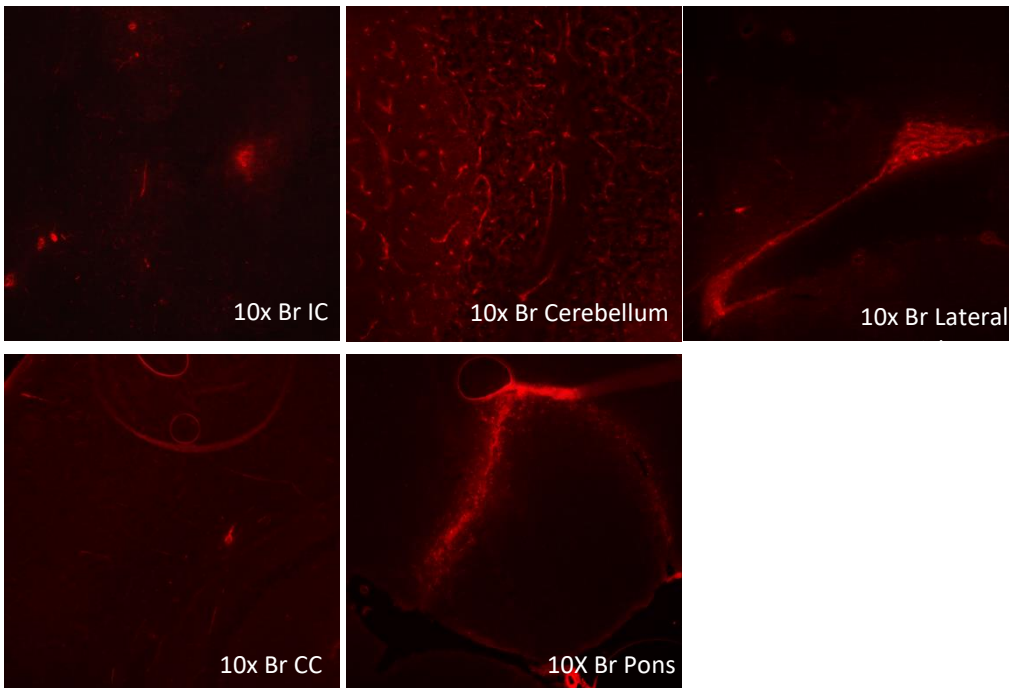


**Figure 40:** Representative photos (10x) of EB from the 1st and 2nd mouse in many brain areas.

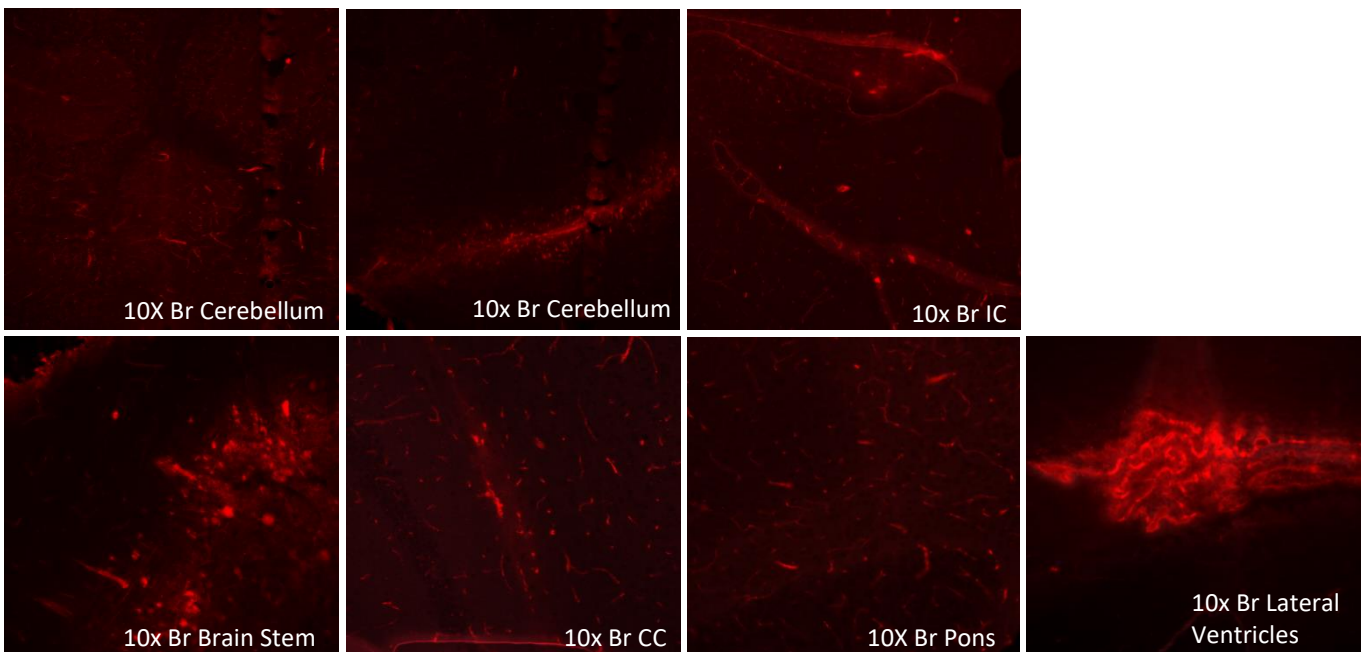


**Figure 41:** Representative photos (10x) of EB from the 3rd and 4th mouse in many brain areas.

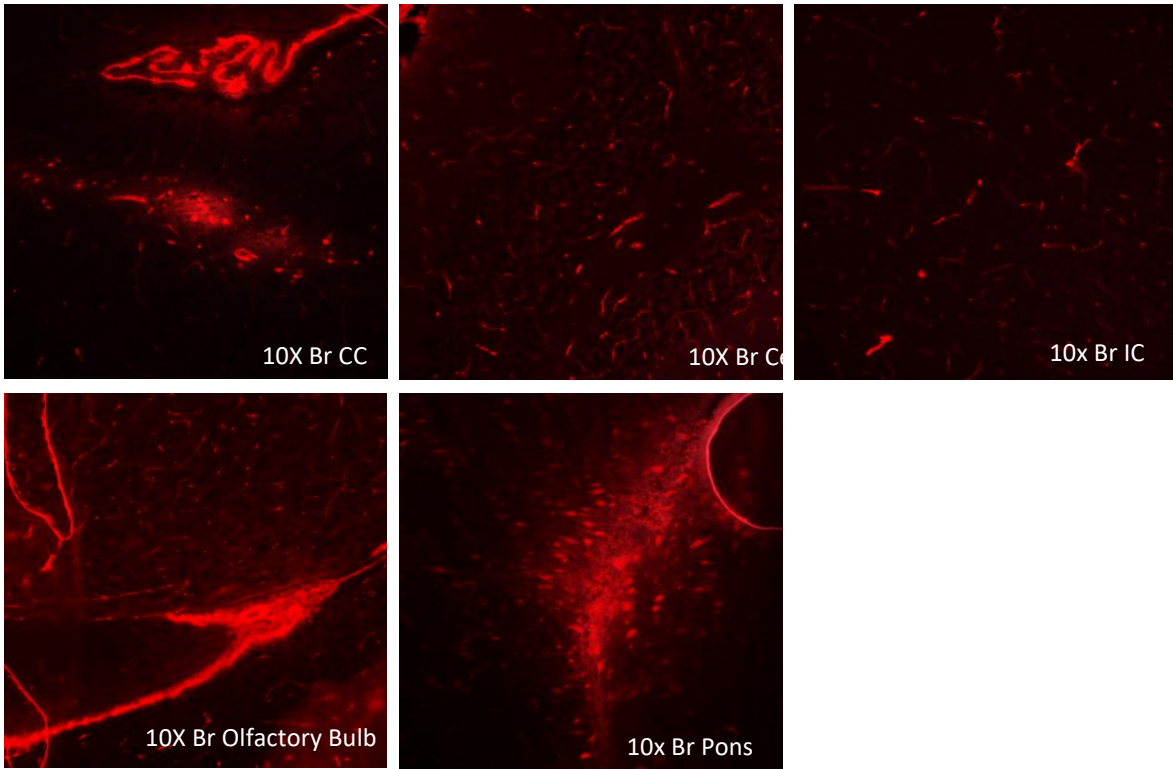


**Figure 42:** Representative photos (10x) of EB from the 5th and 6th mouse in many brain areas.

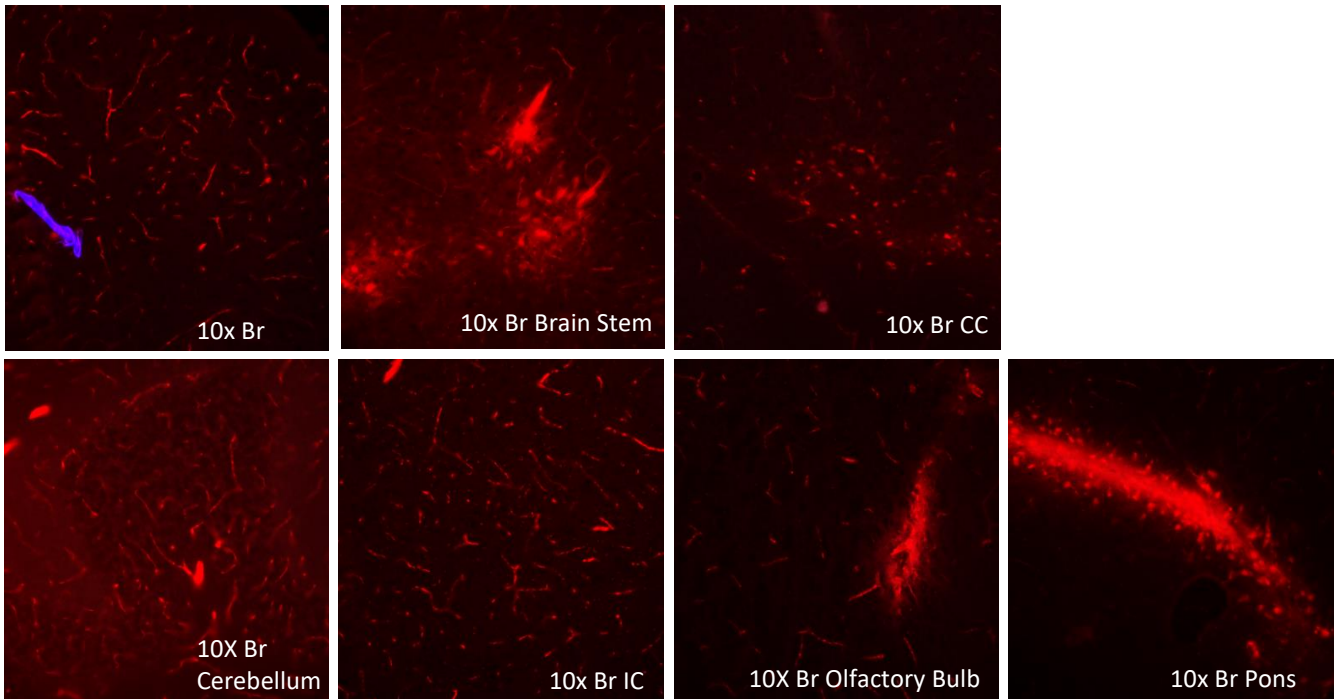


**Figure 43:** Representative photos (10x) of EB from the 7<sup>th</sup> mouse in many brain areas.

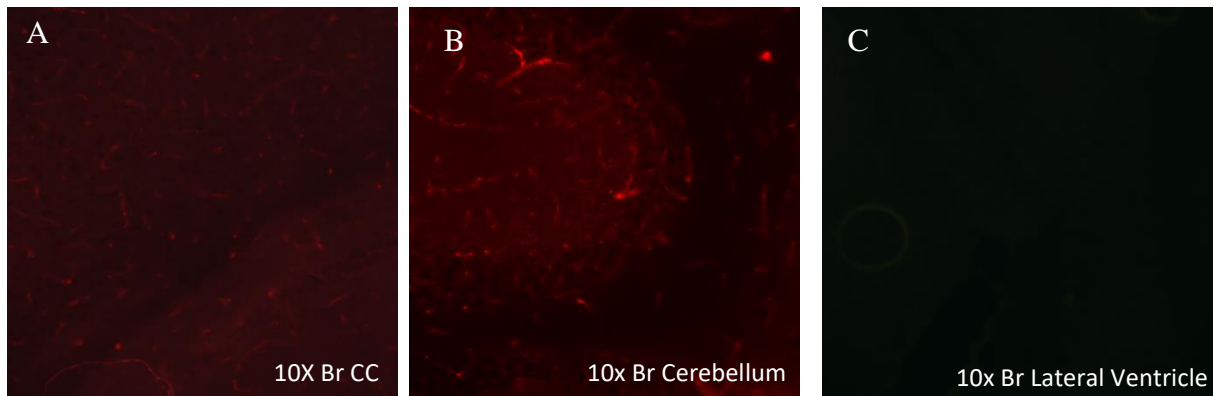


**Figure 44:** Representative photos (10x) of EB from the control mice in brain areas. A-B: Mouse with EB only, C: Non-injected mouse

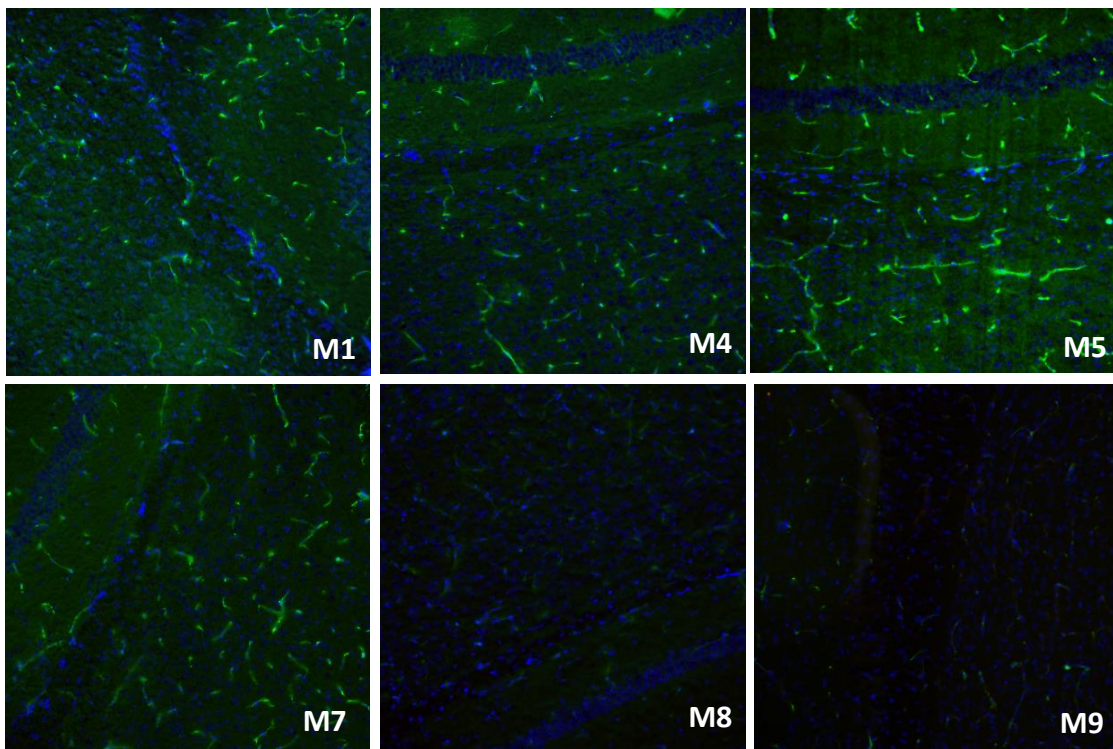


**Figure 45:** Representative photos (10x) from all the tested mice of Fibrinogen immunofluorescence staining in Corpus Callosum. M1: Electric power = 40W, M4: Electric power = 50W, M5: Electric power = 70W. M7: Electric power = 60W, M8: Injected only with EB, M9: Non-injected

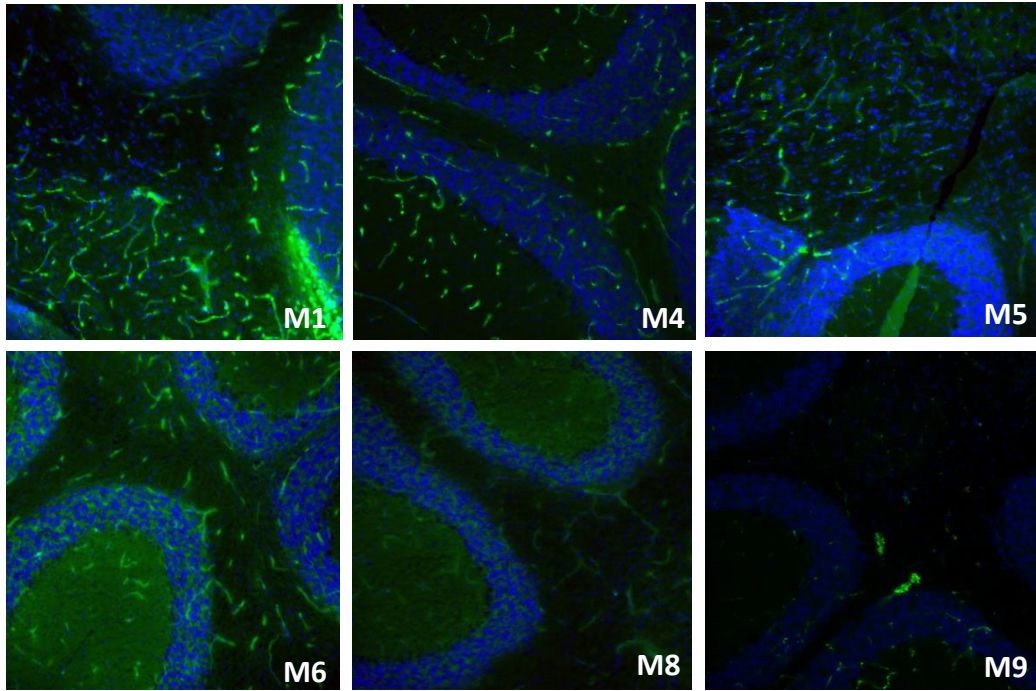


**Figure 46:** Representative photos (10x) from all the tested mice of Fibrinogen immunofluorescence staining in cerebellum. M1: Electric power = 40W, M4: Electric power =50W, M5: Electric power = 70W. M7: Electric power = 60W, M8: Injected only with EB, M9: Non-injected mouse.

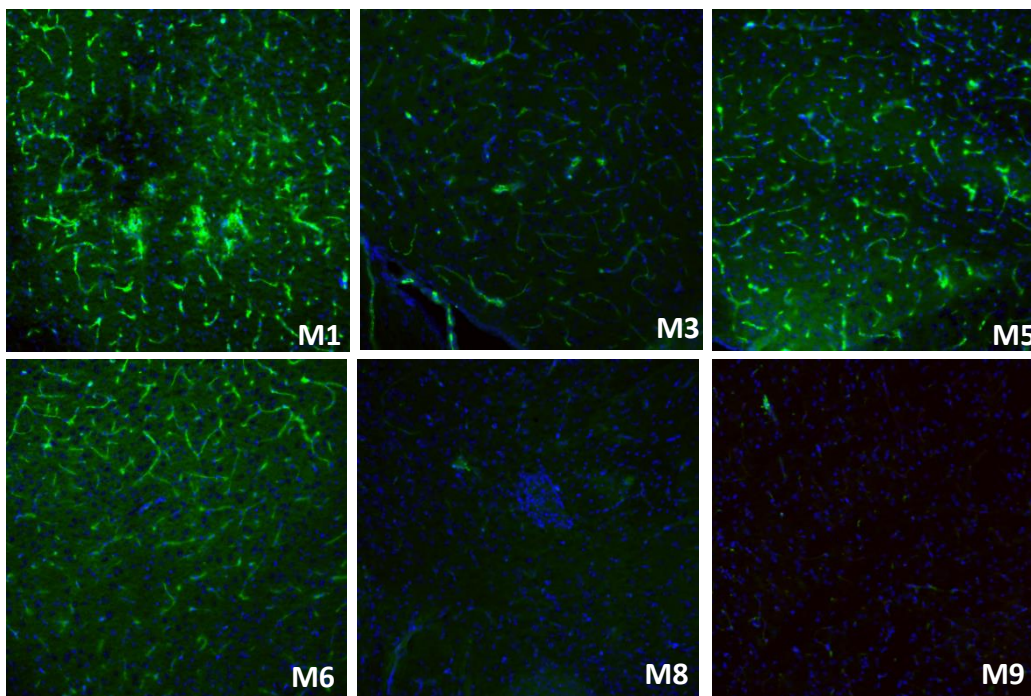


**Figure 47:** Representative photos (10x) from all the tested mice of Fibrinogen immunofluorescence staining in internal capsule. M1: Electric power = 40W, M4: Electric power =50W, M5: Electric power = 70W. M7: Electric power = 60W, M8: Injected only with EB, M9: Non-injected mouse

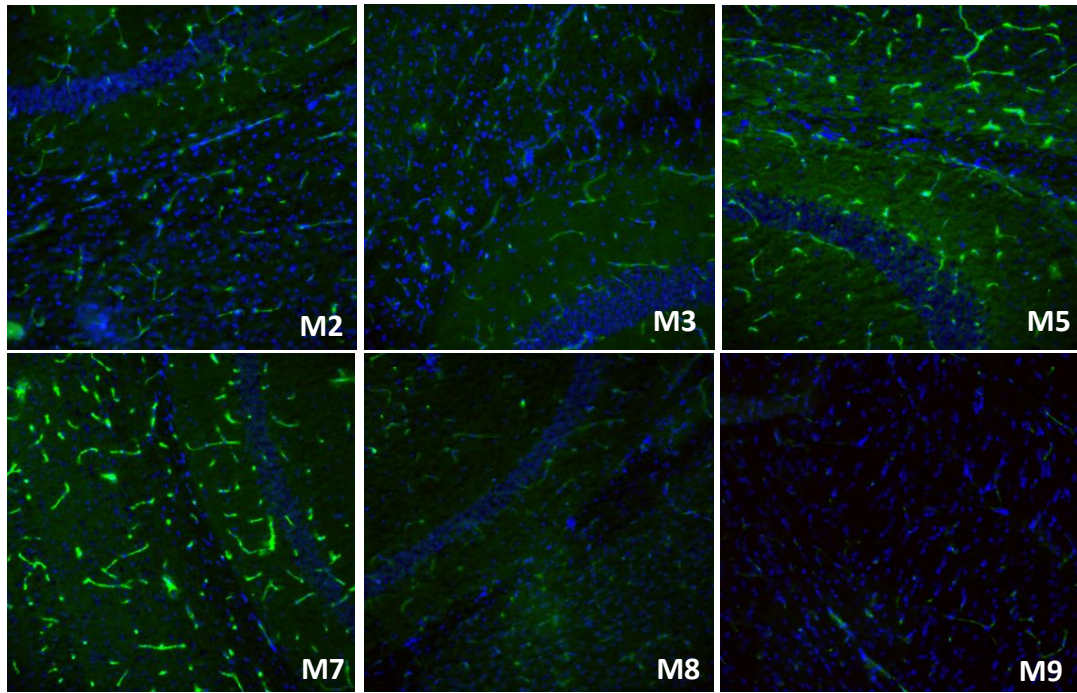


**Figure 48:** Representative photos (10x) from all the tested mice of Fibronectin immunofluorescence staining in Corpus Callosum. M1: Electric power = 40W, M4: Electric power = 50W, M5: Electric power = 70W. M7: Electric power = 60W, M8: Injected only with EB, M9: Non-injected mouse.

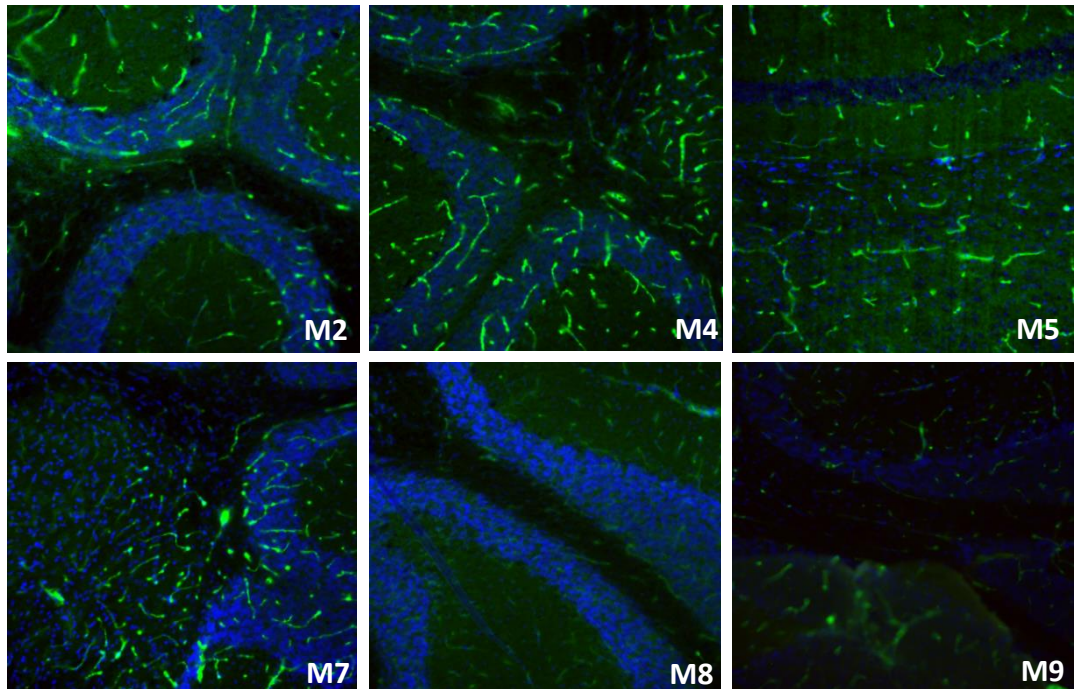


**Figure 49:** Representative photos (10x) from all the tested mice of Fibronectin immunofluorescence staining in cerebellum. M1: Electric power = 40W, M4: Electric power = 50W, M5: Electric power = 70W. M7: Electric power = 60W, M8: Injected only with EB, M9: Non-injected mouse.

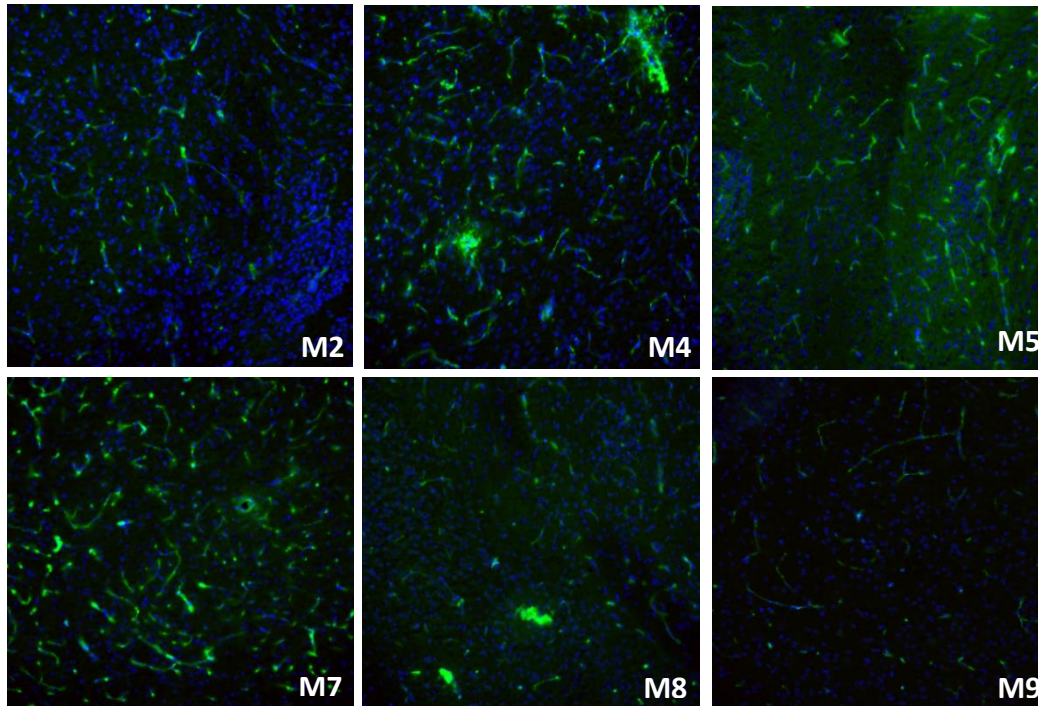


**Figure 50:** Representative photos (10x) from all the tested mice of Fibronectin immunofluorescence staining in internal capsule. M1: Electric power = 40W, M4: Electric power =50W, M5: Electric power = 70W. M7: Electric power = 60W, M8: Injected only with EB, M9: Non-injected mouse.

We also checked the tissue integrity and the lack of hemorrhage with H&E staining. We didn't observe any difference between the FUS treated and control cases in terms of tissue integrity and there was no evidence of hemorrhage (Figures 51-56).

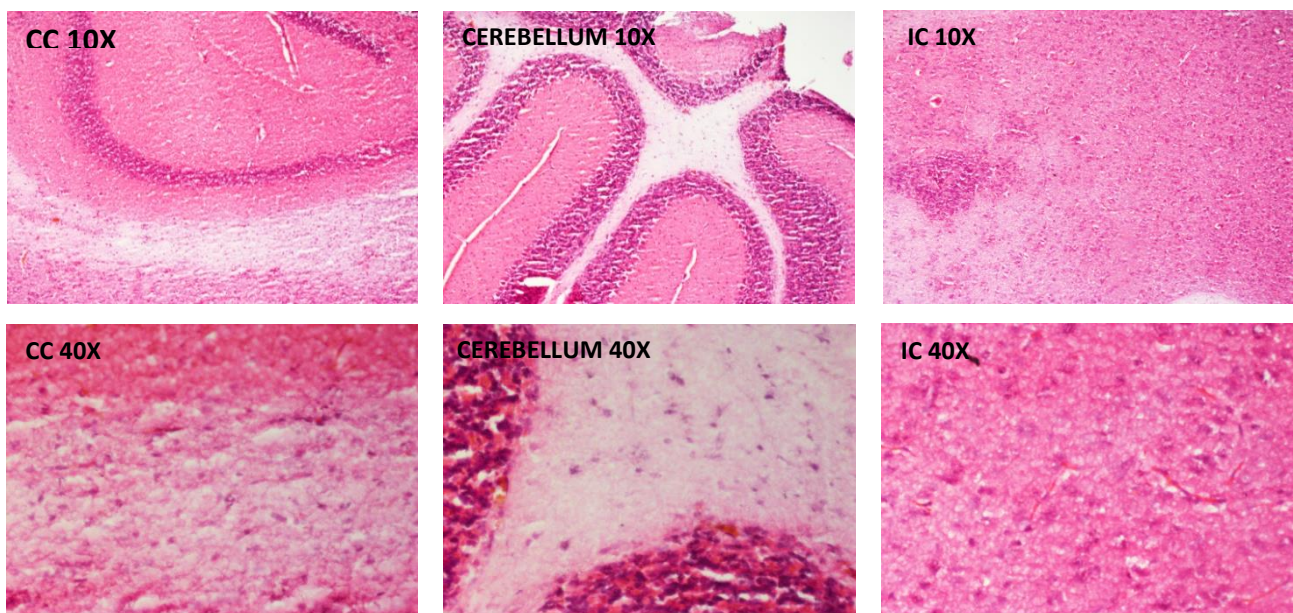


**Figure 51:** Representative photos (10x) of H&E staining from the 1st and 2nd mice in many brain areas.

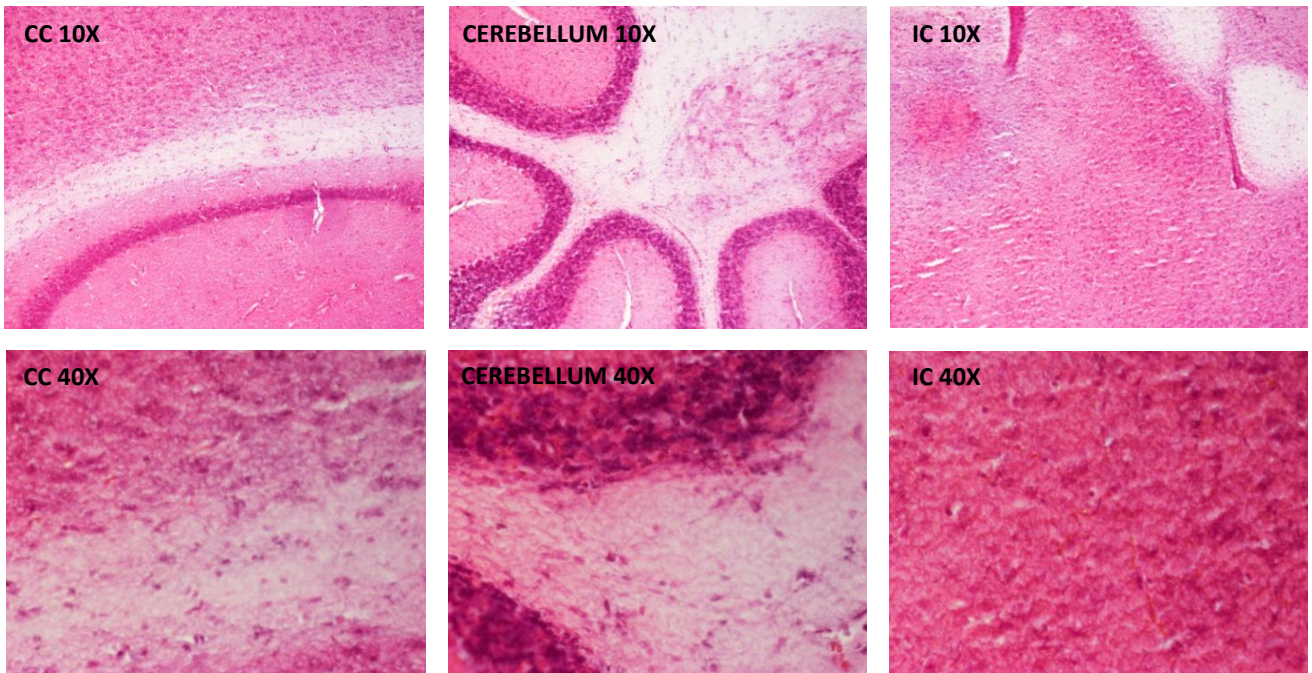


**Figure 52:** Representative photos (10x) of H&E staining from the 3<sup>rd</sup> and 4<sup>th</sup> mice in many brain areas.

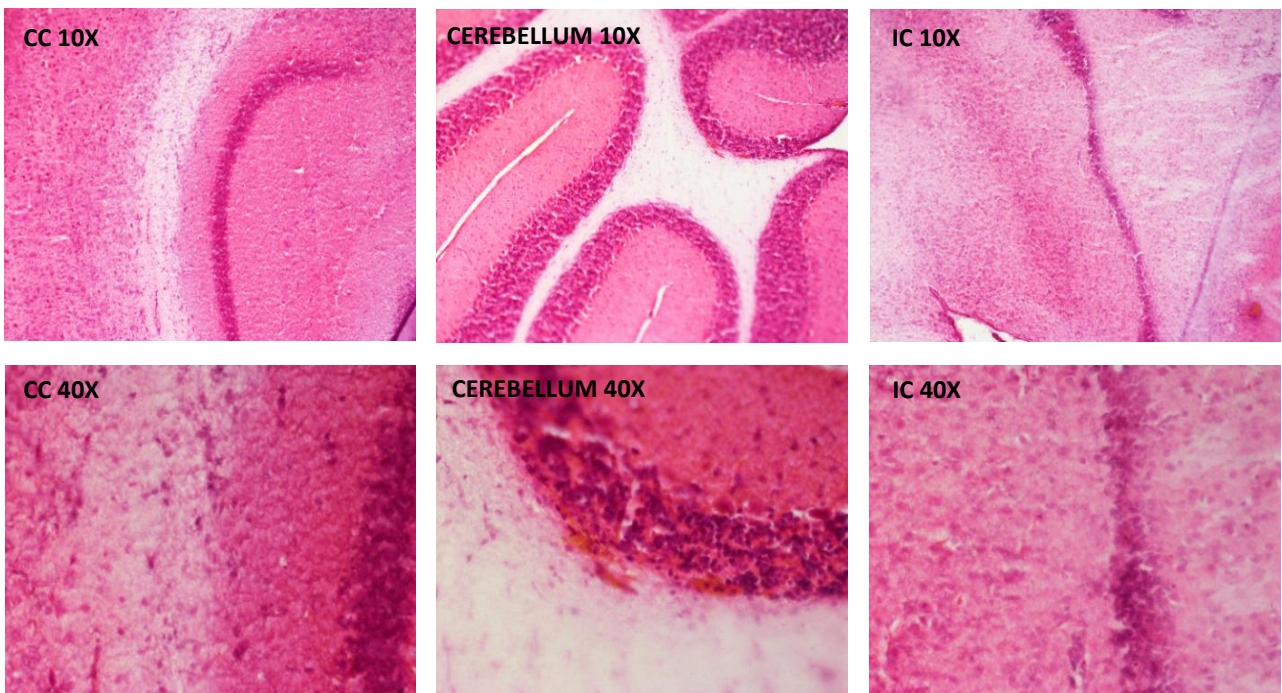


**Figure 53:** Representative photos (10x) of H&E staining from the 3<sup>rd</sup> and 4<sup>th</sup> mice in many brain areas.

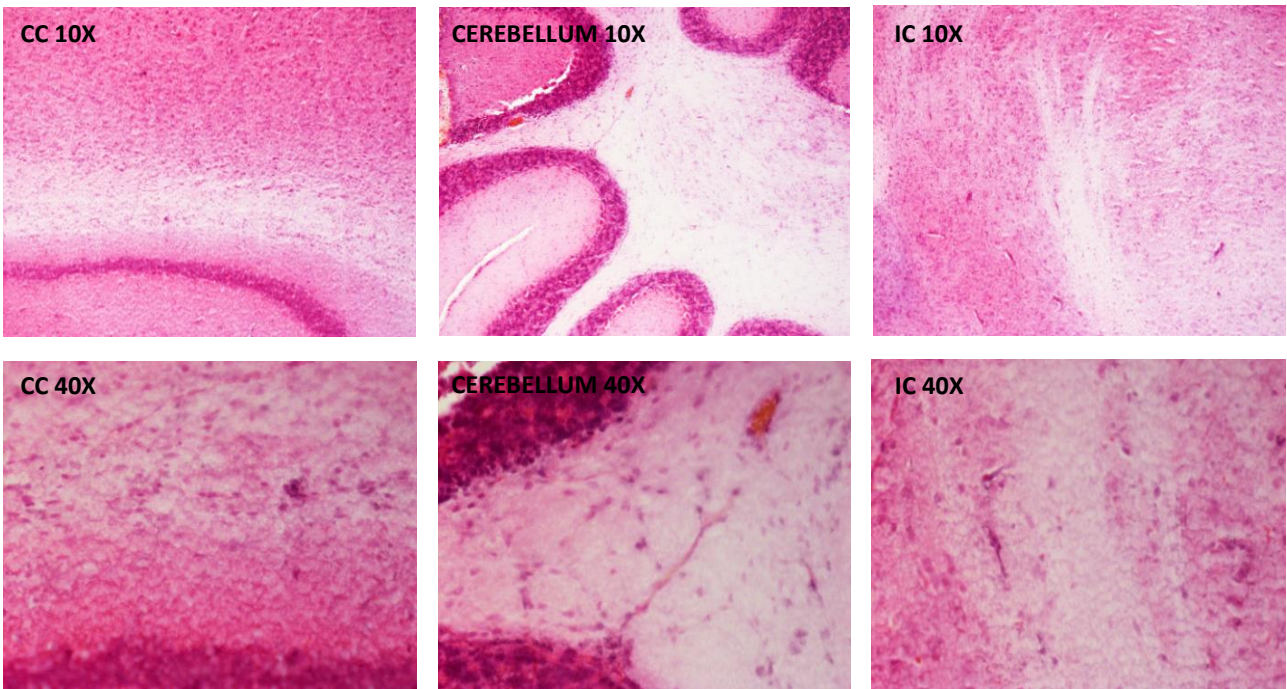


**Figure 54:** Representative photos (10x) of H&E staining from the 5<sup>th</sup> mouse in many brain areas.

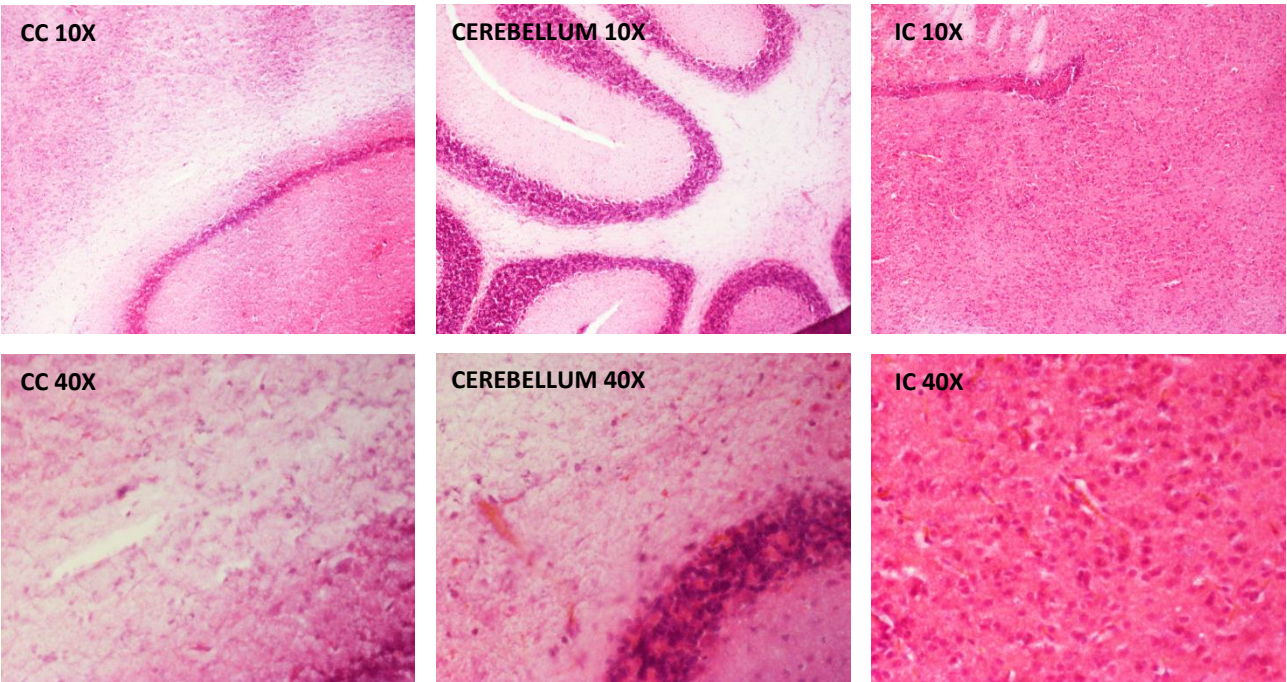


**Figure 55:** Representative photos (10x) of H&E staining from the WT mouse injected with EB only in many brain areas.

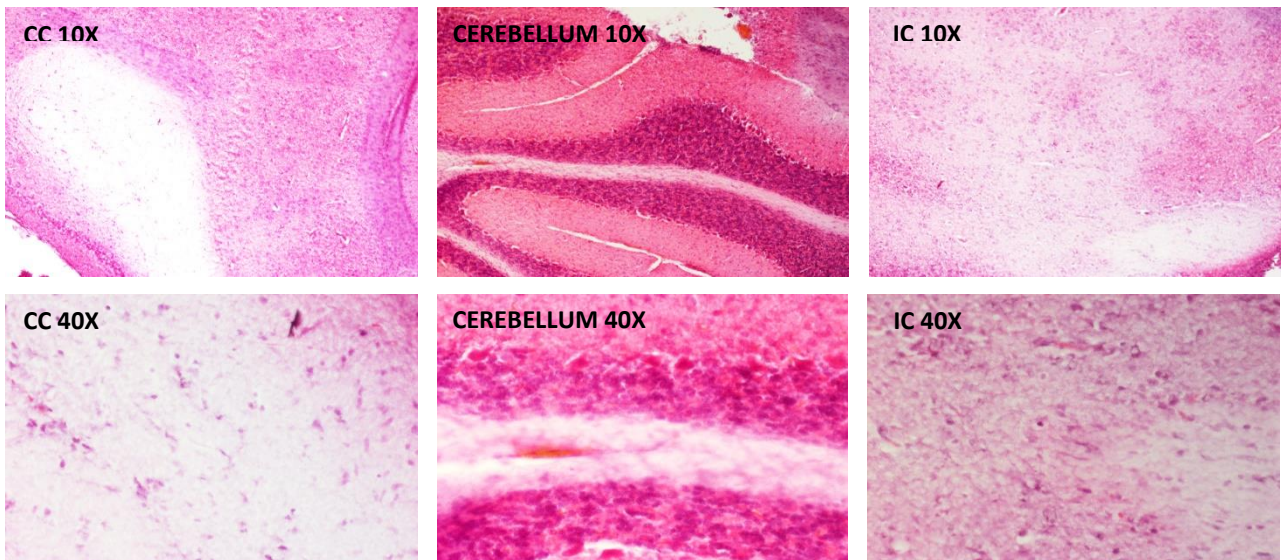


**Figure 56:** Representative photos (10x) of H&E staining from the WT mouse non-injected in many brain areas.

### **Feasibility of delivering A $\beta$ (1-40) antibody in the brain tissue – the effect of antibody amount**

5XFAD mice develop severe amyloid pathology and recapitulate many AD-related phenotypes, thus they are an ideal model of Alzheimer's disease. Drug delivery for therapeutic purposes in Alzheimer's disease is not efficient due to BBB permeability restrictions. The use of this model was essential to investigate the BBB opening with FUS and examine the effect of antibody amount into the brain since **most** of the antibody enters the brain.<sup>36</sup>

An experiment was performed to evaluate the delivery of three different volumes (25, 50, 100  $\mu$ L) of A $\beta$  (1-40) antibody into the brain of three mice via the BBB after sonication with FUS. Three 5XFAD mice were **weighed** and injected with Avertin for rapid and deep anesthesia (Figure 57-59). Hair was removed from the mouse head using hair removal cream. Retro-orbital injection was used to deliver 100  $\mu$ L of A $\beta$  (1-40) antibody and 5  $\mu$ L of MBs. The mouse was placed on the positioning device and coupling gel was applied on the mouse head. FUS was performed within a 3-4 minutes time window. The second mouse was injected with 50  $\mu$ L of A $\beta$  (1-40) antibody and 5  $\mu$ L of MBs and the third mouse with 25  $\mu$ L of antibody and 5  $\mu$ L of MBs. The following sonication parameters were used: Pulsed FUS --> F = 1.04 MHz, P = 50 W, DF = 1 %, PRP = 1000 ms, and PD = 10 ms .

Double immunostaining of coronal brain sections was performed in order to confirm that the injected antibody (A $\beta$  1-40, red colour) successfully passed the BBB and bound to A $\beta$  plaques. Staining with A $\beta$  1-16 antibody (6E10, green colour) was used to identify the amyloid plaques. Therefore, co-localization of both antibodies will confirm the presence of plaques, the specificity of the antibodies to bind the amyloid plaques and the entry of the injected antibody into the brain by a non-invasive microbubble mediated opening of the BBB due to the transcranial application of FUS.

Co-localization of both colours (green and red) confirmed successful binding of the A $\beta$  1-40 injected antibody to A $\beta$  plaques. Brain sections from different regions showed co-localization of the A $\beta$  1-40, (red colour) and A $\beta$  1-16 antibody (6E10, green colour). This was an indication that the injected antibody A $\beta$  1-40, (red colour) entered the brain after the successful opening of the BBB using the following sonication parameters: Pulsed FUS --> F = 1.04 MHz, P = 50 W, DF = 1 %. It was observed that 100  $\mu$ L and 50  $\mu$ L of antibody allowed binding to a higher number of plaques in more brain areas, compared to 25  $\mu$ L (Figures 57-59).

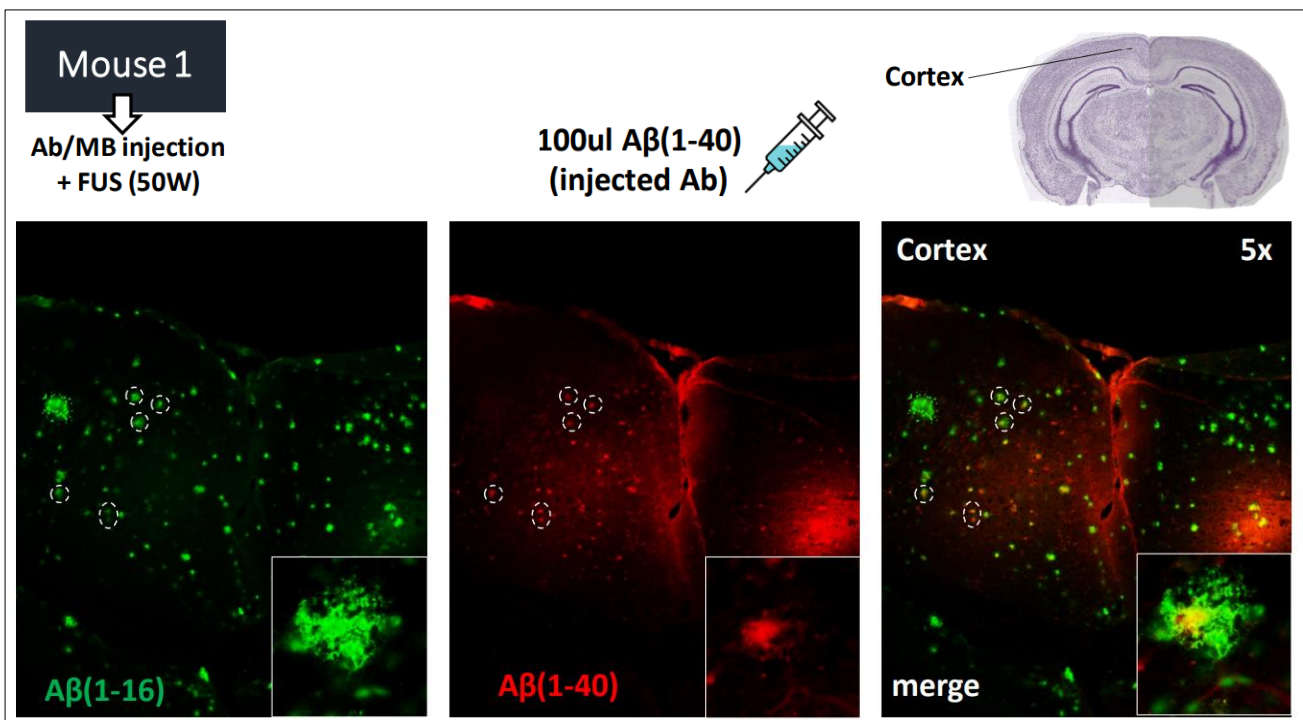
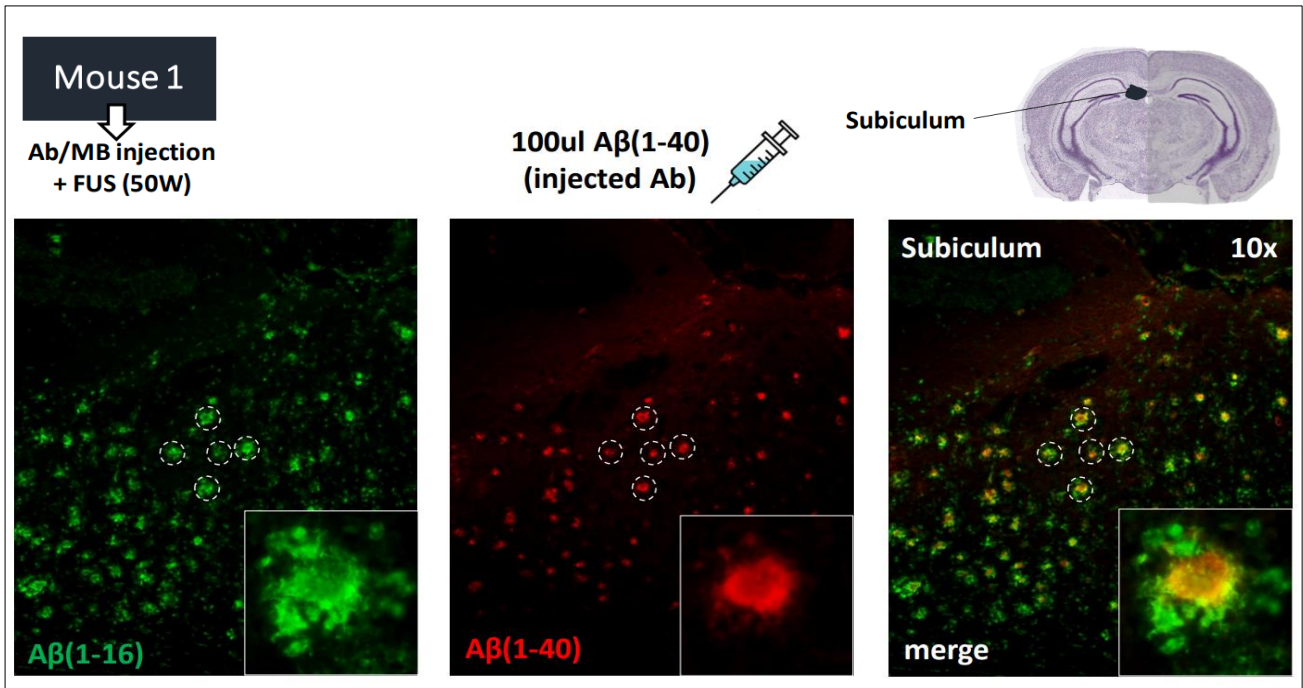


**Figure 57:** Immunohistochemistry analysis of brain tissue sections of a 5XFAD mouse model of Alzheimer's disease injected with 100  $\mu$ L of A $\beta$  1-40 antibody and 5  $\mu$ L of MBs followed by FUS (50W). Co-localization of antibodies (white circles) in different brain regions (subiculum and cortex) confirmed the successful entry and the specificity of the A $\beta$  1-40 antibody.

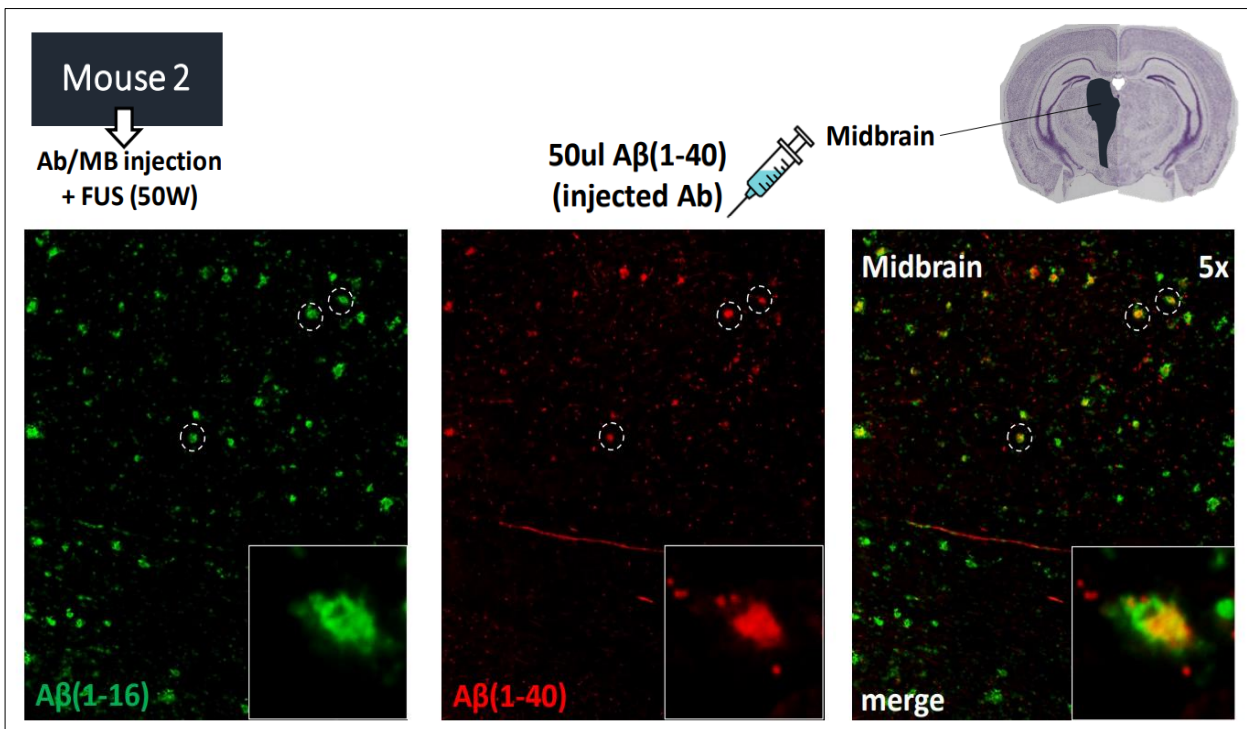
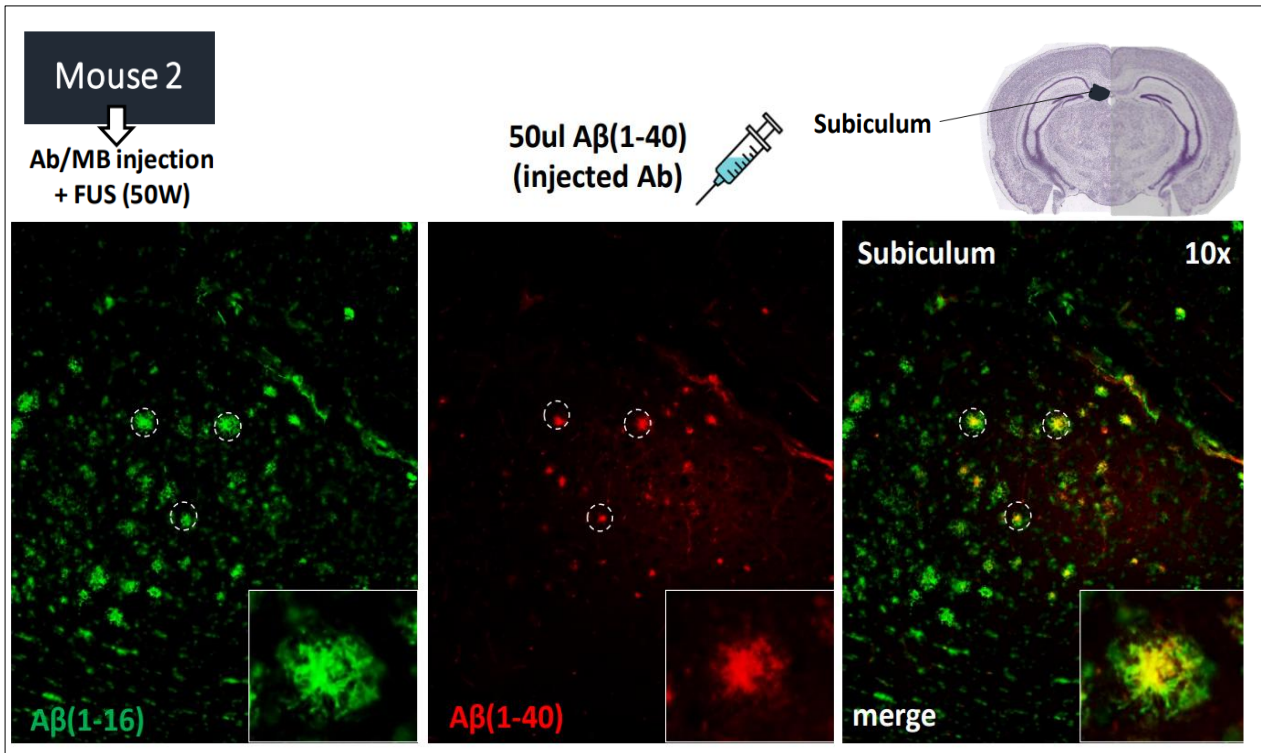


**Figure 58:** Immunohistochemistry analysis of brain tissue sections of a 5XFAD mouse model of Alzheimer's disease injected with 50  $\mu$ L of A $\beta$  1-40 antibody and 5  $\mu$ L of MBs followed by FUS (50W). Co-localization of antibodies (white circles) in different brain regions (subiculum and midbrain) confirmed the successful entry and the specificity of the A $\beta$  1-40 antibody.

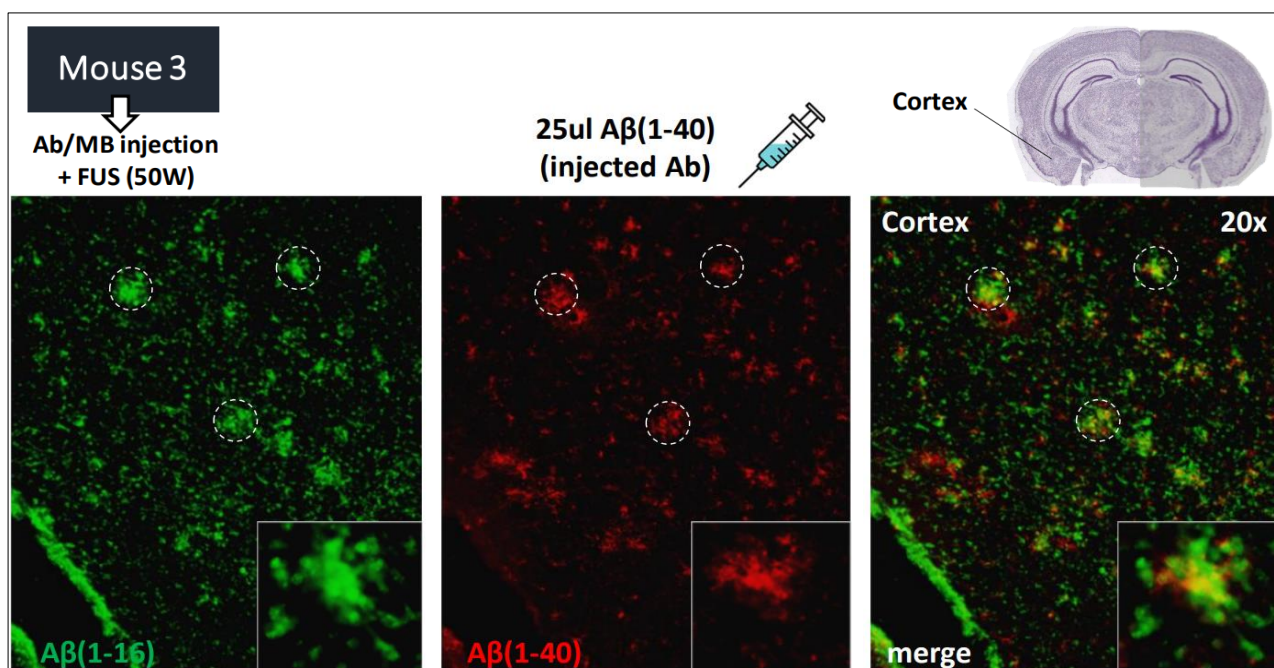


**Figure 59:** Immunohistochemistry analysis of brain tissue sections of a 5XFAD mouse model of Alzheimer’s disease injected with 25  $\mu\text{L}$  of  $\text{A}\beta$  1-40 antibody and 5  $\mu\text{L}$  of MBs followed by FUS (50W). Co-localization of antibodies (white circles) in the cortex confirmed the successful entry into the mouse brain using a non-invasive methodology and the specificity of the  $\text{A}\beta$  1-40 antibody to bind the amyloid plaques.

### **$\text{A}\beta$ (1-40) antibody alone versus antibody plus FUS – constant antibody amount**

Based on these observations, the next experiment was performed using the same sonication parameters (50 W electric power, 100 s duration, 1% DF) and 50  $\mu\text{L}$  of antibody ( $\text{A}\beta$  1-40). Mice were divided into three groups based on the injection and sonication conditions (Table 2).

**Table 2:** The three groups of 5XFAD mice used in this experimental part.

Group	# of mice (5XFAD)	Injection/Sonication Conditions	Saline/Antibody ( $\mu\text{L}$ )	MBs ( $\mu\text{L}$ )
A	5	Saline & FUS+MBs	50	5
B	5	$\text{A}\beta$ (1-40) Antibody Only	50	/
C	10	$\text{A}\beta$ (1-40) Antibody & FUS+MBs	50	5

Transcardiac perfusion was performed to each mouse, followed by brain extraction/dissection, tissue embedding and immunohistochemistry analysis. Co-localization of the  $\text{A}\beta$  1-16 (green colour) and  $\text{A}\beta$  1-40 (injected antibody-red colour) confirmed successful opening of the BBB by the transcranial application of FUS.

Mice from group A were injected with saline and MBs followed by transcranial application of FUS. The brain sections from this group were used as negative controls and they were compared with the coronal brain sections from Groups B and C which were injected with the  $\text{A}\beta$  1-40 antibody (red

colour). As it was expected, mice injected with saline did not have any signs of A $\beta$  1-40 antibody in their brain (Figures 60-62). The same methodology was performed to the mice of group B. Mice were only injected with A $\beta$  1-40 antibody (red colour) without the presence of MBs and FUS application. A $\beta$  1-40 antibody (red colour) was not present in any of the mice brain sections (Figure 63-65). Immunohistochemistry analysis performed on the brain sections of mice from group C showed entry of the A $\beta$  1-40 antibody to their brain (Figure 66-70).

### Group A

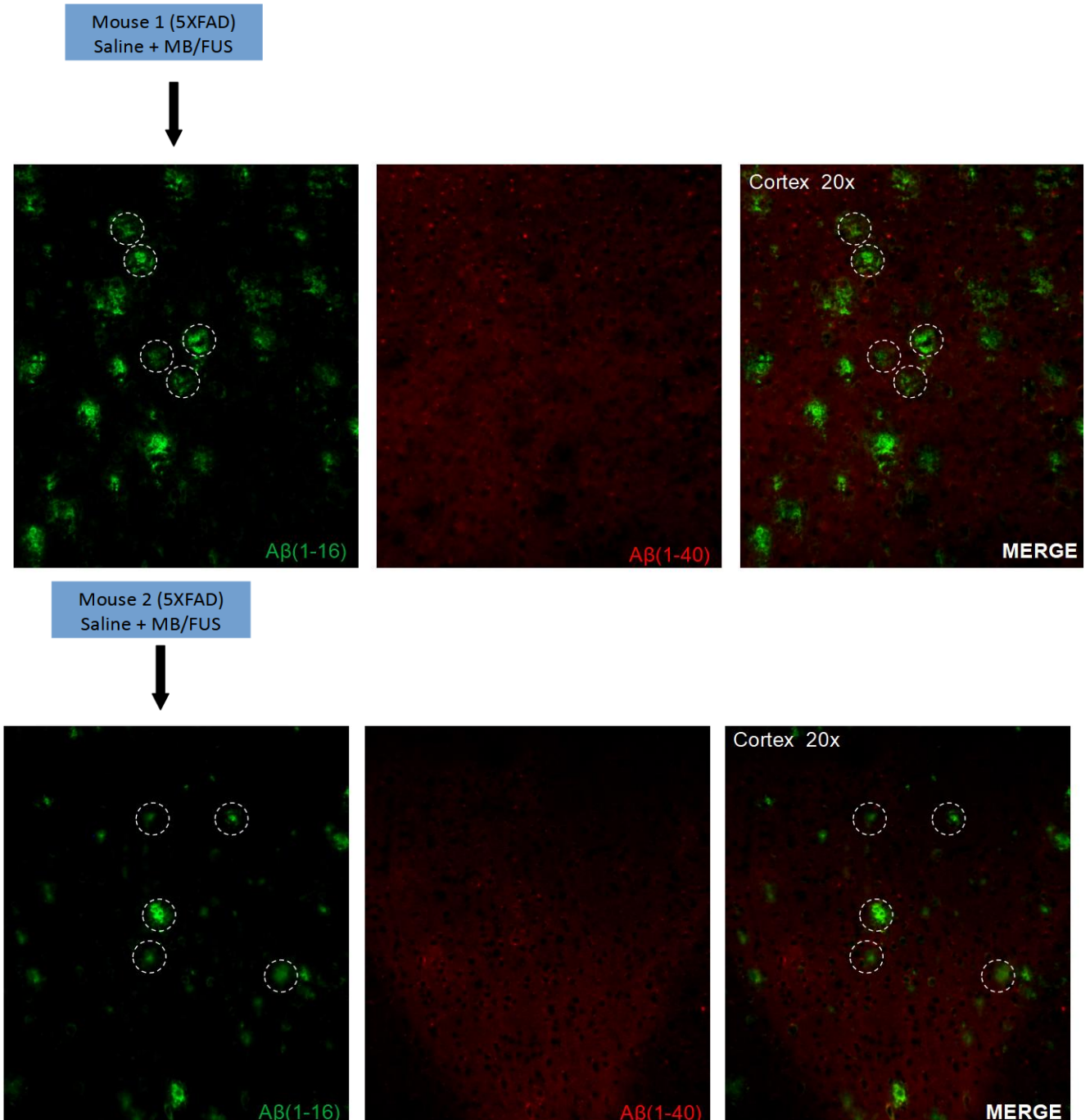


**Figure 60:** Immunohistochemistry analysis of brain tissue sections of 5XFAD mice (Mouse 1&2) injected with 50  $\mu$ L of saline and 5  $\mu$ L of MBs followed by FUS (50W). A $\beta$  (1-16) indicated the presence of amyloid plaques in the cortex. Saline injected mice were used as negative controls (no presence of A $\beta$  1-40 red colour).

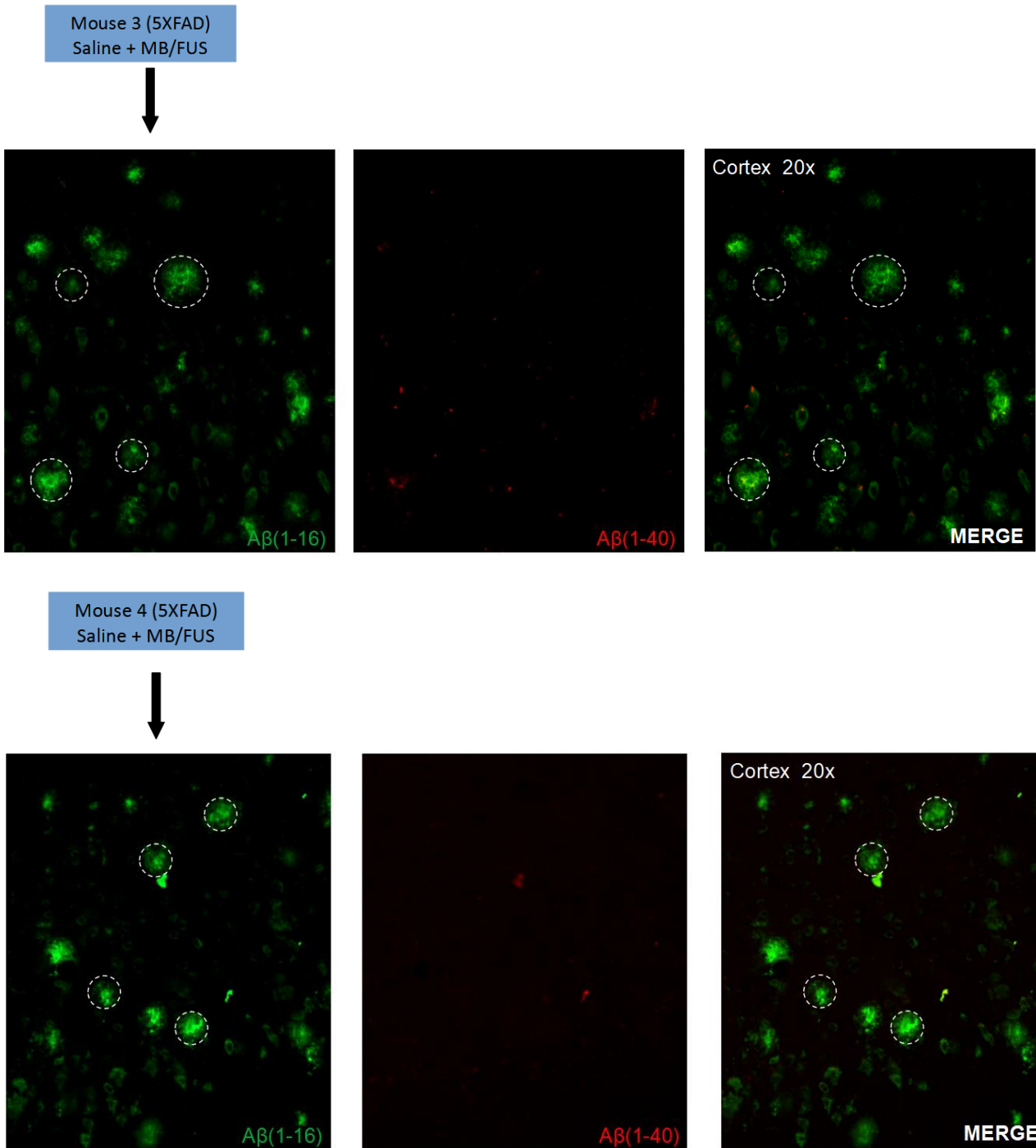


**Figure 61:** Immunohistochemistry analysis of brain tissue sections of 5XFAD mice (Mouse 3&4) injected with 50  $\mu$ L of saline and 5  $\mu$ L of MBs followed by FUS (50W). A $\beta$  (1-16) indicated the presence of amyloid plaques in the cortex.

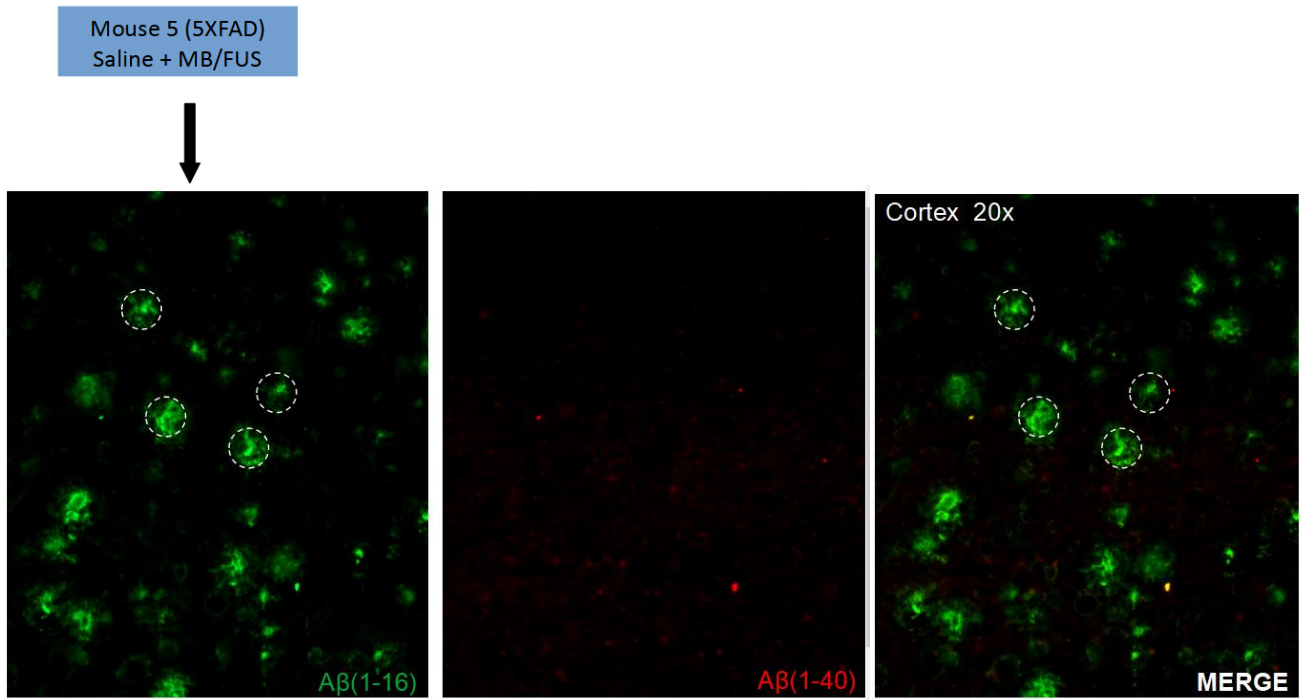


**Figure 62:** Immunohistochemistry analysis of brain tissue sections of 5XFAD mice (Mouse 5) injected with 50  $\mu$ L of saline and 5  $\mu$ L of MBs followed by FUS (50W). A $\beta$  (1-16) indicated the presence of amyloid plaques in the cortex.

### Group B

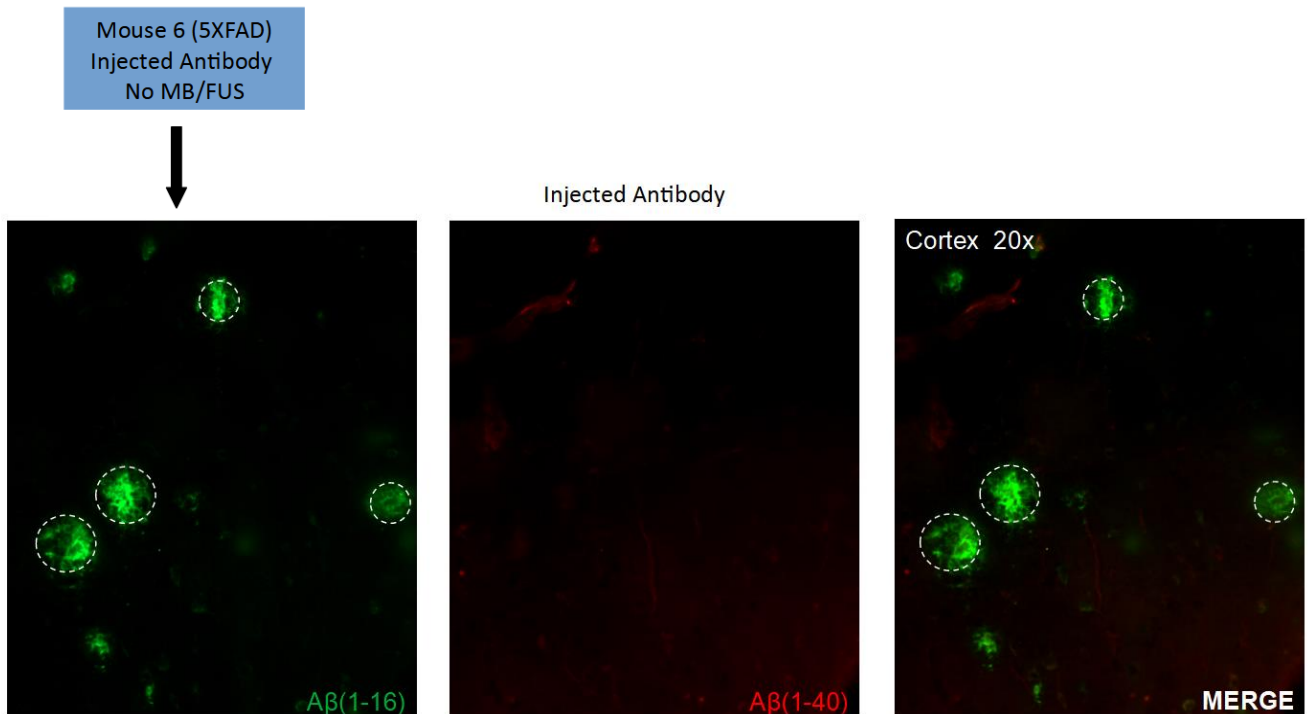


**Figure 63:** Immunohistochemistry analysis of brain tissue sections of 5XFAD mouse (Mouse 6) injected with 50  $\mu$ L of A $\beta$  (1-40, red colour). A $\beta$  (1-16) staining confirmed the presence of amyloid plaques in the cortex. Injected A $\beta$  (1-40, red colour) was not found in the brain.

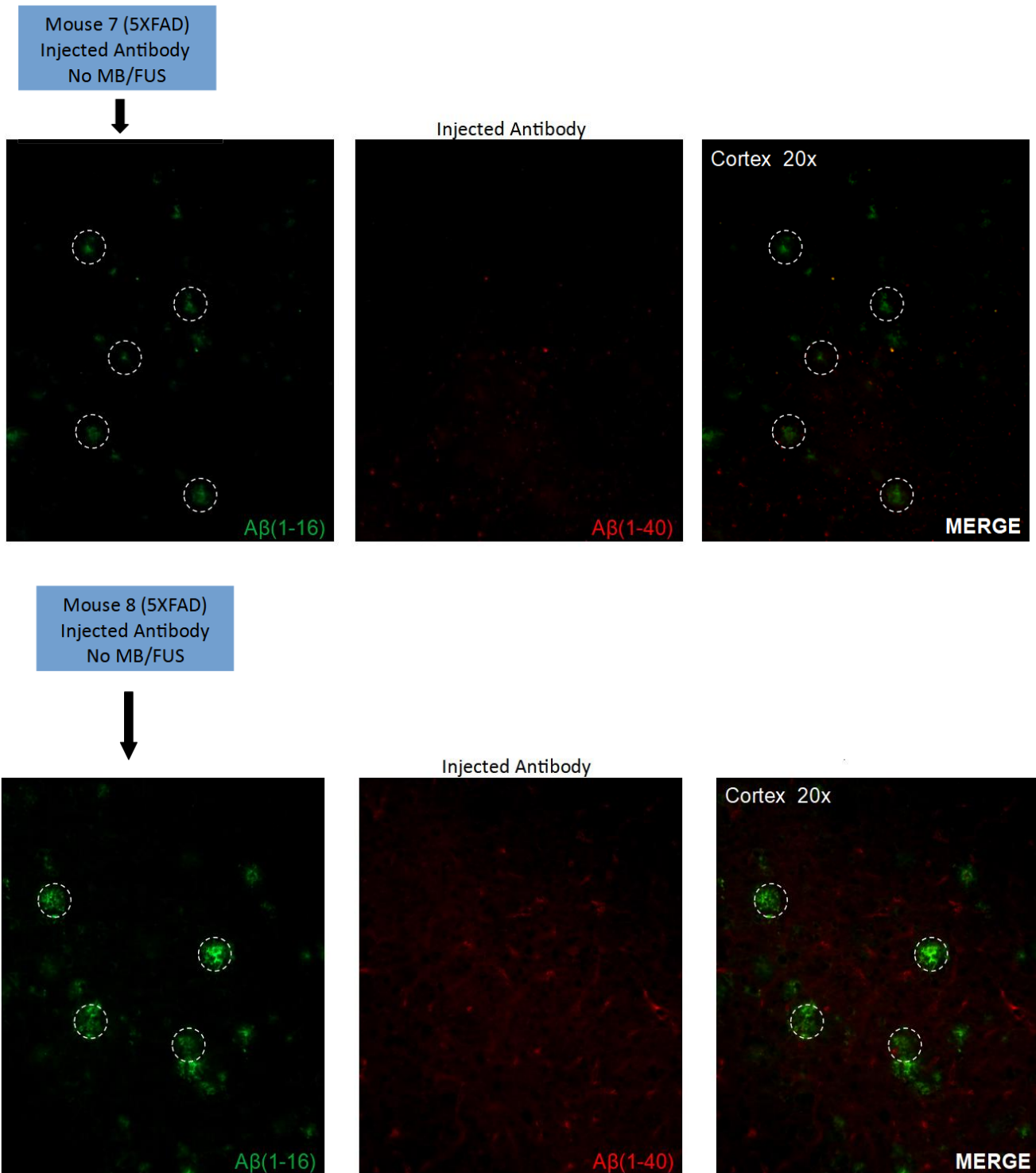


**Figure 64:** Immunohistochemistry analysis of brain tissue sections of 5XFAD mice (Mouse 7&8) injected with 50  $\mu$ L of  $A\beta$  (1-40, red colour).  $A\beta$  (1-16) staining confirmed the presence of amyloid plaques in the cortex. Injected  $A\beta$  (1-40, red colour) was not found in the brain.

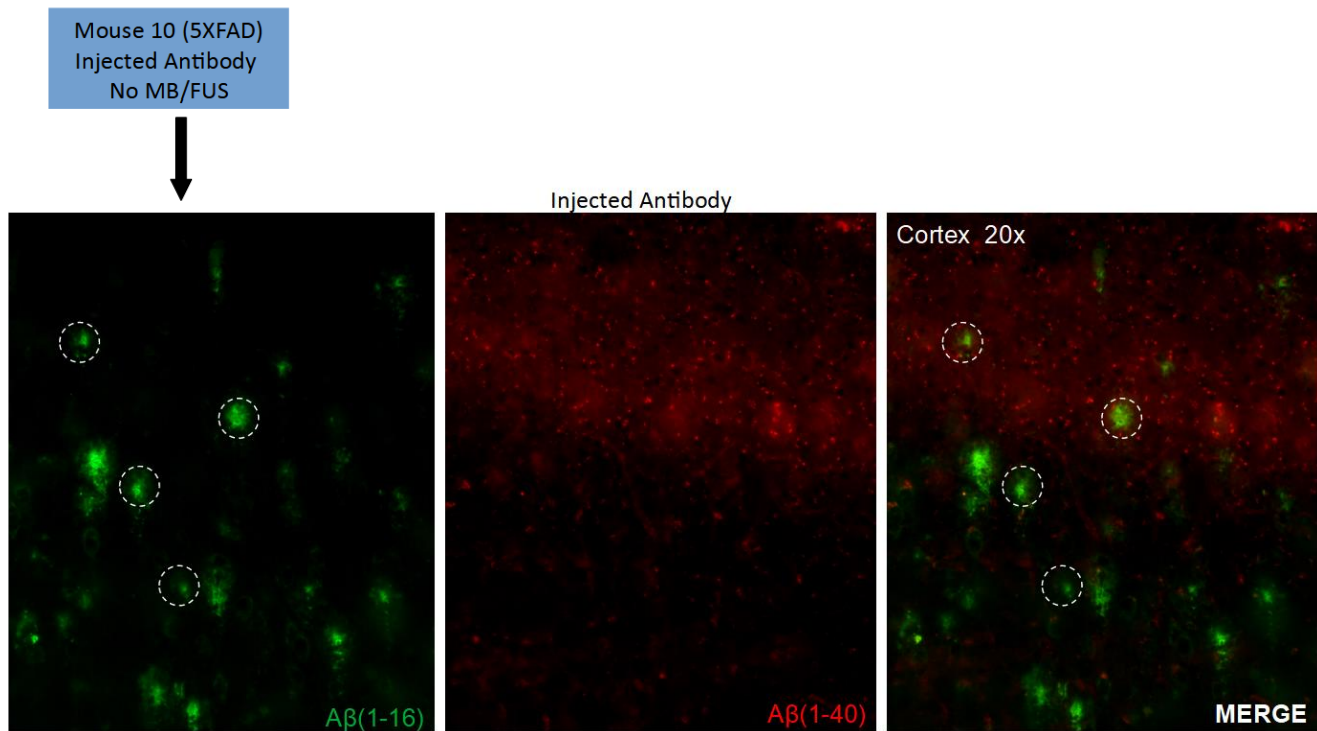
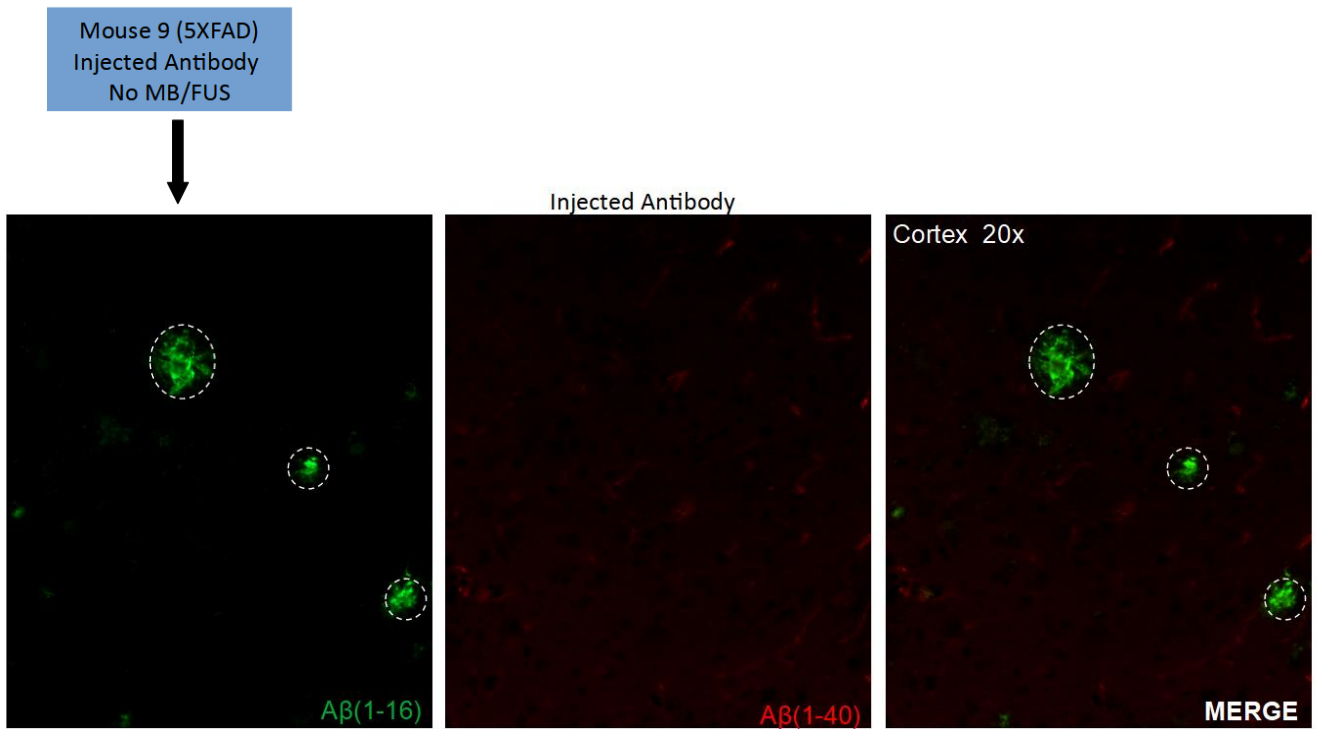


**Figure 65:** Immunohistochemistry analysis of brain tissue sections of 5XFAD mice (Mouse 9&10) injected with 50  $\mu$ L of A $\beta$  (1-40, red colour). A $\beta$  (1-16) staining confirmed the presence of amyloid plaques in the cortex. Injected A $\beta$  (1-40, red colour) was not found in the brain.

## Group C

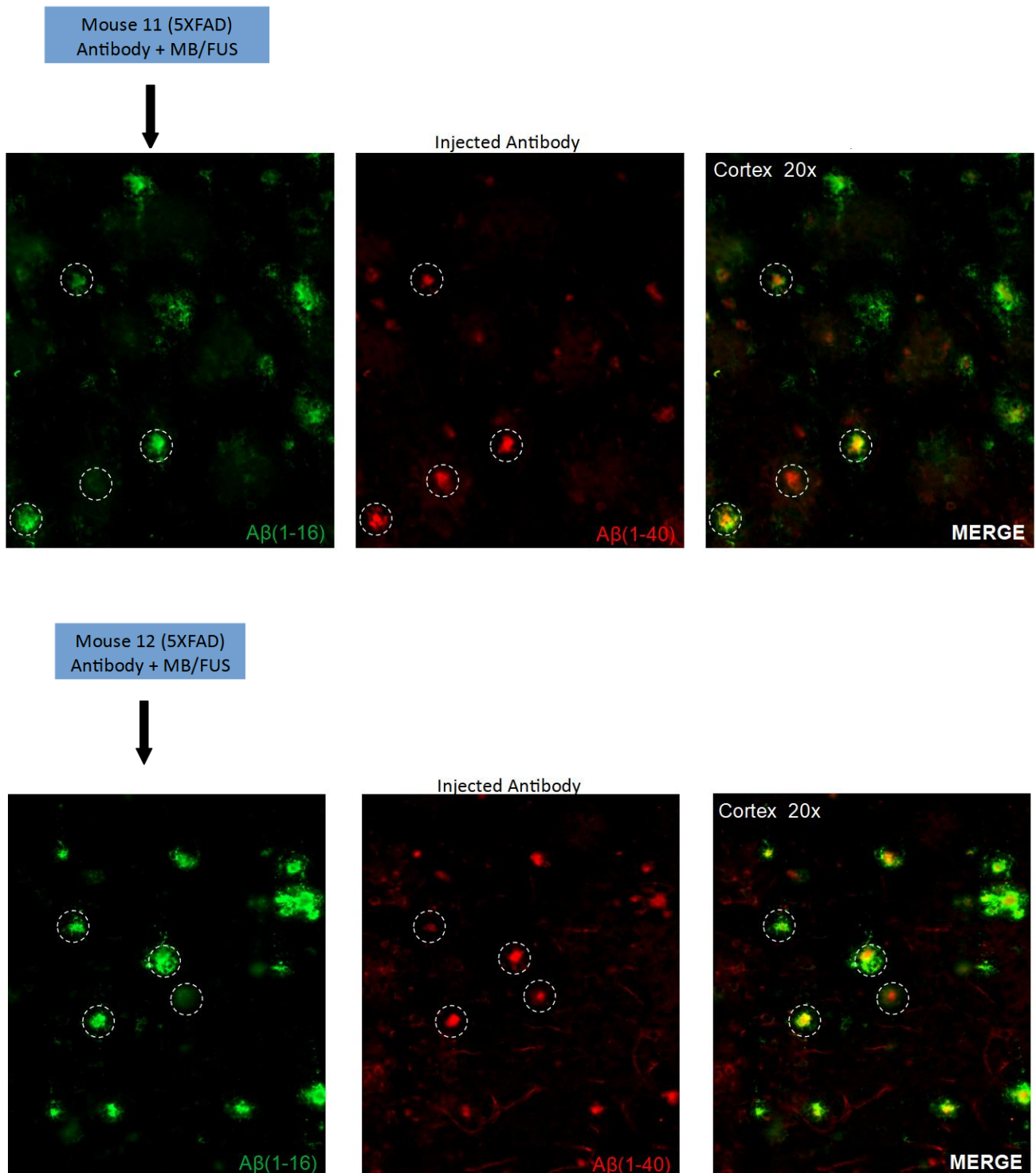


**Figure 66:** Immunohistochemistry analysis of brain tissue sections of 5XFAD mice (Mouse 11&12) injected with 50  $\mu$ L of A $\beta$  (1-40, red colour) and 5  $\mu$ L of MBs followed by FUS (50W). A $\beta$  (1-16) staining confirmed the presence of amyloid plaques in the cortex. Co-localization of antibodies (white circles, green and red colours) in the cortex confirmed the successful entry and specific binding of the A $\beta$  (1-40) into the brain.

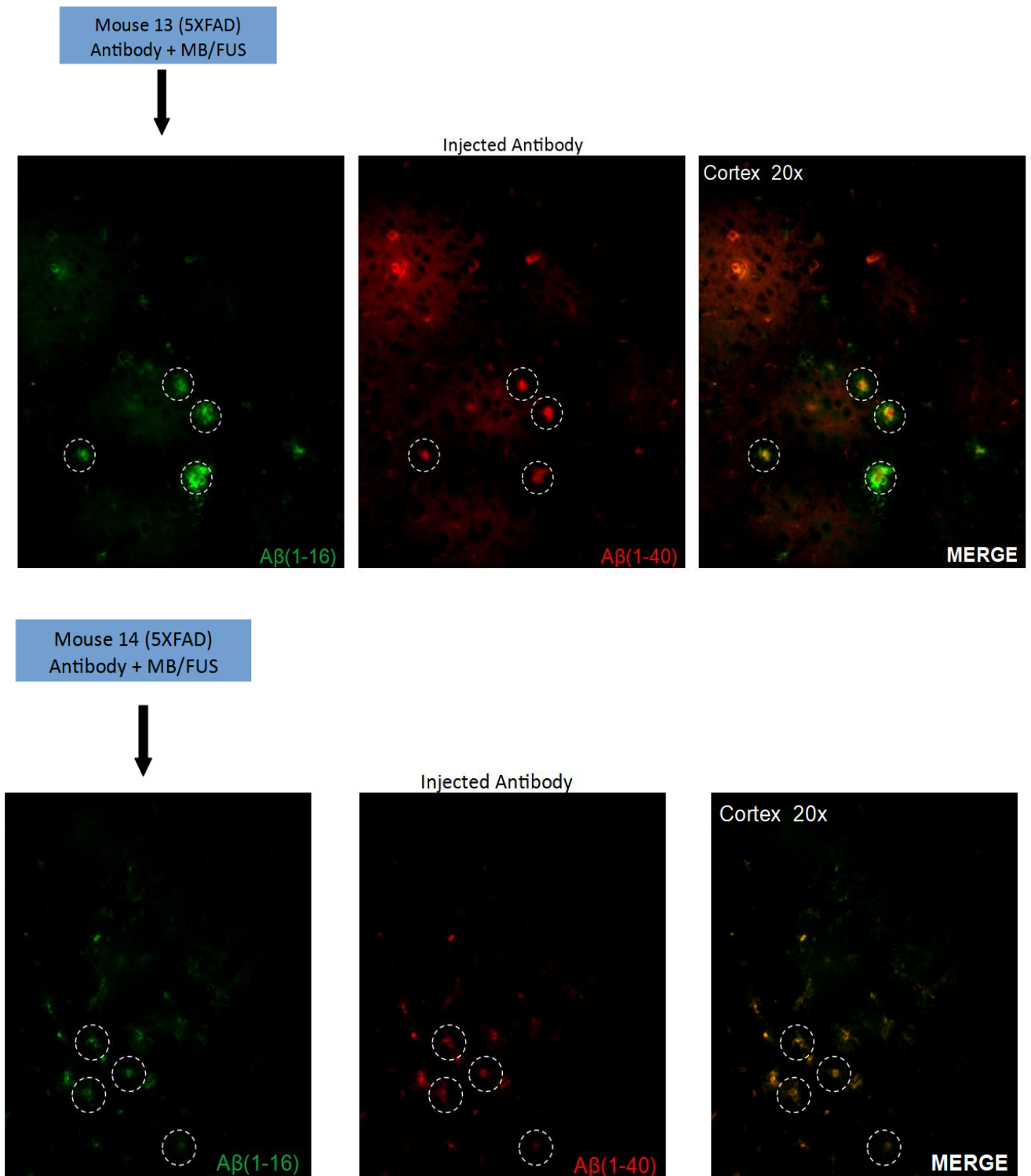


**Figure 67:** Immunohistochemistry analysis of brain tissue sections of 5XFAD mice (Mouse 13 & 14) injected with 50  $\mu$ L of A $\beta$  (1-40, red colour) and 5  $\mu$ L of MBs followed by FUS (50W). A $\beta$  (1-16) staining confirmed the presence of amyloid plaques in the cortex. Co-localization of antibodies (white circles, green and red colours) in the cortex confirmed the successful entry and specific binding of the A $\beta$  (1-40) into the brain.

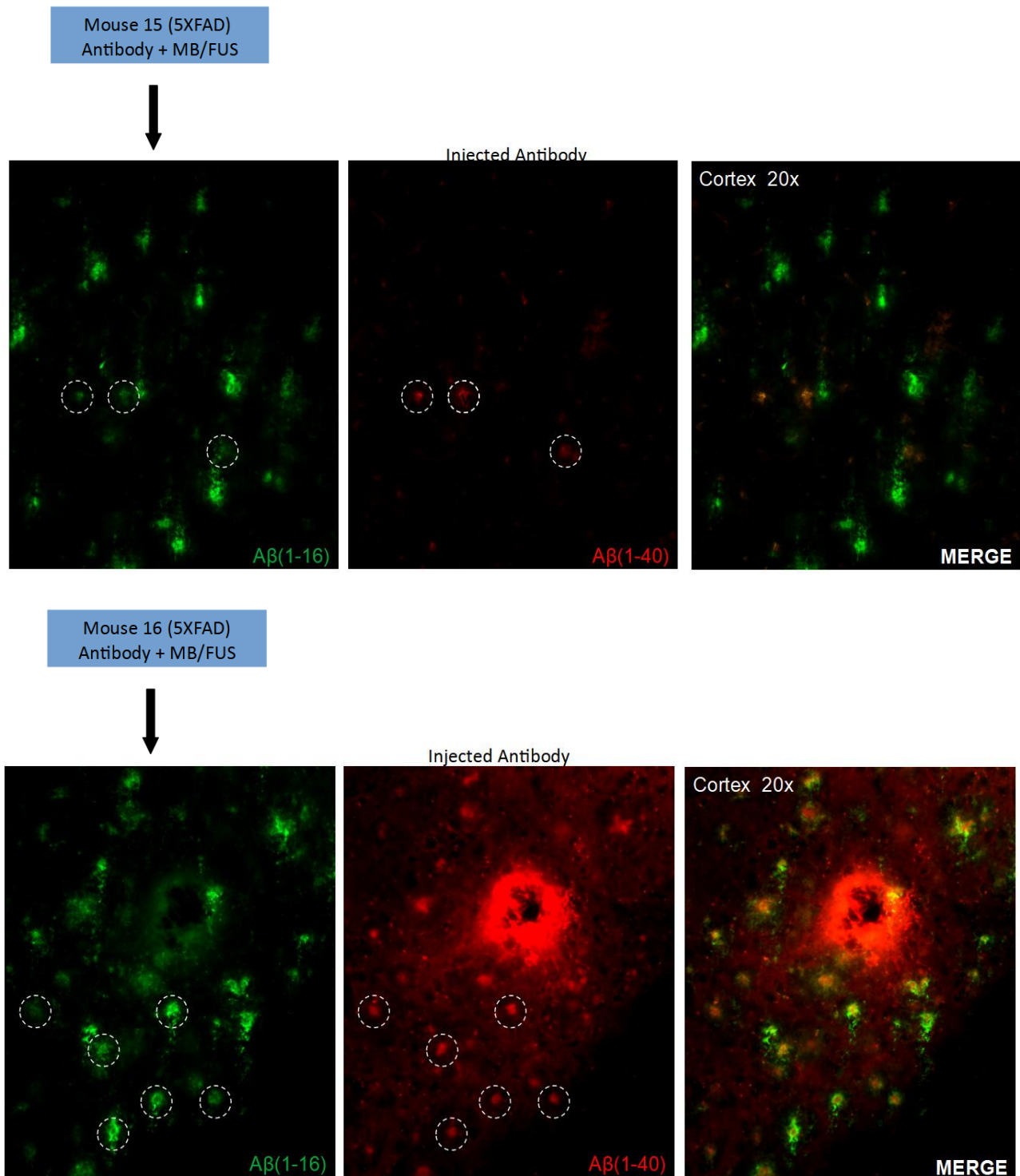


**Figure 68:** Immunohistochemistry analysis of brain tissue sections of 5XFAD mice (Mouse 15 & 16) injected with 50  $\mu$ L of A $\beta$  (1-40, red colour) and 5  $\mu$ L of MBs followed by FUS (50W). A $\beta$  (1-16) staining confirmed the presence of amyloid plaques in the cortex. Co-localization of antibodies (white circles, green and red colours) in the cortex confirmed the successful entry and specific binding of the A $\beta$  (1-40) into the brain.

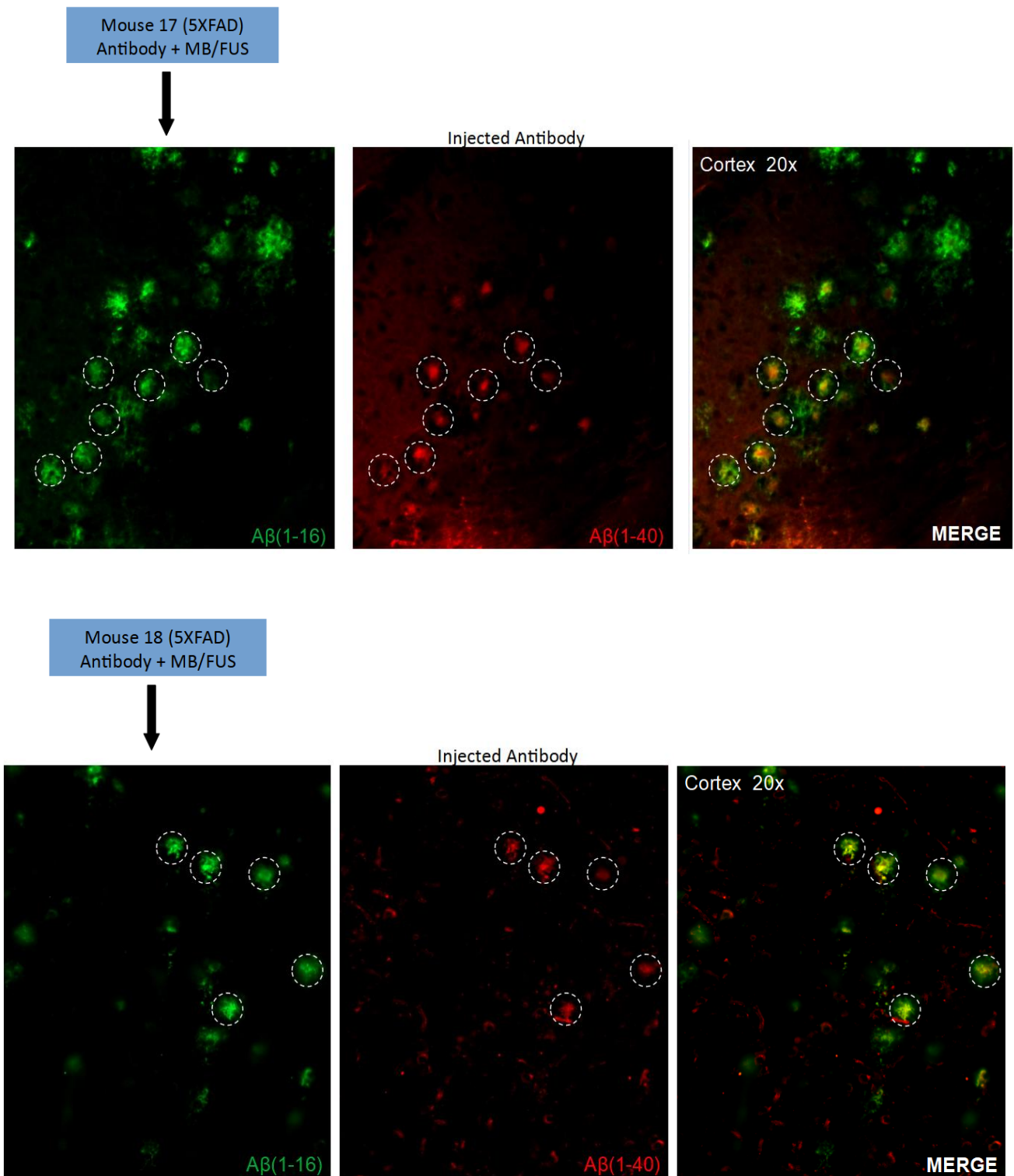


**Figure 69:** Immunohistochemistry analysis of brain tissue sections of 5XFAD mice (Mouse 17 & 18) injected with 50  $\mu$ L of A $\beta$  (1-40, red colour) and 5  $\mu$ L of MBs followed by FUS (50W). A $\beta$  (1-16) staining confirmed the presence of amyloid plaques in the cortex. Co-localization of antibodies (white circles, green and red colours) in the cortex confirmed the successful entry and specific binding of the A $\beta$  (1-40) into the brain.

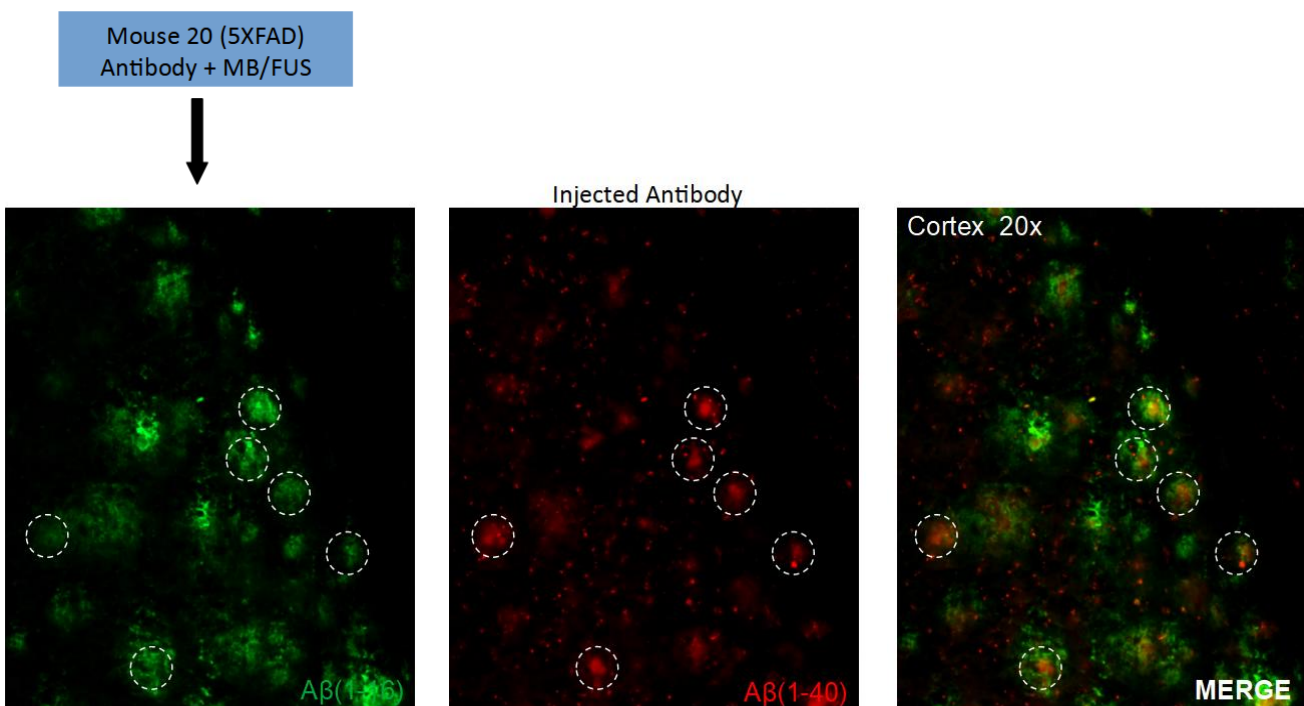
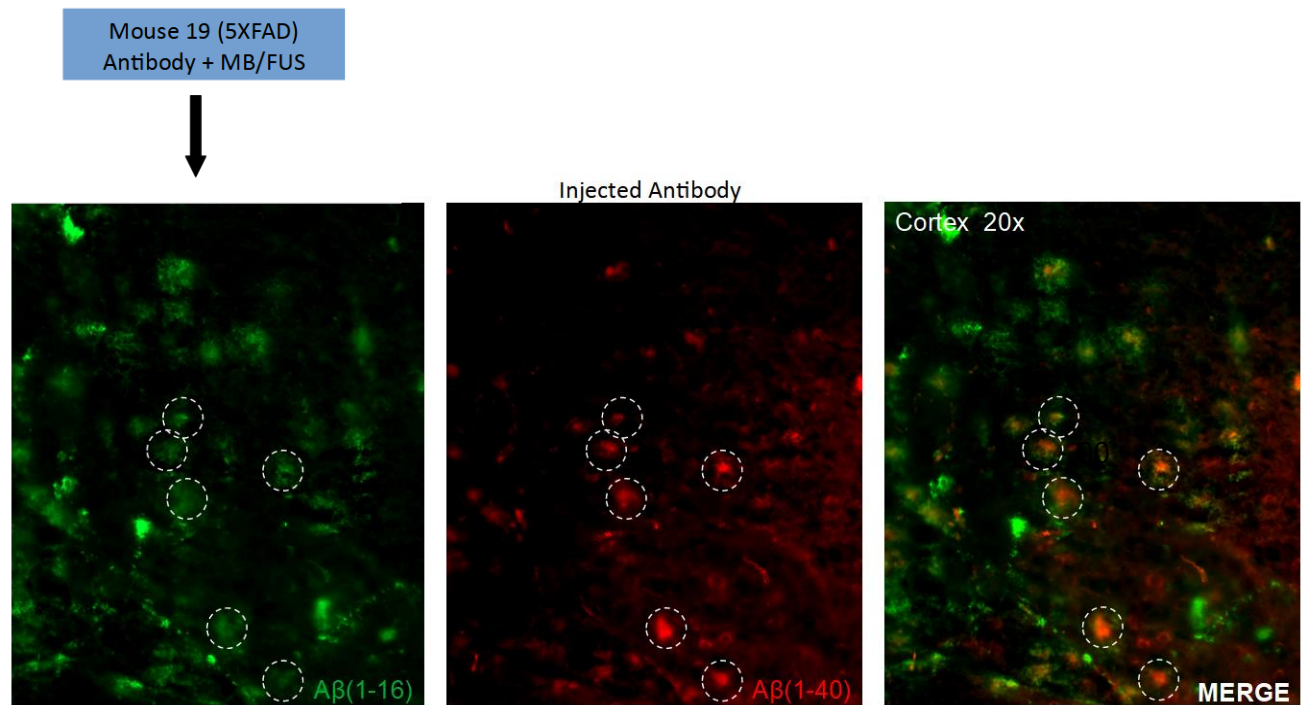


**Figure 70:** Immunohistochemistry analysis of brain tissue sections of 5XFAD mice (Mouse 19 & 20) injected with 50  $\mu$ L of A $\beta$  (1-40, red colour) and 5  $\mu$ L of MBs followed by FUS (50W). A $\beta$  (1-16) staining confirmed the presence of amyloid plaques in the cortex. Co-localization of antibodies (white circles, green and red colours) in the cortex confirmed the successful entry and specific binding of the A $\beta$  (1-40) into the brain.

## Testing whether FUS mediated BBB disruption facilitates AAV9 penetration into the CNS

After we established the optimal parameters for BBBD, we used the AAV9.MBP.EGFP vector for testing the feasibility of FUS induced BBB transient disruption to facilitate AAV9 penetration into the CNS. This vector had been checked before the FUS experiment to 4 WT mice of 1 month-old with tail vein injection (50 $\mu$ L). 5  $\mu$ L/g of body weight of AAV9 vector was injected intravenously into each mouse. Two (2) mice received 50  $\mu$ L of the vector and 2 the half dose (Table 3). The mice were sacrificed with PFA after 4 weeks.

**Table 3:** The groups of mice used in this experimental part, the amount of vector and sonication parameters used in each.

Group	# of mice	Electric power (W)	MBs ( $\mu$ L)	Vector ( $\mu$ L)
A	2	60	5	50 ( $2 \times 10^{12}$ vg)
B	2	60	5	25+25 $\mu$ L (H <sub>2</sub> O) ( $1 \times 10^{12}$ vg)

Slides containing brain sections were directly visualized using a fluorescence microscope. Cryosections from brain were immunostained for EGFP. DNA was extracted from the brain, cerebellum, brainstem, and spinal cord for vector genome copy number determination.

Representative photos of EGFP immunofluorescence are shown in Figures 71-73. Figure 74 shows graphs of the VGCN calculated for the brain and spinal cord areas for each tested treatment protocol.

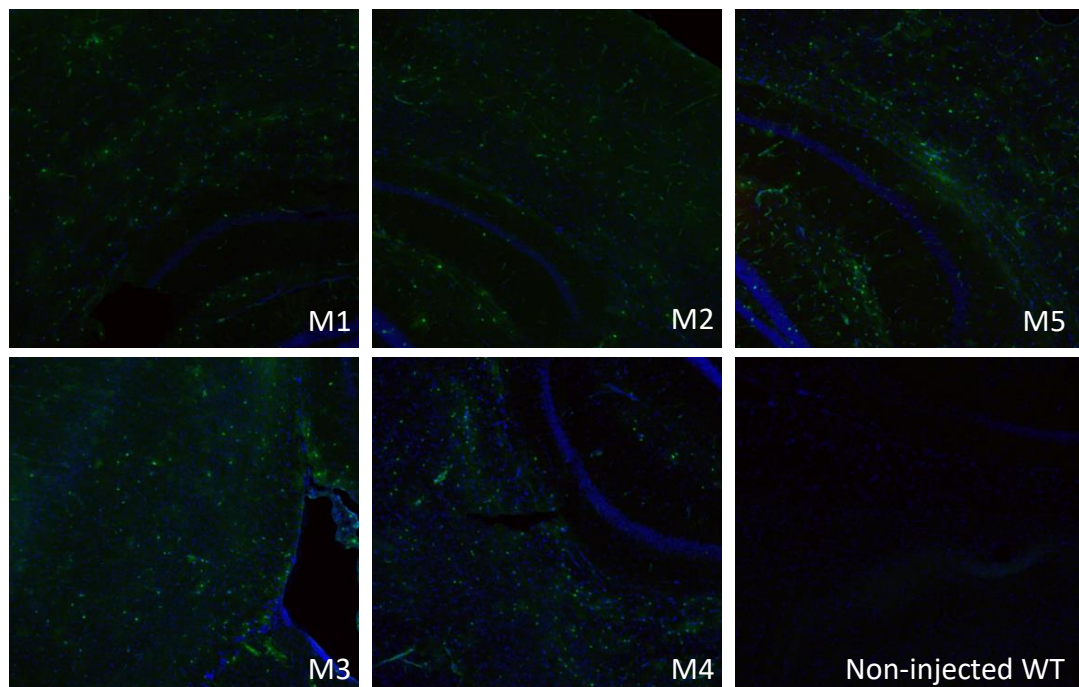


**Figure 71:** Representative photos (10x) from all the tested mice of EGFP immunofluorescence staining in Corpus Callosum. M1-M2: 25 $\mu$ L of vector+ 25 $\mu$ L H<sub>2</sub>O +5 $\mu$ L of MBs, M3-M4: 50 $\mu$ L of vector +5 $\mu$ L of MBs, M5: Injected with 50 $\mu$ L of vector and non-injected mouse.

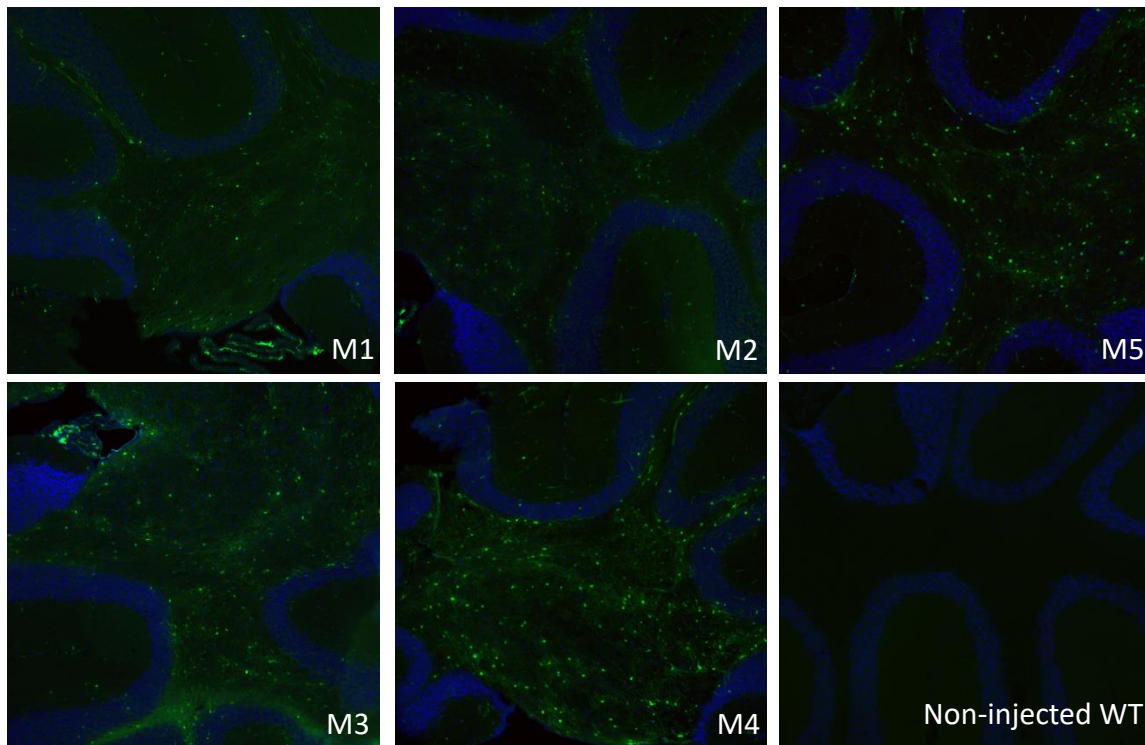


**Figure 72:** Representative photos (10x) from all the tested mice of EGFP immunofluorescence staining in cerebellum. M1-M2: 25 $\mu$ L of vector+ 25 $\mu$ L H<sub>2</sub>O + 5 $\mu$ L of MBs, M3-M4: 50 $\mu$ L of vector +5 $\mu$ L of MBs, M5: Injected with 50 $\mu$ L of vector and non-injected mouse.

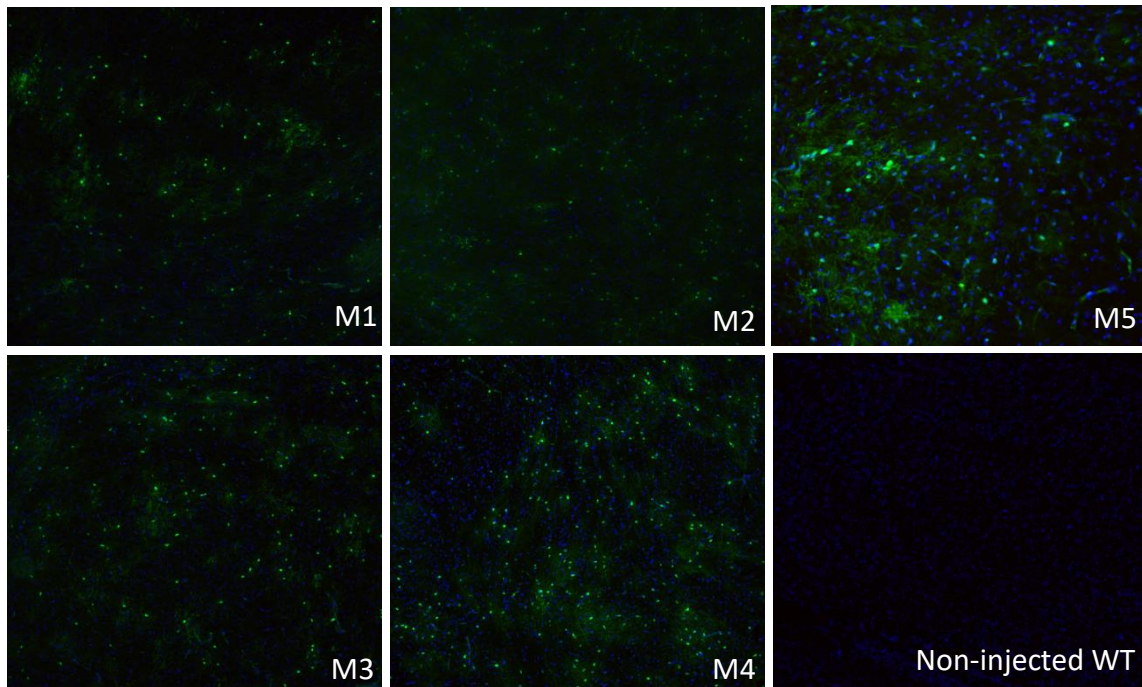


**Figure 73:** Representative photos (10x) from all the tested mice of EGFP immunofluorescence staining in internal capsule. M1-M2: 25 $\mu$ L of vector+ 25 $\mu$ L H<sub>2</sub>O + 5 $\mu$ L of MBs, M3-M4: 50 $\mu$ L of vector +5 $\mu$ L of MBs, M5: Injected with 50 $\mu$ L of vector and non-injected mouse.

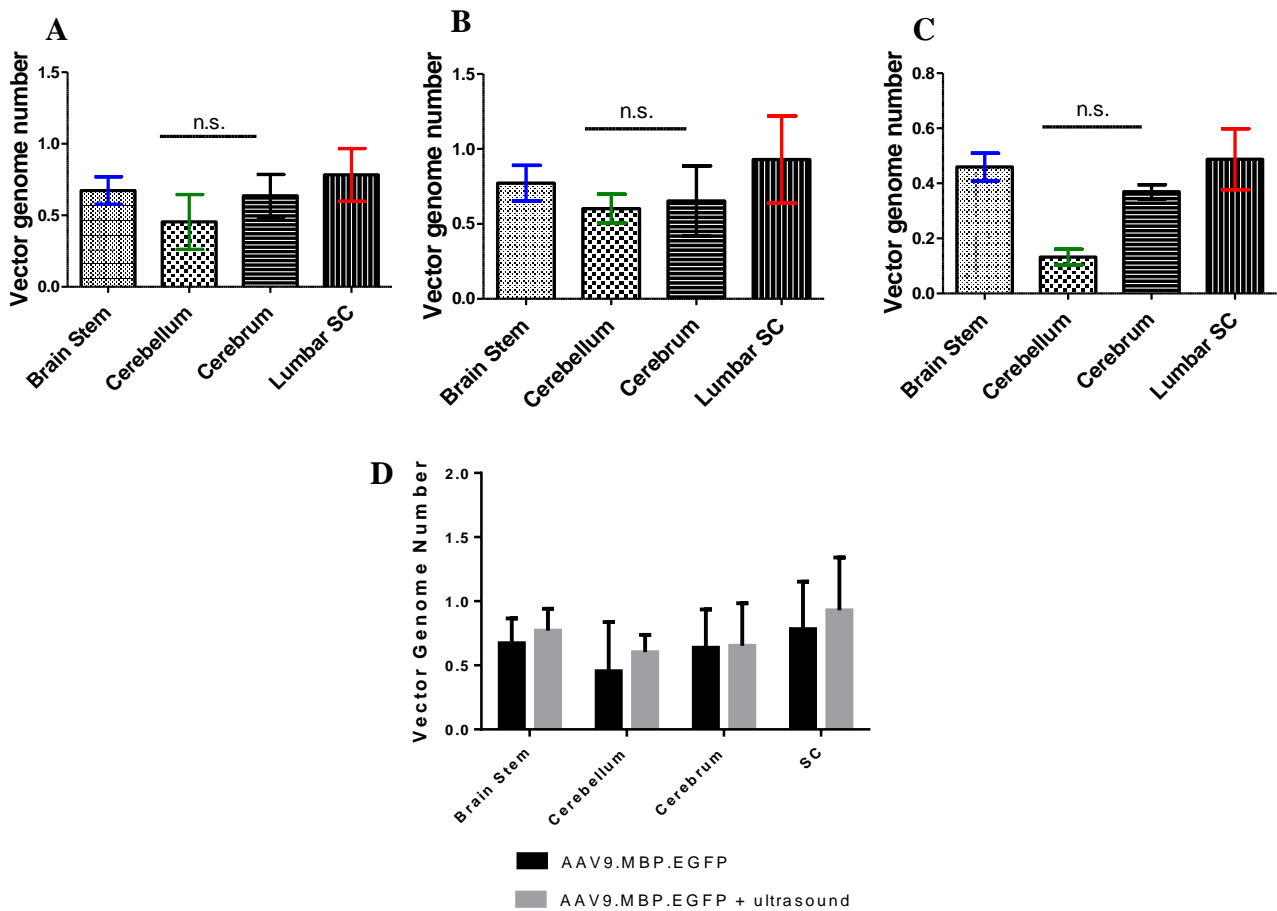


**Figure 74:** Vector genome number (VCN) at A: P30 WT mice injected with AAV9.MBP.EGFP (n=4), B: P30 WT mice injected with 50  $\mu$ L AAV9.MBP.EGFP + MBs (n=2), C: P30 WT mice injected with 25  $\mu$ L of AAV9.MBP.EGFP+ MBs, D: Comparison of VCNs between 2 groups of P30 WT mice injected with 50 $\mu$ L of vector.

All CNS tissues show high rates of EGFP compared to the non-injected mouse (control). Furthermore, we observe that the sonicated mice injected with 5  $\mu$ L MBs and 50  $\mu$ L vector has a tendency for higher levels of EGFP in many brain areas than the mice which injected only with the vector, although this is not consistent. Mice injected with MBs and the half amount of vector show the lower expression, and we do not have a comparison of vector alone with this dose. According to the estimated VCN levels, the mice injected with 5  $\mu$ L MBs and 50  $\mu$ L of the AAV9 vector appear to have the highest transduction rates, however we need to repeat this experiment with more mice and compare the results with and without FUS at both vector doses.

## DISCUSSION

EB leakage in brain parenchyma is clearly visible in mice (WT B6/SJL) treated with FUS and MBs administration, given that proper acoustic coupling is achieved. Mice treated with higher acoustic power showed higher levels of EB dye in the brain tissue covering a larger area. H&E staining showed no damage to the brain by FUS at any electric power.

Based on these observations, electrical power value of 50 W was used in the following experiments in which mice (5XFAD) were injected with the A $\beta$  (1-40) antibody. The use of transcranial application of FUS and MBs was capable to open the BBB and allow the antibody to enter the mouse brain (5XFAD). Mice (5XFAD) injected with the antibody but in the absence of MBs and FUS did not show any signs of the antibody in their brains. This is an indication that without disruption of the BBB with FUS the antibody was unable to pass the BBB. It is well known that only a small number of molecules (hydrophobic molecules such as O<sub>2</sub>, CO<sub>2</sub>, hormones and small non-polar molecules) can pass into the brain.<sup>37</sup> The volume of the antibody is also a significant factor. Identifying the optimal antibody volume will lead to higher number of antibody-bound amyloid plaques. It is also important to address the significance of proper acoustic coupling as insufficient acoustic coupling will not lead to the disruption of the BBB.

Transcranial application of FUS in mice (5XFAD, group C, n=10) injected with 50  $\mu$ L of A $\beta$  1-40 antibody and 5  $\mu$ L MBs opened the BBB with a success rate of 100% as the A $\beta$  1-40 antibody was found in the brain of every mouse. These findings were also validated by the observations from mice (5XFAD, group A) injected with saline and MBs and followed by transcranial application of FUS, which did not have any signs of antibody.

Furthermore, FUS-induced BBBD was performed using electric power of 60 W (and 5  $\mu$ L of MBs) prior to intravenously injecting different doses (50  $\mu$ L or 25  $\mu$ L+25  $\mu$ L H<sub>2</sub>O) of the AAV9-*Mbp-Egfp* vector driving EGFP reporter gene expression in P30 WT mice. The biodistribution of the vector in the CNS was examined by measuring VGCNs in extracted DNA from different CNS areas, as well as oligodendrocyte EGFP expression rates in different CNS areas. The sonicated mice that were injected with 50  $\mu$ L of the AAV9 vector had a tendency for higher levels of EGFP in many brain areas than the non-sonicated mice and appear to have the highest transduction rates. However, further experiments with more mice are required to obtain sufficient evidence and confirm the significance of FUS-mediated BBBD in terms of enhancing the delivery of this specific vector and potentially reducing the amount of vector needed to achieve therapeutic levels in the mouse brain.

All the above, clearly show that the use of FUS in synergy with MBs is a highly accurate and reproducible way to open the BBB, provided the use of optimized parameters, which can be exploited further for therapeutic intervention. The study findings provide clear evidence that FUS plus MBs mediated BBBD enables the delivery of the A $\beta$ (1-40) antibody into the brain parenchyma of a mouse model of the Alzheimer disease, whereas normally this antibody cannot pass through the BBB. The effects of antibody delivery on the plaque pathology is left to be examined. Regarding FUS-mediated biodistribution of the AAV9 vector in the CNS, the results are very promising and further research is required to investigate whether FUS-mediated BBBD allows the use of lower vector doses, which is essential for minimizing side effects.

## REFERENCES

- [1] J. Dobbing, “The Blood-Brain Barrier,” *Dev. Med. Child Neurol.*, vol. 3, no. 6, pp. 610–612, 1961, doi: 10.1111/j.1469-8749.1961.tb10430.x.
- [2] R. Pandit, L. Chen, and J. Götz, “The blood-brain barrier: Physiology and strategies for drug delivery,” *Adv. Drug Deliv. Rev.*, vol. 165–166, pp. 1–14, 2020, doi: 10.1016/j.addr.2019.11.009.
- [3] Z. Ebrahimi, S. Talaei, S. Aghamiri, N. H. Goradel, A. Jafarpour, and B. Negahdari, “Overcoming the blood–brain barrier in neurodegenerative disorders and brain tumours,” *IET Nanobiotechnology*, vol. 14, no. 6, pp. 441–448, 2020, doi: 10.1049/iet-nbt.2019.0351.
- [4] S. Harilal *et al.*, “Revisiting the blood-brain barrier: A hard nut to crack in the transportation of drug molecules,” *Brain Res. Bull.*, vol. 160, pp. 121–140, 2020, doi: 10.1016/j.brainresbull.2020.03.018.
- [5] B. S. Karmur *et al.*, “Blood-Brain Barrier Disruption in Neuro-Oncology: Strategies, Failures, and Challenges to Overcome,” *Front. Oncol.*, vol. 10, 2020, doi: 10.3389/fonc.2020.563840.
- [6] A. Rodriguez, S. B. Tatter, and W. Debinski, “Neurosurgical techniques for disruption of the blood–brain barrier for glioblastoma treatment,” *Pharmaceutics*, vol. 7, no. 3, pp. 175–187, 2015, doi: 10.3390/pharmaceutics7030175.
- [7] A. H. Mesiwala *et al.*, “High-intensity focused ultrasound selectively disrupts the blood-brain barrier in vivo,” *Ultrasound Med. Biol.*, vol. 28, no. 3, pp. 389–400, 2002, doi: 10.1016/S0301-5629(01)00521-X.
- [8] Y. Yang *et al.*, “Cavitation dose painting for focused ultrasound-induced blood-brain barrier disruption,” *Sci. Rep.*, vol. 9, no. 1, pp. 1–10, 2019, doi: 10.1038/s41598-019-39090-9.
- [9] N. Sheikov, N. McDannold, N. Vykhodtseva, F. Jolesz, and K. Hynynen, “Cellular mechanisms of the blood-brain barrier opening induced by ultrasound in presence of microbubbles,” *Ultrasound Med. Biol.*, vol. 30, no. 7, pp. 979–989, 2004, doi: 10.1016/j.ultrasmedbio.2004.04.010.
- [10] J. M. Wasielewska and A. R. White, ““Focused Ultrasound-mediated Drug Delivery in Humans – a Path Towards Translation in Neurodegenerative Diseases,”” *Pharm. Res.*, vol. 39, no. 3, pp. 427–439, 2022, doi: 10.1007/s11095-022-03185-2.
- [11] K. Hynynen, N. McDannold, N. A. Sheikov, F. A. Jolesz, and N. Vykhodtseva, “Local and reversible blood – brain barrier disruption by noninvasive focused ultrasound at frequencies suitable for trans-skull sonications,” vol. 24, pp. 12–20, 2005, doi: 10.1016/j.neuroimage.2004.06.046.
- [12] J. J. Choi, S. Wang, Y.-S. Tung, B. Morrison, and E. E. Konofagou, “Molecules of various pharmacologically-relevant sizes can cross the ultrasound-induced blood-brain barrier opening in vivo,” *Ultrasound Med Biol.*, vol. 36, no. 1, pp. 58–67, 2010, doi: 10.1016/j.ultrasmedbio.2009.08.006.
- [13] K. Chen, K. Wei, and H. Liu, “Theranostic Strategy of Focused Ultrasound Induced Blood-Brain Barrier Opening for CNS Disease Treatment,” vol. 10, no. February, 2019, doi: 10.3389/fphar.2019.00086.
- [14] M. G. Z. Ghali, V. M. Srinivasan, and P. Kan, “Focused Ultrasonography-Mediated Blood-

Brain Barrier Disruption in the Enhancement of Delivery of Brain Tumor Therapies,” *World Neurosurg.*, vol. 131, pp. 65–75, 2019, doi: 10.1016/j.wneu.2019.07.096.

- [15] P. S. Fishman and J. M. Fischell, “Focused Ultrasound Mediated Opening of the Blood-Brain Barrier for Neurodegenerative Diseases,” *Front. Neurol.*, vol. 12, no. November, pp. 1–5, 2021, doi: 10.3389/fneur.2021.749047.
- [16] C. Y. Lin *et al.*, “Focused ultrasound-induced blood-brain barrier opening for non-viral, non-invasive, and targeted gene delivery,” *J. Control. Release*, vol. 212, pp. 1–9, 2015, doi: 10.1016/j.jconrel.2015.06.010.
- [17] “Alzheimer’s Disease International,” *Dementia facts and figures*. [Online]. Available: <https://www.alz.co.uk/research/statistics>. [Accessed: 14-Aug-2022].
- [18] J. J. Choi, S. Wang, T. R. Brown, S. A. Small, K. E. K. Duff, and E. E. Konofagou, “Noninvasive and Transient Blood-Brain Barrier Opening in the Hippocampus of Alzheimer’s Double Transgenic Mice Using Focused Ultrasound,” *Ultrason. Imaging*, vol. 30, no. 3, pp. 189–200, 2008.
- [19] J. F. Jordão *et al.*, “Amyloid- $\beta$  plaque reduction, endogenous antibody delivery and glial activation by brain-targeted, transcranial focused ultrasound,” *Exp Neurol*, vol. 248, pp. 16–29, 2013, doi: 10.1016/j.expneurol.2013.05.008.
- [20] Y. Shen, L. Hua, C. Yeh, L. Shen, M. Ying, and Z. Zhang, “Ultrasound with microbubbles improves memory, ameliorates pathology and modulates hippocampal proteomic changes in a triple transgenic mouse model of Alzheimer’s disease,” *Theranostics*, vol. 10, no. 25, pp. 11794–11819, 2020, doi: 10.7150/thno.44152.
- [21] C. T. Poon *et al.*, “Time course of focused ultrasound effects on  $\beta$ -amyloid plaque pathology in the TgCRND8 mouse model of Alzheimer’s disease,” *Sci. Rep.*, vol. 8, no. 1, pp. 1–11, 2018, doi: 10.1038/s41598-018-32250-3.
- [22] P. H. Hsu *et al.*, “Focused Ultrasound-Induced Blood-Brain Barrier Opening Enhances GSK-3 Inhibitor Delivery for Amyloid-Beta Plaque Reduction,” *Sci. Rep.*, vol. 8, no. 1, pp. 1–9, 2018, doi: 10.1038/s41598-018-31071-8.
- [23] J. L. Frost *et al.*, “An anti-pyroglutamate-3 A $\beta$  vaccine reduces plaques and improves cognition in APPswe/PS1 $\Delta$ E9 mice,” *Neurobiol Aging*, vol. 36, no. 12, pp. 3187–3199, 2015, doi: 10.1016/j.neurobiolaging.2015.08.021.
- [24] K. Xhima, K. Markham-Coultes, R. Hahn Kofoed, H. U. Saragovi, K. Hynynen, and I. Aubert, “Ultrasound delivery of a TrkA agonist confers neuroprotection to Alzheimer-associated pathologies,” *Brain*, vol. 145, no. 8, pp. 2806–2822, 2022, doi: 10.1093/brain/awab460.
- [25] J. F. Jordão *et al.*, “Antibodies targeted to the brain with image-guided focused ultrasound reduces amyloid- $\beta$  plaque load in the TgCRND8 mouse model of Alzheimer’s disease,” *PLoS One*, vol. 5, no. 5, pp. 4–11, 2010, doi: 10.1371/journal.pone.0010549.
- [26] P. Bathini, T. Sun, M. Schenk, S. Schilling, N. J. Mcdannold, and C. A. Lemere, “Acute Effects of Focused Ultrasound-Induced Blood-Brain Barrier Opening on Anti-Pyroglu3 A $\beta$  Antibody Delivery and Immune Responses,” *Biomolecules*, vol. 12, no. 7, p. 951, 2022, doi: 10.3390/biom12070951.
- [27] H. Crehan *et al.*, “Effector function of anti-pyroglutamate-3 A $\beta$  antibodies affects cognitive benefit, glial activation and amyloid clearance in Alzheimer’s-like mice,” *Alzheimer’s Res. Ther.*, vol. 12, no. 1, pp. 1–19, 2020, doi: 10.1186/s13195-019-0579-8.

- [28] T. Sun *et al.*, “Focused ultrasound with anti-pGlu3 A $\beta$  enhances efficacy in Alzheimer’s disease-like mice via recruitment of peripheral immune cells,” *J. Control. Release*, vol. 336, pp. 443–456, 2021, doi: 10.1016/j.jconrel.2021.06.037.
- [29] R. Bajracharya, E. Cruz, J. Götz, and R. M. Nisbet, “Ultrasound-mediated delivery of novel tau-specific monoclonal antibody enhances brain uptake but not therapeutic efficacy,” *J. Control. Release*, vol. 349, pp. 634–648, 2022, doi: 10.1016/j.jconrel.2022.07.026.
- [30] G. Leinenga, W. K. Koh, and J. Götz, “A comparative study of the effects of Aducanumab and scanning ultrasound on amyloid plaques and behavior in the APP23 mouse model of Alzheimer disease,” *Alzheimer’s Res. Ther.*, vol. 13, no. 1, pp. 1–14, 2021, doi: 10.1186/s13195-021-00809-4.
- [31] “Safety and Feasibility of Exablate Blood-Brain Barrier Disruption for Mild Cognitive Impairment or Mild Alzheimer’s Disease Undergoing Aduhelm Therapy,” *ClinicalTrials.gov Identifier: NCT05469009*. [Online]. Available: <https://beta.clinicaltrials.gov/study/NCT05469009>. [Accessed: 10-Jan-2023].
- [32] H. J. Fu, B. Liu, J. L. Frost, and C. A. Lemere, “Amyloid- $\beta$  Immunotherapy for Alzheimer’s Disease,” *CNS Neurol Disord Drug Targets*, vol. 9, no. 2, pp. 197–206, 2010, doi: 10.2174/1871527110791012017.
- [33] S. B. Raymond, L. H. Treat, J. D. Dewey, N. J. Mcdannold, K. Hynynen, and B. J. Bacskaï, “Ultrasound Enhanced Delivery of Molecular Imaging and Therapeutic Agents in Alzheimer’s Disease Mouse Models,” *PLoS One*, vol. 3, no. 5, pp. 1–7, 2008, doi: 10.1371/journal.pone.0002175.
- [34] Yardeni T, Eckhaus M, Morris HD, Huizing M, Hoogstraten-Miller S, “Retro-orbital injections in mice,” *Lab Anim (NY)*. vol. 40, no. 5, pp. 155-60, 2011, doi: 10.1038/labani0511-155.
- [35] Wu J, Cai Y, Wu X, Ying Y, Tai Y, He M, “Transcardiac Perfusion of the Mouse for Brain Tissue Dissection and Fixation,” *Bio Protoc*. vol.11, no. 5, 2021, doi: 10.21769/BioProtoc.3988.
- [36] Oakley H, Cole SL, Logan S *et al.*, “Intraneuronal beta-amyloid aggregates, neurodegeneration, and neuron loss in transgenic mice with five familial Alzheimer’s disease mutations: potential factors in amyloid plaque formation,” *J Neurosci*. vol. 26, no. 40, pp.10129-40, 2006, doi: 10.1523/JNEUROSCI.1202-06.2006.
- [37] Chen J, Tan R, Mo Y, Zhang J, “The blood-brain barrier in health, neurological diseases, and COVID-19,” *Fundamental Research*, 2022.